Interaction Pathways between Breast Cancer Cells and Macrophages

Philip Adrian Vlaicu

Für Pauline und den König

CONTENTS

I. INTRODUCTION

1. The tumour microenvironment is critically involved in cancer development

From its beginning, oncology has primarily focused on the study of tumour cells. Over the decades, great progress has been made regarding cancer diagnosis, therapy and understanding of tumorigenesis. However, it took some time until scientists accepted that tumour cells do not grow and disseminate independently of their surroundings. Yet first evidence of the importance of the tumour microenvironment in the development of cancer was delivered as early as 1889, when the British surgeon Stephen Paget published a "seed and soil" hypothesis of cancer metastasis. From the analysis of 735 necropsies of fatal breast cancer in combination with previously published data, he concluded that tumours of different organs display different patterns of organ-specific metastasis. Paget had realised that, even though disseminating tumour cells spread systemically throughout the body, metastases only establish in organs which support their growth. "When a plant goes to seed, its seeds are carried in all directions; but they can only live and grow if they fall on congenial soil" (Paget, 1889). Today we know that, in solid tumours, cancer cells constitute but one part of a rather complex assembly of different cell types. This assembly develops into an organ-like structure. The tumour microenvironment, or stromal compartment, comprises a cellular part, consisting of fibroblasts, endothelial cells, pericytes and immune cells, as well as its own extracellular matrix (ECM). Rather than being a passive bystander, the stromal compartment constantly interacts with tumour cells and is a source of pro- as well as antitumorigenic factors (Mueller and Fusenig, 2004). Consequently, when a tumour is to grow and progress to metastatic disease, it must employ mechanisms to generate a supportive microenvironment. The most obvious process that illustrates the necessity of tumour-stromal interactions is the delivery of oxygen and nutrients to proliferating tumour cells. In order to grow beyond a size of 1-2 mm in diameter, tumours must trigger an angiogenic response, during which endothelial cells and associated pericytes establish a functional tumour vascular network (Folkman, 2003). Cancer-associated fibroblasts (CAF) can actively assist tumour growth and progression by secreting growth factors, metalloproteases and ECM components (De Wever et al., 2004; Lewis et al., 2004; Li et al., 2003). In order to invade locally and establish distant metastases, tumours must remodel the surrounding ECM compartment. The breakdown of the basal lamina surrounding benign tumours is a key step in the progression to locally invasive disease. During dissemination to distant organs, cancer cells often encounter microenvironments very different from the organ of origin. In order to thrive, they again need to modulate these microenvironments to their own benefit.

Immune escape is another key aspect of interactions between tumour and stromal cells. As the hallmark of all tumour cells is an instable genome, cancer cells express aberrant proteins that can trigger the immune system to reject the tumour (Burnet, 1970; Smyth et al., 2001). Thus, in order to avoid rejection, tumours must modulate infiltrating immune cells. Figure 1 compares micrographs of immunohistochemical samples of normal mammary epithelial ducts and an invasive mammary carcinoma.

A

B

normal mammary ducts

cancer cells   stromal compartment
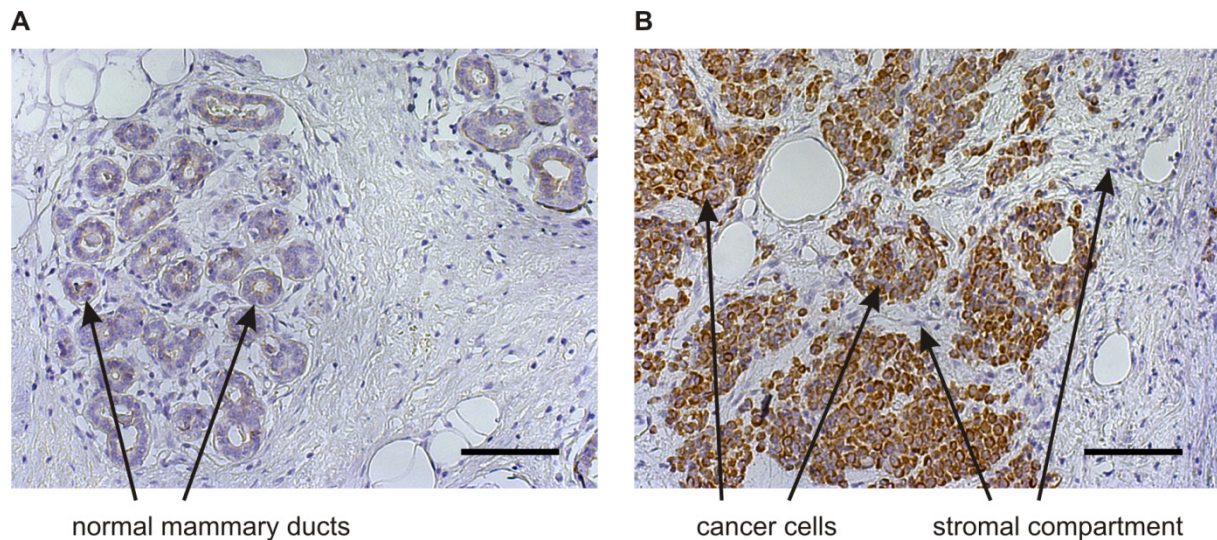
FIGURE 1. The stromal compartment is an integral part of solid tumours. (A) Micrograph depicting normal mammary ducts. (B) Tumour cells live in intimate contact to surrounding stromal cells in an invasive mammary carcinoma sample. Cancer cells have been selectively stained with a specific antibody. Scale bar: 100 µm.

2.   Immune escape is a hallmark of cancer

Of all stromal cells, infiltrating immune cells exert the most puzzling roles during cancerogenesis. *Per se*, these cells are fully equipped to eradicate a developing tumour. However, once a tumour has established, immune cells rarely reject it.

All immune cells develop from a common hematopoietic stem cell (HSC). At the cellular level, lineage-committed HSC progenitors give rise to two major lineages of immune cells. The myeloid lineage comprises monocytes, macrophages (MΦ), mast cells, basophils, eosinophils, neutrophils and subsets of dendritic cells (DC). T lymphocytes, B lymphocytes, natural killer (NK) cells and certain DC subsets constitute the lymphoid lineage. Functionally, we distinguish the innate from the adaptive immune system. The former represents the primordial defense mechanism of all multicellular organisms. Upon recognizing conserved constituents of microbes, its effector cells initiate an immediate reaction that results in killing of pathogens and pathogen-infested cells. Innate immune reactions are swift, do not require previous activation and clonal expansion of cell populations, but lack a memory function which would speed up reactions upon repeated exposure to the same pathogen. In contrast, the adaptive immune system initiates a slow

reaction upon its first contact to a given pathogen. Following recognition of pathogen-derived antigens, T lymphocytes activate individual B lymphocytes that express antigen-specific antibodies. Activated B lymphocytes proliferate clonally, generating plasma cells that secrete large quantities of antibodies. The released antibodies bind antigens on the surface of pathogens during a process called opsonization, marking pathogens for subsequent ingestion and destruction by innate immune cells. At the end of an adaptive immune reaction, the majority of activated T and plasma cells are cleared from the body by undergoing apoptosis. However, certain subsets of these cells survive and differentiate into long-lived resting memory cells. Once reencountering the same antigen, these cells immediately assume effector functions and trigger a memory reaction, so fast and efficient that it usually proceeds unnoticed. In that case, the host enjoys immunity against the previously encountered pathogen. Although innate and adaptive immunity are functionally distinct, we cannot draw a clear line between these processes at the cellular level. As an example, phagocytic macrophages represent workhorses of the innate immune system, yet at the same time they present antigens of engulfed pathogens to T lymphocytes, speeding up adaptive immune reactions.

The adaptive immune system's ability to recognize an almost unlimited number of antigens and the provision of long-lasting immunity constitute the formula of success of vaccination strategies directed against infectious diseases, which led to the eradication of smallpox in 1980 (Fenner, 1982). Thus, it is not surprising that scientists and clinicians explore the feasibility of vaccination and autologous transfer approaches as means of cancer prophylaxis and treatment (Hunder et al., 2008; Jaini et al., 2010; Tyagi and Mirakhur, 2009).

In 1863, Rudolf Virchow first noted that tumour samples were infiltrated by immune cells, preparing the ground for the field now known as tumour immunology. From his observations, Virchow postulated that tumours originate from sites of chronic inflammation.

The early view regarded tumour-infiltrating leukocytes as indicative of an active immune response against the tumour (Friedell et al., 1965; Kreider et al., 1984). Sure enough, gastric and colorectal carcinomas heavily infiltrated by NK cells exhibit a favourable prognosis (Coca et al., 1997; Ishigami et al., 2000). Paradoxically, epidemiological studies have revealed that inflammatory processes predispose to cancer, suggesting that immune cells can also act in a tumour-promoting fashion. *Helicobacter pylori* infection leads to chronic gastritis, which predisposes to gastric cancer (De Luca and Iaquinto, 2004). Infection with hepatitis B or hepatitis C viruses promotes hepatocellular carcinoma by causing chronic hepatitis (Brechot, 2004). Such tumour-promoting inflammatory processes are not necessarily linked to pathogens, as they are also induced by exposure to toxic substances or irritants. It is well-established that asbestos and tobacco smoke cause chronic inflammation of the lung, greatly increasing lung cancer risk (Manning et al., 2002; Takahashi et al., 2010). Conversely, chronic administration of non-steroidal anti-inflammatory drugs (NSAID) reduces cancer risk, further strengthening the causative link

between inflammation and cancer (Dannenberg and Subbaramaiah, 2003; Peter et al., 2010a; Peter et al., 2010b).

Recent studies of the tumour microenvironment have emphasized that all manifest tumours employ mechanisms to elude the immune system, establishing immune subversion as a true hallmark of cancer (Dunn et al., 2004). Tumour cells not only manage to avoid rejection by the host's immune system, but effectively reprogram infiltrating immune cells to render them tumour-supportive (Johansson et al., 2008). Interestingly, cancer cells employ analogous mechanisms to circumvent therapeutic targeting on the one hand and to escape immunosurveillance on the other. Just as therapeutic targeting of cancer cells selects for resistant clones, an immune reaction against tumour cells selects cancer cell clones that escape immunosurveillance, a process termed immunoediting (Dunn et al., 2004). The cancer immunoediting process is comprised of three phases: during the initial elimination phase, neoplastic cells are actively targeted by cells of the innate and adaptive immune system, eventually leading to tumour eradication. However, the immune response will spare cancer cells that have, owing to their inherent genomic instability, developed means of circumventing or actively inhibiting immunosurveillance. If eradication fails, the tumour enters an equilibrium phase, during which the ongoing immune response further selects for resistant cancer cells by killing immunogenic clones. As more and more resistant clones emerge, the immune reaction against the tumour fails, and cancer cells enter the escape phase, growing unrestrained of immune pressure. It is at this stage that the tumour becomes clinically detectable. To escape immune recognition, tumour cells alter their antigen processing and presentation pathways, e.g. by downregulating expression of HLA class I proteins (Algarra et al., 2000). Alternatively, tumour cells secrete immunosuppressive cytokines such as TGF-β or IL-10 (Khong and Restifo, 2002), or impede the maturation of antigen-presenting dendritic cells (Wang et al., 2004).

3.   The role of tumour-associated mononuclear cells in cancerogenesis

Tumour-associated macrophages (TAM) are key participants in the crosstalk between tumour and immune cells. TAM density correlates with poor prognosis in a considerable number of human tumours (Bingle et al., 2002). In some cases, macrophages (MΦ) already participate in the very early steps of cancer initiation, by fostering a mutagenic, growth-promoting environment (Coussens and Werb, 2002). However, their best studied contribution to malignancy is the involvement in tumour progression. In a mouse breast carcinoma model, Pollard and colleagues have shown that MΦ ablation inhibits metastasis (Lin et al., 2001). Surprisingly, the macrophage ablation model uncovered striking parallels between the role of MΦ in metastasis promotion and in the development and maintenance of certain organs. Macrophage ablation affects branching morphogenesis, leading to atrophic mammary glands (Gouon-Evans et al., 2000; Pollard and Hennighausen, 1994). Moreover, it

leads to defects in pancreatic islet formation (Banaei-Bouchareb et al., 2004). Wound healing studies have highlighted that MΦ exert important functions as trophic agents (Martin and Leibovich, 2005), and they are known to secrete a plethora of growth factors and metalloproteases (Kessenbrock et al., 2010; Pollard, 2004). While TAM are the best studied components of the innate immune system influencing tumour progression, little is known about functional implications of tumour-associated monocytes. Yet, populations of Tie2-expressing infiltrating monocytes promote angiogenesis in mouse tumour models (De Palma et al., 2005; Venneri et al., 2007).

4. Epidermal growth factor receptor family members are key players in cancer development

The molecular cloning of the epidermal growth factor receptor (EGFR) in 1984 marks a milestone of biochemical research (Ullrich et al., 1984). As scientists step by step unravelled structural and functional features of the EGFR, they gained fundamental new insights into the biology of receptor tyrosine kinases (RTK). The EGFR peptide sequence was found to be homologous to the protein encoded by an avian oncoprotein, v-erbB (Downward et al., 1984). This early observation established a connection between a growth factor receptor and cancer. The other three EGFR/ERBB family members, human EGFR-related 2 (*HER2/ERBB2*), *HER3* (*ERBB3*) and *HER4* (*ERBB4*), were also shown to be important proto-oncogenes. A screening conducted on 189 breast cancer specimens revealed that *HER2*, which was overexpressed in 30 % of the samples, was a strong negative prognostic factor (Slamon et al., 1987). This finding lead to the development of Herceptin, a monoclonal antibody directed against HER2, as the first molecular anticancer therapeutic. Mouse knockout studies confirmed that, apart from their roles in cancer development, all EGFR family members are essential for development and homeostasis (Gschwind et al., 2004).

EGFR family members display a modular architecture, composed of an extracellular ligand-binding domain, a transmembrane domain and a cytoplasmic tyrosine kinase domain with adjacent regulatory regions. Ligand binding induces conformational changes that lead to receptor dimerization and autophosphorylation of tyrosine residues in the activation loops of the kinase domains, which further stimulates kinase activity (Schlessinger, 1988). Activation of HER2 and HER3 differs from that of the other EGFR family members. HER3 is missing a functional kinase domain, while HER2 has no described ligand. Instead, the conformation of HER2 resembles that of ligand-activated EGFR members, which facilitates receptor dimerization. Thus, it is not surprising that HER2 is the preferred dimerization partner of all EGFR family members (Graus-Porta et al., 1997).

EGFR family ligands are produced as transmembrane proforms, and active ligands are shed into the extracellular space by membrane-anchored ADAM (a disintegrin and metalloprotease) metalloproteases. Based on their receptor binding preferences, EGFR

family ligands are divided into four groups: epidermal growth factor (EGF), transforming growth factor alpha (TGFα) and amphiregulin (AREG) specifically bind to EGFR, whereas betacellulin (BTC), heparin-binding EGF-like growth factor (HB-EGF) and epiregulin (EREG) display dual specificity towards EGFR and HER4. Neuregulins 1 and 2 (NRG1 and NRG2) bind to HER3 and HER4, and neuregulins 3 and 4 (NRG3 and NRG4) bind to HER4 exclusively. The differential receptor-binding preferences of EGFR family ligands and the variety of receptor homo- and heterodimers provide great signalling diversity (Figure 2), which is further increased by alterations in signal transduction downstream of the activated receptor kinases.
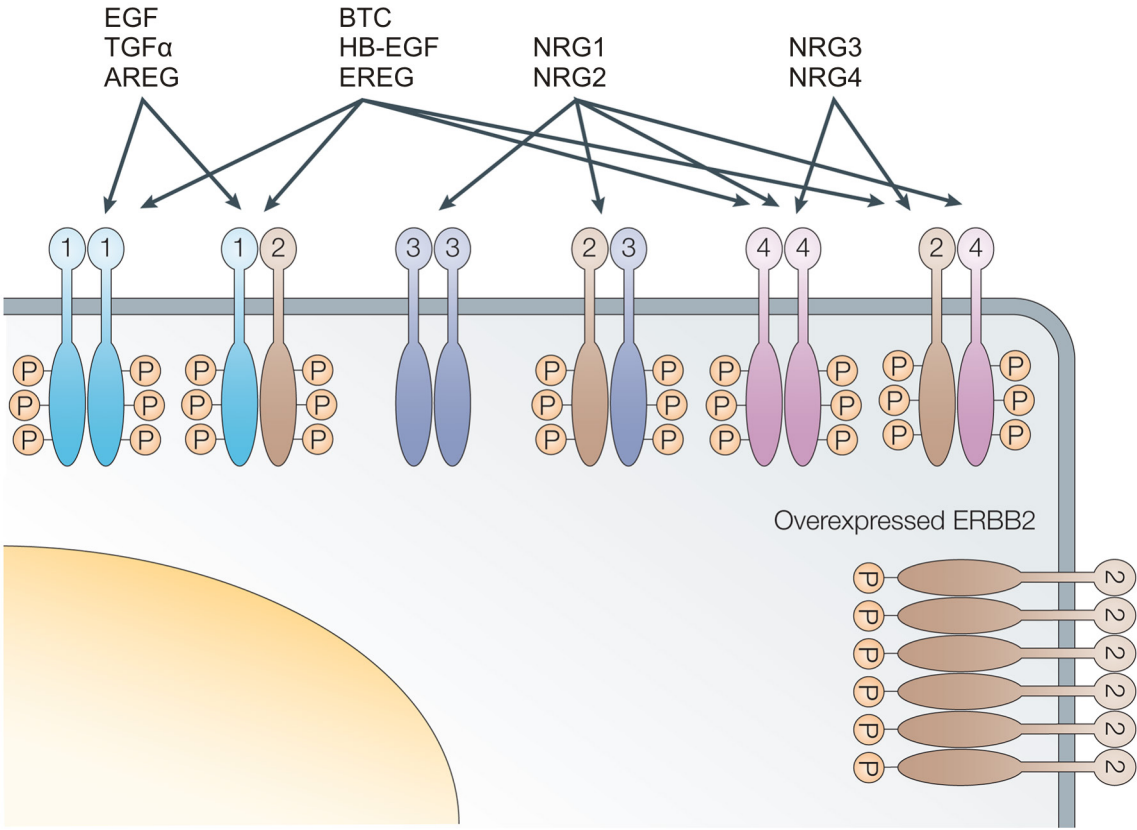
FIGURE 2. Signalling diversity of ERBB family members. Ligands of the epidermal growth factor (EGF) family display different preferential binding properties towards ERBB receptors. Ligand binding induces the formation of various receptor homo- and heterodimers and the activation of the cytoplasmic kinase domain, resulting in phosphorylation of specific tyrosine residues within the cytoplasmic tail. Image adapted from Hynes and Lane (Hynes and Lane, 2005).

Active EGFR family receptors present several phosphorylated tyrosine residues on their cytoplasmic tails. These serve as docking sites for SH2 domain-containing Grb2 adaptor proteins which initiate the classical RTK downstream signalling cascade that leads to activation of Ras, Raf, MEK and ERK oncoproteins. Apart of the RTK-Grb2-Sos-Ras-Raf-MEK-ERK signalling cascade, EGFR family members activate a wide range of oncoproteins, including PLCγ1, PI3K, AKT, Src, mTOR and STAT family members (Gschwind et al., 2004).

Several mechanisms lead to deregulated EGFR family member signalling, which is a major contributor to cancer development. One such mechanism is receptor overexpression, as the already mentioned amplification of *HER2* in breast cancer. Activating *EGFR* mutations occur frequently in non-small cell lung carcinomas (NSCLC) and open a therapeutic window by rendering these tumours sensitive to treatment with EGFR tyrosine kinase inhibitors (Paez et al., 2004). Finally, aberrant auto- or paracrine secretion of EGFR family ligands persistently activates ERBB receptors in a wide range of cancers (Kramer et al., 2007; Tateishi et al., 1990; Thogersen et al., 2001; Umekita et al., 2000).

The importance of EGFR family members as oncoproteins has spurred the development of an ever increasing number of anticancer therapeutics. Two basic approaches are being used to interfere with EGFR family member-mediated tumorigenesis: neutralising antibodies and small-molecule tyrosine kinase inhibitors (TKI). More than thirteen anticancer agents targeting EGFR family oncoproteins either have obtained approval by the U.S. Food and Drug Administration (FDA) or are currently undergoing clinical examination. The list of neutralising antibodies comprises HER2-targeted herceptin and pertuzumab, EGFR-interfering erbitux and panitumumab, and HER3-targeted U3 P1287 and MM-121. MM-111 represents a new approach, being an antibody with dual specificity for HER2 and HER3. CI-1033 and EKB-569 are dual-specificity irreversible TKI targeting EGFR and HER2. Most TKI, however, are reversible inhibitors, like gefitinib (EGFR), erlotinib (EGFR), lapatinib (EGFR/HER2) and AEE788 (EGFR/HER2/VEGFR).

5. STAT3 transcription factors in cancerogenesis

Proteins of the STAT family fulfil dual roles: they are cytoplasmic signal transducers on the one hand, and nuclear transcription factors on the other hand. The STAT family comprises STAT1, STAT3, STAT4, STAT6 and the closely related STAT5A and STAT5B members. Following activation, cytokine receptors activate associated Janus kinases (JAK). These phosphorylate tyrosine residues on the cytoplasmic tail of the activated cytokine receptors, creating docking sites for monomeric STAT proteins. Upon binding to the receptor, STAT monomers are themselves phosphorylated at selected tyrosine residues, and form homo- or heterodimers via reciprocal interaction of SH2 domains and phosphotyrosine moieties. STAT dimers translocate to the nucleus, where they bind to specific DNA promoter sequences and initiate transcription of their respective target genes. STAT proteins represent versatile

signalling hubs, as they can be activated by a multitude of cytokine receptors, growth factor receptors (EGFR, Her2, HGFR, PDGFR, IGFR) and non-receptor tyrosine kinases, such as Src and Abl (Bollrath and Greten, 2009).

STAT3 was discovered as a transcription factor whose activation was mediated by EGF and IL-6 (Zhong et al., 1994). Its ablation in mice leads to embryonic lethality, proving that STAT3 activity is essential during development (Takeda et al., 1997). However, soon after its discovery, STAT3 was also shown to be deeply implicated in cancerogenesis. Cell transformation by the viral oncogenes *V-SRC* and polyoma virus middle T antigen (*PyMT*) triggered constitutive activation of STAT3, whose activity was required for *V-SRC*-mediated transformation (Bromberg et al., 1998; Garcia et al., 1997; Yu et al., 1995). A constitutively active form of STAT3 lead to cell transformation and tumorigenesis in mice (Bromberg et al., 1999). In cancer patients, STAT3 was found to be persistently active in solid tumours of the brain, breast, head and neck, skin, ovary, pancreas and prostate, as well as in lymphomas and leukemias (Turkson and Jove, 2000). Oncogenic *STAT3* mutations are rare. Instead, STAT3 activation in tumours happens almost exclusively due to upstream events, like gain-of-function mutations of tyrosine kinases, cytokine receptors, or alternatively due to aberrant auto- or paracrine secretion of growth factors or cytokines (Yu et al., 2009). Depending on the cellular context, STAT3 activity in tumour cells elicits a plethora of cellular responses, including proliferation, survival, migration and angiogenesis (Epling-Burnette et al., 2001; Garcia et al., 2001; Grandis et al., 1998; Niu et al., 2002; Yamashita et al., 2002). Paracrine crosstalk mechanisms between tumour cells and stromal cells establish feed-forward loops that result in the constitutive activation of STAT3 in both tumour compartments (Yu et al., 2007). Cancer cells trigger the activation of STAT3 in tumour-associated immune cells, a key step in blunting antitumour immune reactions. In tumour-associated myeloid cells, STAT3 activity promotes the accumulation of myeloid-derived suppressor cells (MDSC), which inhibit DC maturation, suppressing an antitumour reaction of the adaptive immune system (Cheng et al., 2008). Conversely, disruption of STAT3 signalling in hematopoietic cells leads to enhanced immunosurveillance mediated by DC, NK and T cells *in vivo* (Cheng et al., 2003; Kortylewski et al., 2005).

Inflammation-related cancer involves pathways that converge on two transcription factors: NFκB and STAT3. While STAT3 activation in tumour cells and stromal cells is clearly protumorigenic, NFκB activity elicits pro- as well as antitumour effects (Baud and Karin, 2009). However, when both transcription factors are activated during tumorigenesis, STAT3 activity inhibits the expression of NFκB antitumour target genes, skewing NFκB actions towards a pro-tumour response (Lee et al., 2009; Yu et al., 2007). In inflammation-related cancer, persistent STAT3 activation is achieved via two mechanisms: oncogenic alterations in the transformed cells lead to constitutive activation of pathways that are upstream of STAT3 (intrinsic pathway). However, receptors and non-receptor kinases upstream of STAT3 are also activated by environmental factors that promote inflammation (extrinsic pathway, Figure 3). Such extrinsic factors are chronic infections with *Helicobacter pylori*,

papillomavirus, hepatitis B virus, or alternatively inflammatory agents like UV light and cigarette smoke (Arredondo et al., 2006; Bronte-Tinkew et al., 2009; Choudhari et al., 2007; Sano et al., 2005; Sun and Steinberg, 2002).
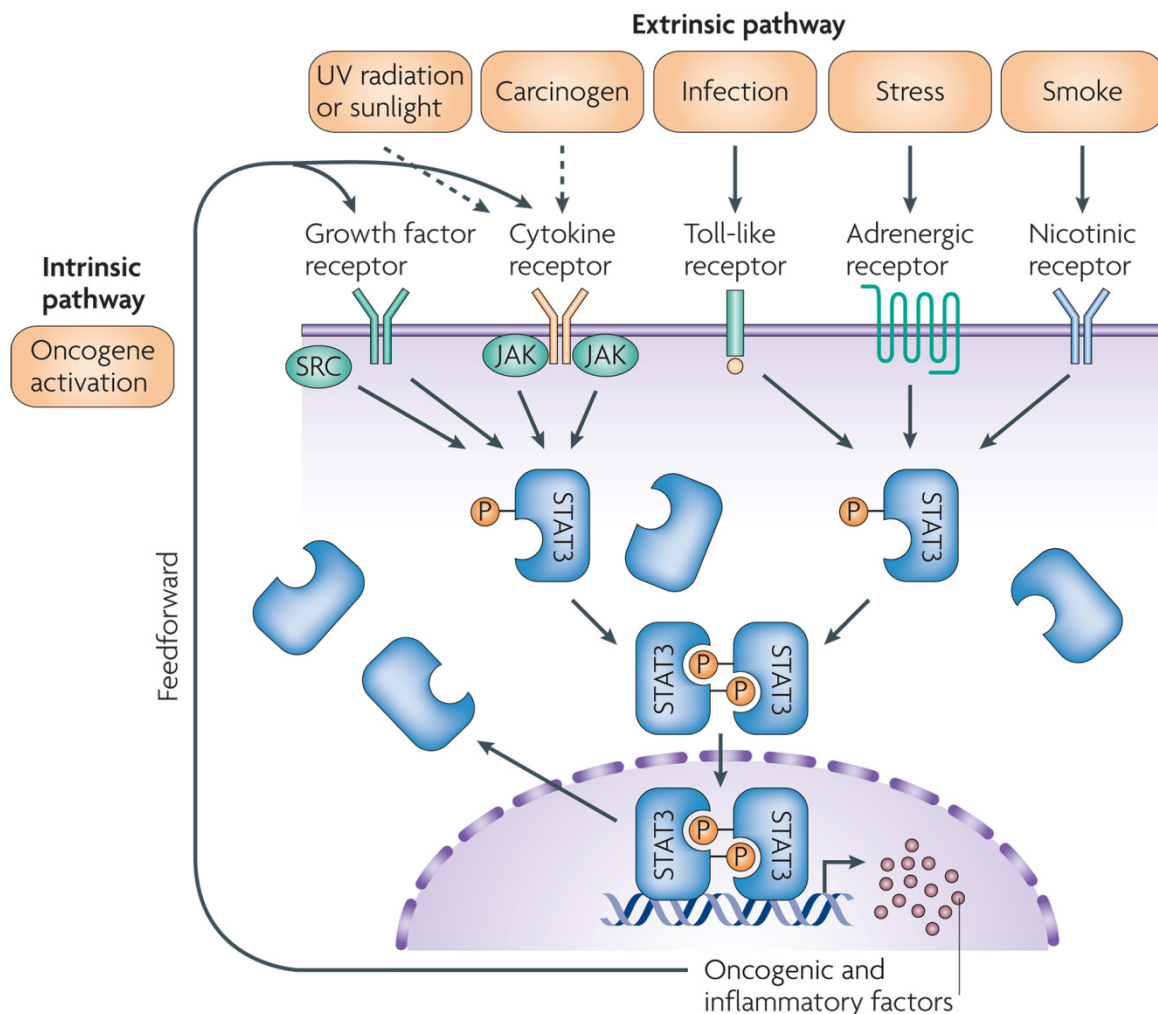
FIGURE 3. Inflammatory and oncogenic pathways converge at the level of STAT3 transcription factors. The intrinsic pathway of STAT3 activation is governed by underlying oncogenic DNA alterations. Alternatively, proinflammatory environmental factors such as UV radiation, carcinogens, infection, stress or tobacco smoke activate STAT3 via extrinsic pathways (Yu et al., 2009).

Although STAT3 has been long validated as a target for anticancer therapy, so far no therapeutics aimed at inhibiting its activity in tumours are available to clinicians. Without doubt this is, at least partly, due to two factors: the intracellular localization of STAT3 prevents the use of inhibitory antibodies. Moreover, the lack of an enzymatic activity in STAT proteins poses a further challenge to drug development. Nevertheless, small molecule and peptide inhibitors interfering with protein-protein or protein-DNA interactions have been developed (Mandal et al., 2009; Schust et al., 2006; Turkson et al., 2004). Alternative approaches include small interfering RNA (siRNA) mediated downregulation of gene expression, decoy DNA binding oligonucleotides and inhibition of upstream Janus kinases

(Kong et al., 2008; Leong et al., 2003; Ling and Arlinghaus, 2005; Nefedova et al., 2005). Antitumour effects of novel multitargeted kinase inhibitors Sunitinib and Sorafenib are partly mediated by inhibition of STAT3 phosphorylation, further supporting the rationale of targeting STAT3 in anticancer therapy (Xin et al., 2009; Yang et al., 2010). Currently, three STAT3 inhibitors are undergoing clinical trials. Small molecule inhibitors OPB-31121 and AZD1480 target STAT3 and JAK2, respectively, whereas a STAT3 decoy is being tested in patients with head and neck squamous cell carcinoma (http://clinicaltrials.gov/ct2/home).

II. AIMS

We studied the influence of tumour cells on ligand secretion and transcription patterns of monocytes and differentiated macrophages. Given the pivotal roles that the oncogenic STAT3 and EGFR pathways play in tumour development, we focused primarily on the repertoire of interleukin-6-like STAT3 activators and EGFR agonists secreted by tumour-primed monocytes and МФ.

Recent *in vivo* studies have revealed that IL-6 and STAT3 are essential for the development of colitis-associated cancer (Bollrath et al., 2009; Grivennikov et al., 2009). Patients with colorectal carcinoma display elevated IL-6 protein serum levels, which indicate a poor prognosis (Knupfer and Preiss, 2010). The family of interleukin-6-like cytokines contains several ligands, including interleukin-6 (IL-6), interleukin-11 (IL-11), leukemia inhibitory factor (LIF), ciliary neurotrophic factor (CNTF), cardiotrophin-1 (CT-1) and oncostatin-M (OSM). To date, little is known about the possible implications of tumour-associated mononuclear cells as secretory sources of IL-6-like cytokines.

Several lines of evidence point to a role of TAM-secreted EGFR ligands in malignant progression. McGee and colleagues provided clues for EGFR ligand production by TAM in breast carcinoma biopsies (O'Sullivan et al., 1993). TAM number and EGFR expression levels correlate in human breast tumours (Leek et al., 2000), and TAM comigrate with tumour cells in an EGFR dependent manner in a murine breast carcinoma model (Wyckoff et al., 2004). However, the exact repertoire of EGFR agonists that TAM secrete is unknown, as are the related regulatory pathways.

We analysed oncogenic ligands secreted by mononuclear cells in response to tumour cell-derived factors. In a first step, we established a monocytic cell line model and have screened its secretome to identify monocyte-secreted ligands that are relevant to tumour progression *in vitro*. To validate our findings, we have analysed primary human PBMC and МФ exposed to tumour cell supernatants, as well as plasma samples from breast cancer patients.

III. MATERIALS AND METHODS

1. Material sources

1.1 Laboratory chemicals and biochemicals

Acrylamide	Serva, Heidelberg
Active human serum	Prepared in our department
AG1478	Alexis Biochemicals, USA
Agarose	BRL, Eggenstein
Aprotinin	Sigma, Taufkirchen
APS (ammonium peroxodisulfate)	Bio-Rad, München
Bisacrylamide	Roth, Karlsruhe
Bromphenol blue	Sigma, Taufkirchen
BSA (bovine serum albumin)	Sigma, Taufkirchen
Cholera toxin	Sigma, Taufkirchen
Coomassie G250	Serva, Heidelberg
Crystal violet	Sigma, Taufkirchen
Deoxynucleotides (dGTP/dATP/dTTP/dCTP)	Roche, Mannheim
Ethidium bromide	Sigma, Taufkirchen
FCS (fetal calf serum)	Gibco, USA
Formaldehyde	Roth, Karlsruhe
Gelatine from bovine skin, tissue culture grade	Sigma, Taufkirchen
Glycerol	Merck, Darmstadt
HEPES (N-(2-hydroxyethyl) piperazine-N'-(2-ethanesulfonic acid))	Serva, Heidelberg
L-glutamine	Invitrogen, Eggenstein
Normal human male AB serum	Sigma, Taufkirchen
PMSF (phenylmethylsulfonyl fluoride)	Sigma, Taufkirchen
Ponceau S	Sigma, Taufkirchen
Saponin	Sigma, Taufkirchen
SDS (sodium dodecyl sulfate)	Serva, Heidelberg
Sodium azide	Serva, Heidelberg
Sodium fluoride	Sigma, Taufkirchen
Sodium orthovanadate	Sigma, Taufkirchen
Streptavidin, horseradish peroxidase-linked	Jackson ImmunoResearch, USA
TEMED (N,N,N',N'-tetramethylethane-1,2-diamine)	Serva, Heidelberg
TMB substrate (3,3′,5,5′-tetramethylbenzidine)	Calbiochem, Darmstadt
Triton X-100	Roth, Karlsruhe

Trypsin/EDTA (0.05 %/0.02 % in PBS)	PAA, Austria
Tween$_{20}$	Sigma, Taufkirchen
Xylenecyanol	Merck, Darmstadt
β-Mercaptoethanol	Merck, Darmstadt

All other chemicals were purchased in analytical grade from Merck (Darmstadt).

1.2 Chemicals for SILAC and MS analysis

Acetonitrile for HPLC	Sigma, Taufkirchen
Ammoniumbicarbonate	Sigma, Taufkirchen
Ammonium hydroxide	Merck, Darmstadt
Antioxidance	Invitrogen, Eggenstein
2,5-Dihydroxybenzoic acid	Fluka, Taufkirchen
DTT (dithiothreitol)	Sigma, Taufkirchen
Fetal bovine serum, dialyzed	Gibco, USA
Iodoacetamide	Sigma, Taufkirchen
L-Arginine	Gibco, USA
L-Arginine: HCl, U-$^{13}C_6{}^{14}N_4$	Euriso-Top, France
L-Arginine: HCl, U-$^{13}C_6{}^{15}N_4$	Euriso-Top, France
L-Glutamine	Gibco, USA
L-Lysine	Gibco, USA
L-Lysine: 2 HCl, $^2H_4$	Euriso-Top, France
L-Lysine: 2 HCl, U-$^{13}C_6{}^{15}N_2$	Euriso-Top, France
Lys-C	WAKO, Neuss
n-octosylglucoside	Roche, Mannheim
Nonidet™ P 40 Substitute	Sigma, Taufkirchen
Penicillin/Streptomycin, 100x	PAA, Austria
SILAC RPMI	Gibco, USA
Thio urea	Invitrogen, Eggenstein
Trypsin (seq. grade modified)	Promega, USA
Urea	Merck, Darmstadt

1.3 Enzymes

AMV reverse transcriptase	Roche, Mannheim
Trypsin	Invitrogen, Eggenstein

1.4 Kits and other materials

Cell culture materials	Greiner, Solingen
	Nunclon, Denmark
	Falcon, UK
Cellulose nitrate 0.45 µm	Schleicher & Schüll, Dassel
Colloidal Blue Staining Kit	Invitrogen, Eggenstein
Fast SYBR® Green Master Mix	Applied Biosystems, USA
Ficoll-Paque™ PLUS	GE Healthcare, USA
Hyperfilm MP	Amersham Pharmacia, Freiburg
MACS MultiStand	Miltenyi Biotech, Bergisch Gladbach
MaxiSorp™ 96 well plates for ELISA	Thermo Fisher Scientific, USA
Micro BCA Protein Assay Kit	Pierce, Sankt Augustin
MidiMACS Separation Unit	Miltenyi Biotech, Bergisch Gladbach
LS Columns	Miltenyi Biotech, Bergisch Gladbach
Parafilm	Dynatech, Denkendorf
Protein A-Sepharose	Amersham Pharmacia, Freiburg
Protein G-Sepharose	Amersham Pharmacia, Freiburg
QIAquick PCR Purification Kit (50)	Qiagen, Hilden
ReadyMix™ redtaq™ PCR reaction mix	Sigma, Taufkirchen
RNeasy Mini Kit	Quiagen, Hilden
Sterile filter 0.22 µm, cellulose acetate	Nalge Company, USA
Sterile filter Millex-GV, 0.22 µm, PVDF	Millipore, USA
Sterile filter 0.45 µm, cellulose acetate	Nalge Company, USA
VIVASPIN ultrafiltration columns	Sartorius, France
Western Lightning™-ECL Kit	PerkinElmer, USA
Whatman 3MM	Whatman, USA

1.5 Growth factors and ligands

AREG (human)	R&D Systems, USA
EGF (human)	Peprotech, USA
HB-EGF (human)	R&D Systems, USA
Hydrocortisone (human)	Sigma, Taufkirchen
IL-6 (human)	Invitrogen, Eggenstein
Insulin (bovine)	Sigma, Taufkirchen
OSM (human)	R&D Systems, USA
TGFα (human)	R&D Systems, USA

2.   Cell culture media

Gibco™ media and additives were obtained from Invitrogen (Eggenstein). Media were supplemented to the requirements of each cell line. Freezing medium contained 95 % heat inactivated FCS and 5 % DMSO.

3.   Stock solutions and commonly used buffers

Collecting gel buffer (4x)	0,5 M	Tris/HCl pH6.
	0,4 %	SDS
ELISA wash buffer	0.05 %	Tween$_{20}$ in PBS
ELISA blocking buffer	1 %	BSA
	5 %	Sucrose in PBS
ELISA dilution buffer	1 %	BSA in PBS
FACS buffer (FB)	3 %	FCS in PBS
	0.04 %	NaN$_3$
FACS fixation buffer	2 %	Formaldehyde in PBS
HNTG	20.0 mM	HEPES pH 7.5
	150 mM	NaCl
	0.1 %	Triton X-100
	10.0 %	Glycerol
	10.0 mM	Na$_4$P$_2$O$_7$
Hypotonic buffer	20 mM	HEPES pH 7.2
	10 mM	KCl
	1.5 mM	MgCl$_2$
	0.1 mM	EGTA
	10 mM	Na$_4$P$_2$O$_7$
	2 mM	Na$_3$VO$_4$
	10 mM	NaF
	1 mM	PMSF
	10 µg/ml	Aprotinin

DNA loading buffer (6x)	0.05 %	Bromphenol blue
	0.05 %	Xylencyanol
	30.0 %	Glycerol
	100.0 mM	EDTA pH 8.0
Laemmli buffer (3x)	100 mM	Tris/HCl pH 6.8
	3.0 %	SDS
	45.0 %	Glycerol
	0.01 %	Bromphenol blue
	7.5 %	ß-Mercaptoethanol
Mass spectrometry lysis buffer	50 mM	Tris-HCl pH 7.5
	150 mM	NaCl
	1 %	NP-40
	0.1 %	Sodium deoxycholate
	1 mM	EDTA
	1 mM	Na_3VO_4
	1 mM	PMSF
	0.1 µg/ml	Aprotinin
	10 mM	NaF
Membrane solubilisation buffer	50 mM	HEPES pH 7.5
	1 %	Triton X-100
	150 mM	NaCl
	10 mM	EDTA
	10 %	glycerol
	10 mM	$Na_4P_2O_7$
	2 mM	Na_3VO_4
	10 mM	NaF
	1 mM	PMSF
	10 µg/ml	Aprotinin
NET	50.0 mM	Tris/HCl pH 7.4
	5.0 mM	EDTA
	0.05 %	Triton X-100
	150.0 mM	NaCl

PBS	137.0 mM	NaCl
	27.0 mM	KCl
	80.9 mM	Na_2HPO_4
	1.5 mM	KH_2PO_4
	pH 7.4	
SAP buffer	3 %	FCS in PBS
	0.04 %	NaN_3
	0.1 %	Saponin
SD-Transblot	50.0 mM	Tris/HCl pH 7.5
	40.0 mM	Glycine
	20.0 %	Methanol
	0.004 %	SDS
Separating gel buffer (4x)	0.5 M	Tris/HCl pH 8.8
	0.4 %	SDS
"Strip" buffer	62.5 mM	Tris/HCl pH 6.8
	2.0 %	SDS
	100.0 mM	β-Mercaptoethanol
TAE	40.0 mM	Tris/Acetate pH 8.0
	1.0 mM	EDTA
TE10/0.1	10.0 mM	Tris/HCl pH 8.0
	0.1 mM	EDTA pH 8.0
Tris-Glycine-SDS	25.0 mM	Tris/HCl pH 7.5
	200.0 mM	Glycine
	0.1 %	SDS

4.   Cells

4.1   Cell lines

Name	Description	Origin/Reference
HL-60	Human promyelocytic leukemia	ATCC, USA
MAD-NT	Macrophage differentiation, non-terminal; partly adherent HL-60 clone	Pjotr Knyazev
MCF 10A	Human mammary breast hyperplasia	ATCC, USA
MCF7	Human mammary breast carcinoma	ATCC, USA
MDA-MB-231	Human mammary breast carcinoma	ATCC, USA
MDA-MB-435S	Human mammary breast carcinoma	ATCC, USA
MDA-MB-468	Human mammary breast carcinoma	ATCC, USA
SCC-9	Human squamous cell carcinoma (tongue)	ATCC, USA
T-47D	Human mammary breast carcinoma	ATCC, USA

4.2   Primary cells

Name	Description	Origin/Reference
HMEC	Human mammary epithelial cells	Clonetics, Switzerland
PBMC	Human peripheral blood monocytes	Venous blood from healthy donors

5.   Antibodies

5.1   Primary antibodies

Antibody	Description/Use	Origin
Donkey IgG	Donkey polyclonal, used as Fc blocking antibody for flow cytometry experiments	Jackson Immunoresarch, USA
Mouse IgG_1 PE	Mouse monoclonal, PE conjugated control antibody, used for flow cytometry experiments	BD Biosciences, USA
Mouse IgG_{2A} FITC	Mouse monoclonal, FITC conjugated control antibody, used for flow cytometry experiments	BD Biosciences, USA
Mouse IgG_{2B}	Mouse monoclonal, used as control antibody	R&D Systems, USA
Mouse IgG_{2B} PE	Mouse monoclonal, PE-conjugated, used as control antibody for flow cytometry experiments	R&D Systems, USA

Normal goat IgG	Goat polyclonal, used as control antibody	R&D Systems, USA
Rat IgG$_1$	Rat monoclonal, used as control antibody	R&D Systems, USA
αADAMTS-1	Mouse monoclonal, recognizes human ADAMTS-1, used for IP and WB experiments	R&D Systems, USA
αAREG	Goat polyclonal, recognizes human AREG, used for neutralisation experiments	R&D Systems, USA
αAREG	Mouse monoclonal, recognizes human AREG, used as ELISA capture antibody	R&D Systems, USA
αAREG	Goat polyclonal, biotin-conjugated, recognizes human AREG, used as ELISA detection antibody	R&D Systems, USA
αCD14	Mouse monoclonal, conjugated to MicroBeads, recognizes human CD14, used to isolate PBMC	Miltenyi Biotech, Bergisch Gladbach
αCD14 FITC	Mouse monoclonal, recognizes human CD14, used for flow cytometry experiments	BD Biosciences, USA
αCD64 PE	Mouse monoclonal, recognizes human CD64, used for flow cytometry experiments	BD Biosciences, USA
αEGFR	Rabbit polyclonal, recognizes human EGFR, used for WB experiments	Cell Signaling, USA
αEREG	Affinity-purified goat polyclonal, recognizes human EREG, used for neutralisation experiments	R&D Systems, USA
αEREG PE	Mouse monoclonal, PE-conjugated, recognizes human EREG, used for flow cytometry	R&D Systems, USA
αHB-EGF	Human monoclonal, recognizes human HB-EGF, used as ELISA capture antibody	a gift from U3 Pharma, Martinsried
αHB-EGF	Affinity-purified goat polyclonal, recognizes human HB-EGF, used for neutralisation experiments and as ELISA capture antibody	R&D Systems, USA
αHB-EGF	Goat polyclonal, biotin-conjugated, recognizes human HB-EGF, used as ELISA detection antibody	R&D Systems, USA
αHGF	Mouse monoclonal, recognizes human HGF, used for neutralisation experiments	R&D Systems, USA
αHGFR	Rabbit polyclonal, recognizes human HGFR, used for IP and WB experiments	Santa Cruz Biotechnology, USA

αIL-6	Rat monoclonal, recognizes human IL-6, used for neutralisation experiments	BioLegend, USA
αOSM	Mouse monoclonal, recognizes human OSM, used as ELISA capture antibody	R&D Systems, USA
αOSM	Affinity-purified goat polyclonal, recognizes human OSM, used for neutralisation experiments	R&D Systems, USA
αOSM	Goat polyclonal, biotin-conjugated, recognizes human OSM, used as ELISA detection antibody	R&D Systems, USA
αpAKT	Rabbit polyclonal, recognizes human phospho-AKT (Thr308), used for WB experiments	Cell Signaling, USA
αpEGFR	Rabbit monoclonal, recognizes human phospho-EGFR (Tyr1173), used for WB experiments	Cell Signaling, USA
αpSTAT3	Rabbit polyclonal, recognizes human phospho-STAT3 (Tyr705), used for WB experiments	Cell Signaling, USA
αpTYR (4G10)	Mouse monoclonal, recognizes phospho-tyrosine residues, used for IP and WB experiments	Produced in house
αSCARA1	Mouse monoclonal, recognizes human scavenger receptor A 1, used for flow cytometry experiments	R&D Systems, USA
αSTAT3	Rabbit polyclonal, recognizes human STAT3, used for WB experiments	Cell Signaling, USA
αTGFα	Goat polyclonal, recognizes human TGFα, used as ELISA capture antibody	R&D Systems, USA
αTGFα	Goat polyclonal, biotin-conjugated, recognizes human TGFα, used as ELISA detection antibody	R&D Systems, USA
αTGFα	Goat polyclonal, recognizes human TGFα, used for neutralisation experiments	R&D Systems, USA
αtubulin	Mouse monoclonal, recognizes human alpha-tubulin, used for WB experiments	Sigma, Taufkirchen

5.2   Secondary antibodies

Antibody	Dilution	Origin
Donkey anti-mouse-PE	1:200	Jackson Immunoresarch, USA
Goat anti-mouse-HRP	1:10,000	Sigma, Taufkirchen
Goat anti-rabbit-HRP	1:25,000	BioRad, München

6.   Oligonucleotides

Target	Use	Sequence (forward/reverse primer)	Reference
AREG	qPCR and semiquantitative PCR	TGGTGCTGTCGCTCTTGATA GCCAGGTATTTGTGGTTCGT	Andreas Gschwind (Gschwind et al., 2003)
BTC	Semiquantitative PCR	GAAACTAATGGCCTCCTCTGTG TCCGCTTTGATTGTGTGG;	This study
Cyclophilin A	qPCR	GCCG-CGTCTCCTTTGAGCT CACCACATGCTTGCCATCC	Pjotr Knyazev
EGF	Semiquantitative PCR	GCCAAGCAGTCTGTGATTGA CTGATGGCATAGCCCAATCT	This study
EMR1	Semiquantitative PCR	CCAAGGGGGATAAGATGAAG CACCAAGGAGATGATAATGCC	Wael Khazen (Khazen et al., 2005)
EPGN	Semiquantitative PCR	TGACAGCACT-GACCGAAGAG AATCCAACACCAATCCCAAT	This study
EREG	qPCR and semiquantitative PCR	GGGGAGGAGGATGGAGATG TGAGGACTGCCTGTAGAAGATG	This study
GAPDH	Semiquantitative PCR	TTCCAGTATGACTCCACTCACGGC GCAGAAGGGGCGGAGATGATG	Philipp Mertins
GP130	Semiquantitative PCR	TGCCTCCTTTTGAAGCCAAT CCTTTGGAAGGTGGAGCTTG;	This study

HBEGF	qPCR and semiquantitative PCR	TTATCCTCCAAGCCACAAGC TGACCAGCAGACAGACAGATG	Andreas Gschwind (Gschwind et al., 2003)
IL6	Semiquantitative PCR	TGAACTCCTTCTCCACAAGCG TCTGAAGAGGTGAGTGGCTGTC	A. Tchirkov (Tchirkov et al., 2001)
IL6R	Semiquantitative PCR	GAGGGAGACAGCTCTTTCTACATAG CTTCTTGAACCTCAGAACAATGGC	Mihiro Okabe (Okabe et al., 1995)
LIF	Semiquantitative PCR	CGGGACCAGAAGATCCTCAA GCCCAGCTTCTTCTTCTGGA	This study
LIFR	Semiquantitative PCR	TGACTGGAGCCCTGTGAAGA GCGGATTGTGAGCATTCAAA	This study
OSM	Semiquantitative PCR	TGGGGGTACTGCTCACACAG CCTCAGGGTCTCCTCACTGG	This study
OSM	qPCR	CAAGGCCTG-GATGTTCCTAA CCAGACCTCTCCAAATCCTG	This study
OSMRβ	Semiquantitative PCR	GGCA-CAGAGGGTGGATTCTC GTGTTCATCCGGAGTCGTGA	This study
TGFA	qPCR and semiquantitative PCR	TGTGTCTGCCATTCTGGGTA GACCTGGCAGCAGTGTATCA	This study
Tubulin	Semiquantitative PCR	AAGTGACAAGACCATTGGGGGAGG GGGCATAGTTATTGGCAGCATC	Markus Hutterer (Hutterer et al., 2008)

7. Cell culture

7.1 General cell culture techniques

Cell lines were grown in a humidified 93 % air, 7 % CO_2 incubator (Heraeus B 5060 EC-CO2, Heraeus, Hanau) at 37 °C and routinely assayed for mycoplasma contamination using a bisbenzimide staining kit (Sigma). Before seeding, cells were counted with a Z1 Coulter™ Particle Counter (Beckman Coulter, Krefeld).

7.2 Monocyte isolation

Peripheral blood was collected from healthy human donors after obtaining informed consent in accordance with the guidelines of the local ethics committee. 15 ml of EDTA-treated blood were layered over a Ficoll-Paque™ PLUS column (GE Healthcare) and centrifuged at 400 g for 30 minutes, at 18 °C. Leukocytes were washed twice with ice-cold PBS and transferred into RPMI containing 10 % heat-inactivated fetal bovine serum and 5 % active human serum. Following adherence to gelatine-coated culture plates (Sigma) that had been freshly precoated with human plasma, monocytes were washed 5 times with warm washing buffer (RPMI and PBS; 1:1), then detached using 5 mM EDTA in washing buffer. Cells were collected, centrifuged at 400 g for 15 minutes at 4 °C then washed twice with ice-cold washing buffer. PBMC were plated at a density of 1.0×10^6 cells/ml in 6 well culture plates (Corning, USA) in monocyte culture medium (RPMI supplemented with 5 % normal human male AB serum, Sigma).

Alternatively, CD14$^+$ monocytes were isolated from fresh blood samples using magnetic nanobeads coated with a CD14 specific antibody, according to the manufacturer's instructions (Miltenyi Biotech).

7.3 Macrophage differentiation

Following isolation, PBMC were cultured in monocyte culture medium for 4 days. Subsequently, cells were washed 3 times with RPMI and received fresh culture medium. Between day 4 and 10, medium was changed every third day. After seven days of culture, macrophages had completed spontaneous differentiation.

7.4 Monocyte/macrophage priming

To obtain media for PBMC/MΦ priming experiments, cells were plated into 15 cm culture plates, using their respective culture media. After 24 hrs, 60 % confluent cells were washed 3 times with PBS and incubated in 20 ml monocyte culture medium for 24 hrs. Conditioned media were collected, filtered through a 0.22 μm filter (Millipore, USA), shockfrozen and stored at -70 °C. For priming of PBMC/MΦ, a 1:1 mixture of conditioned medium and fresh monocyte culture medium was used. Priming of PBMC was done for 24 hrs immediately after isolation. For short-time priming of differentiated macrophages, cells were incubated in control medium or priming medium for 24 hrs from day 10 to 11. For long-time priming, macrophages were incubated in control medium or priming medium from day 4 to 10, and medium was changed every third day. At day 10 cells received fresh control or priming medium for 24 hrs.

8.   Protein analytical methods

8.1   Cell lysis

Cells were lysed on ice with a buffer containing 50 mM HEPES (pH 7.5), 150 mM NaCl, 1 % Triton X-100, 1 mM EDTA, 10 % glycerol, 10 mM $Na_4P_2O_7$, 2 mM Na_3VO_4, 10 mM NaF, 1 mM PMSF and 10 µg/ml aprotinin. Lysates were precleared by centrifugation at 17,000 g, 4 °C for 10 minutes.

8.2   Determination of protein concentration in cell lysates

The Micro BCA Protein Assay Kit (Pierce, Sankt Augustin) was used according to the manufacturer's recommendations.

8.3   Immunoprecipitation of proteins

An equal volume of HNTG buffer was added to the precleared cell lysates that had been adjusted for equal protein concentration. Proteins of interest were immunoprecipitated using the respective antibodies and 20 µL of protein A- or G-Sepharose for 4 hrs at 4°C. Precipitates were washed four times with 1 ml of HNTG buffer, suspended in 3 × Laemmli buffer, boiled for 5 minutes, and subjected to SDS-PAGE.

8.4   SDS-polyacrylamide-gel electrophoresis (SDS-PAGE)

SDS-PAGE was conducted as described previously (Laemmli, 1970). The following proteins were used as molecular weight standards:

Protein	MW (kDa)	Protein	MW (kDa)
Myosin	205.0	Ovalbumin	42.7
ß-Galaktosidase	116.2	Carboanhydrase	29.0
Phosphorylase b	97.4	Trypsin inhibitor	21.5
BSA	66.2	Lysozyme	14.4

8.5   Coomassie staining of polyacrylamide gels

Polyacrylamide gels were stained with Coomassie-brilliant-blue G-250 using a colloidal staining method. In brief, gels were fixed in 12 % TCA solution for one hour and stained thereafter over night in Coomassie-brilliant-blue solution (0.1 % Coomassie-brilliant-blue G-250, 2 % H_3PO_4, 10 % $(NH_4)_2SO_4$, 20 % methanol). Destaining was performed in 25 %

methanol for 2 hrs. For drying, gels were fixed between two cellophane foils and dried in a fan heater.

8.6 *Transfer of proteins onto nitrocellulose membranes*

For immunoblot analysis proteins were transferred to nitrocellulose membranes (Gershoni and Palade, 1982) for 2 h at 0.8 mA/cm^2 using a "Semidry"-Blot device in the presence of Transblot-SD buffer. Following transfer, proteins were stained with Ponceau S (2 g/l in 2 % TCA) in order to visualize and mark standard protein bands. The membrane was destained in water.

8.7 *Immunoblot detection*

After electroblotting the transferred proteins were bound to the surface of the nitrocellulose membrane, providing access for reaction with immunodetection reagents. Remaining binding sites were blocked by immersing the membrane in 1x NET, 0.25 % gelatine for at least 1 hr. The membrane was then probed with primary antibody (typically overnight). Antibodies were diluted 1:500 to 1:2000 in 1 x NET, 0.25 % gelatine. The membrane was washed 3 x 5 min in 1 x NET, 0.25 % gelatine, incubated for 1 hr with secondary antibody and washed again 3 x 10 min. Antibody-antigen complexes were identified using horseradish peroxidase coupled to the secondary anti-IgG antibody. Luminescent substrates were used to visualize peroxidise activity. Signals were detected with X-ray films. Membranes were stripped of bound antibody by shaking in strip-buffer for 1 hr at 50°C. Stripped membranes were blocked and reprobed with a different primary antibody to confirm equal protein loading.

9. Gene Expression Analysis

9.1 *RT-PCR*

Total RNA was isolated using the Quiagen RNeasy Mini Kit (Quiagen) and reverse-transcribed with AMV reverse transcriptase (Roche). Semiquantitative PCR was performed using the ReadyMix™ redtaq™ PCR reaction mix (Sigma). PCR products were subjected to electrophoresis in 2 % agarose gels and were visualised by ethidium bromide staining.

9.2   Quantitative PCR

Quantitative PCR was performed on a StepOnePlus™ instrument using the Fast SYBR® Green Master Mix (Applied Biosystems). Data analysis and calculation of 95 % confidence intervals was performed using the StepOne™ Software version 2.0.

10.   Analysis of whole cell-based assays

10.1   Flow cytometry

Following detachment, cells were fixed with 2 % paraformaldehyde. All further steps were carried out on ice. Fc receptors were blocked by a 10 minute incubation step with mouse IgG$_{2B}$ or donkey IgG. Cells were incubated with primary antibodies for 45 minutes, washed twice with PBS + 2 % FCS and incubated with fluorescence-labelled secondary antibodies for 45 minutes. After 2 washing steps, cells were analysed in a FACSCalibur flow cytometer (BD Biosciences). Data analysis was done using CellQuest Pro software (BD Biosciences). CD14/CD64 double staining was performed with prelabelled BD Oncomark CD14 FITC/CD64 PE mouse monoclonal antibodies (BD Biosciences). The Simultest™ Control prelabelled antibody mixture was used. Epiregulin was stained with a PE-labelled mouse monoclonal antibody and PE-labelled mouse isotype control (R&D Systems). Scavenger Receptor A 1 staining was done with a mouse monoclonal primary antibody (R&D Systems) and a PE-labelled donkey anti-mouse IgG secondary antibody F(ab)$_2$ fragment (Jackson ImmunoResearch). Mouse isotype control antibody was from R&D Systems, donkey IgG from Jackson ImmunoResearch.

10.2   Migration assays

Unless otherwise stated, cells were plated into transwell migration inserts (BD Biosciences) using RPMI + 0.1 % BSA. The lower compartments contained either serum-free MΦ supernatants, culture media or RPMI + 0.1 % BSA with or without OSM/HB-EGF. Where indicated, a 1 hr preincubation with neutralising antibodies, DMSO or AG1478 was performed prior to cell plating. At the end of the migration period, cells were fixed and stained with 20 % methanol, 0.5 % crystal violet and cotton swabs were used to remove the cells from the upper side of the membrane. An Axio Observer.A1 microscope (Carl Zeiss, Jena) was used to record 5 micrographs per well. Photoshop CS4 (Adobe, USA) and a proprietary script were used for automated quantification of migration. 5 x 10^4 SCC-9 cells were allowed to migrate for 6 hrs (chemotaxis) or 17 hrs (intrinsic motility). 1.5 x 10^5 MCF 10A cells were allowed to migrate for 17 hrs. 1.5 x 10^5 MCF7 cells were allowed to migrate for 48 hrs.

10.3 Proliferation assays

1.5×10^5 cells were plated per well in 6 well culture plates (MDA-MB-231, MDA-MB-435S, MDA-MB-468, T-47D, MCF7) or 2.5×10^4 cells were plated per well in 12 well culture plates (MCF 10A). At the indicated timepoints, cells were detached using Trypsin/EDTA (0.05 %/0.02 % in PBS; PAA) and counted with a Z1 Coulter™ Particle Counter (Beckman Coulter, Krefeld).

11. Enzyme-linked immunosorbent assays

Nunc MaxiSorp™ 96 well plates (Thermo Fisher Scientific, USA) were coated with capture antibodies at room temperature overnight. Plates were washed 4 times with washing buffer containing 0.05 % Tween$_{20}$ in PBS, pH 7.4. Next, plates were incubated for 2 hrs at room temperature with 150 µl/well blocking buffer containing 5 % sucrose, 1 % BSA in PBS. Following 4 washing steps, 100 µl of 1:10 diluted samples or concentration standard were added per well. Concentration standards were prepared in PBS using 10 % control plasma or culture medium. After 2 hrs of incubation at room temperature, plates were washed 6 times and 100 µl of biotinylated detection antibodies were applied for 2 hrs. Samples were washed 6 times, incubated with 50 ng/ml peroxidase-streptavidin (Jackson ImmunoResearch) for 15 minutes, followed by 6 further washing steps. The colorimetric reaction was performed in 100 µl of TMB substrate (Calbiochem) and stopped by addition of 50 µl 1 M H_2SO_4. The optical densities at 405 and 570 nm were measured with a spectrophotometer. HB-EGF capture was performed using a monoclonal antibody (a gift from U3 Pharma, Martinsried) or an affinity-purified goat polyclonal antibody (R&D Systems), with very similar results. OSM and AREG were captured using monoclonal antibodies from R&D Systems. A goat polyclonal anti-TGFα capture antibody and all biotinylated detection antibodies were from R&D Systems. Antibody and streptavidin dilutions were prepared using 1 % BSA in PBS.

12. SILAC experiments and MS-analysis

12.1 MAD-NT membrane preparation

Cells were scraped in PBS, pelleted by centrifugation (400 g, 5 minutes, 4 °C) and incubated in hypotonic buffer (20 mM HEPES pH 7.2, 10 mM KCl, 1.5 mM $MgCl_2$, 0.1 mM EGTA, 10 mM $Na_4P_2O_7$, 2 mM Na_3VO_4, 10 mM NaF, 1 mM PMSF and 10 µg/ml aprotinin) for 30 minutes at 4 °C. Cells were broken using a Dounce homogenizer (30 strokes) and nuclei were pelleted by centrifugation (750 g, 10 minutes, 4 °C). The supernatant was subjected to

ultracentrifugation at 1×10^5 g for 1 hr at 4 °C to separate the membrane (pellet) from the cytosolic fraction (supernatant). The pellet was washed with hypotonic buffer and solubilised with membrane solubilisation buffer (50 mM HEPES pH 7.5, 1 % Triton X-100, 150 mM NaCl, 10 mM EDTA, 10 % glycerol, 10 mM $Na_4P_2O_7$, 2 mM Na_3VO_4, 10 mM NaF, 1 mM PMSF and 10 μg/ml aprotinin), followed by centrifugation at 1×10^5 g for 1 hr at 4 °C.

12.2   SILAC labelling of MDA-MB-231 cells

Isotope labelling was performed according to Mann and colleagues (Ong et al., 2002). Cells were grown for seven days in media containing either normal L-arginine (Arg-0) and L-lysine (Lys-0) (Sigma), L-arginine-U-$^{13}C_6$$^{14}N_4$ (Arg-6) and L-lysine $^2H_4$ (Lys-4) or L-arginine-U-$^{13}C_6$-$^{15}N_4$ (Arg-10) and L-lysine-U-$^{13}C_6$-$^{15}N_2$ (Lys-8) (Euriso-Top, France). MAD-NT cells were grown in light medium (Arg-0, Lys-0) and serum-free supernatants were collected, cleared of debris by centrifugation at 1,000 g, filtered through a 0.22 μm filter and concentrated using a 50 kDa cutoff filter. The retentate was used to stimulate heavy labelled (Arg-10, Lys-8) MDA-MB-231 cells for 10 minutes. Medium labelled (Arg-6, Lys-4) MDA-MB-231 cells were stimulated in parallel with control medium.

12.3   Cell lysis and anti-pTyr immunoprecipitation

After stimulation, cells were lysed for 20 minutes in ice-cold lysis buffer (50 mM Tris-HCl pH 7.5, 150 mM NaCl, 1 % NP40, 0.1 % sodium deoxycholate, 1 mM EDTA, 1 mM Na_3VO_4, 1 mM PMSF, 0.1 μg/ml aprotinin, 10 mM NaF). Lysates were precleared by centrifugation at 17,000 g for 15 minutes. Protein amount determination was performed using the BCA assay (Pierce). Cell lysates derived from different SILAC states were mixed in equal amounts per label after determination of protein amounts. For immunoprecipitation, 200 μg anti-pTyr 4G10 antibody (produced in-house) and 40 μl protein A-Sepharose (GE Healthcare) were added to mixed cell lysates containing up to 20 mg total protein of each label and incubated for 4 hrs at 4 °C. Precipitates were washed four times with lysis buffer and precipitated proteins were eluted with LDS-sample buffer (Invitrogen).

12.4   In-gel protein separation and digestion

Proteins were separated by SDS-PAGE using NuPAGE Novex Bis-Tris gels (Invitrogen) according to the manufacturer's instructions. The gel was stained with Coomassie blue using the Colloidal Blue Staining Kit (Invitrogen). The resulting lane was cut into 12 slices (pTyr proteome analysis), 9 slices (MAD-NT secretome analysis), or 10 slices (MAD-NT membrane proteome) which were then subjected to in-gel digestion essentially performed as described (Shevchenko et al., 1996). Gel slices were cut into small cubes and washed with 50 mM ammonium bicarbonate (ABC)/50 % ethanol until the cubes were fully destained.

Gel cubes were dehydrated with ethanol and re-hydrated with 50 mM ABC containing 10 mM DTT. Proteins were reduced for 1 hr at 56 °C. Resulting free thiol groups were then alkylated by adding 55 mM iodoacetamide in 50 mM ABC for 1 hr at 25 °C in the dark. Gel pieces were washed twice with a 50 mM ABC/50 % ethanol solution, dehydrated with 100 % ethanol and dried in a vacuum concentrator. Each gel fraction was rehydrated in 50 mM ABC solution containing 0.4 µg trypsin and samples were incubated at 37 °C over night. Supernatants were transferred to new tubes and residual peptides were extracted out of the gel pieces by double incubation with 30 % MeCN in 3 % TFA and double incubation with 100 % MeCN. All extracts were combined and MeCN was evaporated in a vacuum concentrator. Subsequently, samples were desalted using home-made RP-C$_{18}$ STAGE Tip columns (Rappsilber et al., 2003) and the eluted peptides were used for MS analysis.

12.5 NanoLC-MS/MS analysis

All peptide samples were separated by online reverse phase (RP) nanoscale capillary liquid chromatography (nanoLC) and analysed by electrospray tandem mass spectrometry (ES MS/MS). Using an Agilent 1100 nanoflow system (Agilent Technologies, USA), samples were injected onto a 15 cm RP, fused-silica capillary column (inner diameter 75 µM, packed in-house with 3 µm ReproSil-Pur C18-AQ media (Dr. Maisch, Ammerbuch-Entringen). The LC setup was connected to an LTQ Orbitrap mass spectrometer (Thermo Fisher Scientific) equipped with a nano-electrospray ion source (Proxeon Biosystems, Denmark). Loaded peptides were eluted with 140 minute gradients from 5 to 40 % MeCN in 0.5 % acetic acid. Data-dependent acquisition was performed on the LTQ-Orbitrap using the Xcalibur 2.0 software in the positive ion mode. The instrument was recalibrated in real-time by co-injection of an internal standard from ambient air into the C-trap ("lock mass option") (Olsen et al., 2005). Survey spectra were acquired with a resolution of 60,000 in the orbitrap. In parallel, up to five of the most intense multiple-charged ions per cycle were isolated, fragmented and analysed in the LTQ part of the instrument. Ions selected for MS/MS were dynamically excluded for 90 s after fragmentation.

12.6 Identification and quantification of peptides and proteins

Mass spectra were processed using the MaxQuant software (version 1.0.12.0) (Cox and Mann, 2008), in combination with the Mascot search engine version 2.2.0 (Matrix Science, UK). For peptide identification a concatenated forward and reversed International Protein Index protein sequence database (IPI version 3.37, human) was queried. The mass tolerance for the precursor ions and for fragment ions was set to 7 ppm and 0.5 Da, respectively. Cysteine carbamidomethylation was searched as a fixed modification, whereas oxidation on methionine and N-acetylation (Protein) were considered as variable modifications. The enzyme specificity was set to trypsin and cleavage N-terminal of proline and between

aspartic acid and proline. A maximum of up to 3 missed cleavages was allowed. The results of the Mascot search were further processed and statistically evaluated by MaxQuant. For peptide and protein identification the maximum peptide and protein false discovery rate (FDR) was set to 1 %. Proteins were considered to be identified with at least two assigned peptides including one unique peptide. For quantitation experiments at least 2 different peptides were required for each quantified protein. All proteins that were induced ($p<0.01$) in MDA-MB-231 by conditioned media from MAD-NT cells together with proteins from the MAD-NT secretome analysis were uploaded into the STRING 8.0 database (Jensen et al., 2009) and the following settings were used to analyse interaction networks: interactions from database entries and experiments only, high level of confidence ($p>0.9$) and up to 10 interactions per node. The resulting protein network was exported and further analysed using Cytoscape 2.7.0 (Shannon et al., 2003). Proteins found in the BioCarta Met pathway (BioCarta, San Diego, CA) and Kegg Jak-Stat pathway (Kanehisa, 1997) were highlighted. Annotations of protein lists to pathway databases were performed in the DAVID 8.0 database (Dennis et al., 2003; Huang da et al., 2009).

13.   Patient sample collection

Plasma samples of human donors were obtained in accordance with the guidelines of the local ethics committee and after obtaining informed consent. Patient samples were collected at the Red Cross Hospital, Munich. Samples from control donors were collected at the Red Cross Hospital and at the Max Planck Institute of Biochemistry (Martinsried). After collection of peripheral blood into heparinized tubes, cells were pelleted at 2,500 g, 4 °C for 15 minutes. Plasma was cleared at 17,000 g, 4 °C for 15 minutes, aliquoted, shockfrozen and stored at -70 °C. Prior to ELISA, samples were heat-inactivated and cleared at 17,000 g, 4 °C for 15 minutes.

14.   Statistical analysis

Two-tailed Mann-Whitney U-Tests were used for pPCR and ELISA experiments. For immunoblot, motility and chemotaxis experiments we used the two-tailed Student's T-Test. Differences were considered significant when $p<0.05$. Data are presented as means ± SEM or SD.

IV. RESULTS

1.   MAD-NT cells are a model of spontaneously differentiating monocytes

HL-60 leukaemia cells represent a model system to study the differentiation of promyelocytes into monocytic and granulocytic lineages (Collins, 1987; Gallagher et al., 1979). We have isolated MAD-NT (macrophage differentiation, non-terminal), an HL-60 clone that has undergone spontaneous monocytic differentiation. Approximately 50 % of cells adhere to tissue culture dishes and display the irregular morphology of adherent monocytes (Figure 4A). Sub-passaging either the adherent or floating cell population generates the same proportions of adherent and floating cells. We were interested in establishing a cell model for the identification of monocyte-secreted ligands. Even in the absence of specific stimuli, adherent MAD-NT express the monocyte-specific marker CD64 (Figure 4B) and EGF-like module receptor 1 (*EMR1*) transcripts, the human homologue of the mouse F4/80 macrophage marker (Figure 4C).
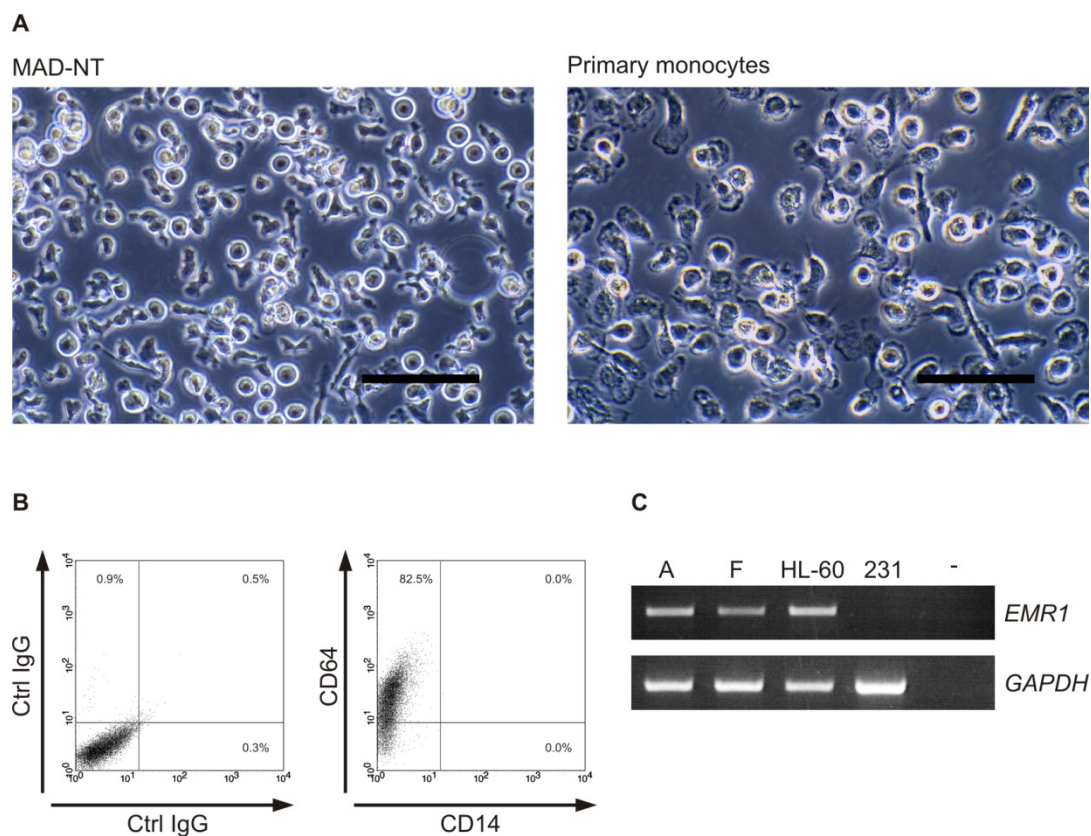

FIGURE 4. MAD-NT cells resemble adherent primary monocytes and express monocyte markers CD64 and EMR1. (A) Morphology of MAD-NT and primary human monocytes at day 3 post-isolation. Scale bar: 100 μm. **(B)** MAD-NT cells present CD64. Flow cytometry of MAD-NT cells double-stained with CD14 FITC/CD64 PE or control antibodies. **(C)** MAD-NT cells express *EMR1*. RT-PCR of adherent (A), floating (F) MAD-NT and parental HL-60 cells. MDA-MB-231 breast carcinoma cells (231) served as a control. -: water control.

To get a broader overview of the lineage markers present in the membrane proteome of adherent MAD-NT cells, we performed mass spectrometry of membrane fractions. Analysis confirmed the expression of CD64 seen in flow cytometry, and found further lineage markers: from general leukocyte markers like CD45, CD54 and CD18, to myeloid markers like CD33 and CD11c. We also identified monocyte and macrophage markers, like CD11a, CD11b, the macrophage mannose receptor 2, macrophage-capping protein and monocyte/neutrophil elastase inhibitor (Table 1). Together, these data indicate that adherent MAD-NT cells represent a valid model system for spontaneously differentiating monocytes

TABLE 1. Differentiation markers identified by mass spectrometric analysis of MAD-NT membrane fractions.

Protein	Expression	Peptides
CD64; IgG Fc receptor I	Macrophages; monocytes; neutrophils	1
CD280; Macrophage mannose receptor 2	Macrophages; non-hematopoietic cells	2
Macrophage-capping protein	Macrophages	10
CD11a; Integrin alpha-L	Macrophages; monocytes; granulocytes	3
CD11b; Integrin, alpha M	Macrophages; monocytes; granulocytes	5
CD11c; Integrin alpha-X	Myeloid cells	17
Myeloid-associated differentiation marker	Myeloid cells	2
CD33; Myeloid cell surface antigen	Myelomonocytic lineage	2
Monocyte/neutrophil elastase inhibitor	Monocytes; neutrophils	3
Myeloid cell nuclear differentiation antigen	Monocytes; granulocytes; myeloid cells	2
CD31; PECAM-1	Monocytes; neutrophils; platelets	2
CD36L2; Lysosome membrane protein 2	Monocytes; platelets	5
CD35; Complement receptor type 1	Monocytes; B cells; neutrophils; eosinophils	20
CD18; Integrin beta-2	Leukocytes	24
CD49d; Integrin alpha-4	Leukocytes	7
CD45; Leukocyte common antigen	Leukocytes	47
CD54; ICAM-1	Leukocytes	8
MOP-4; Monocyte protein 4	Leukocytes; non-hematopoietic cells	8
MOP-5; Monocyte protein 5	Leukocytes; non-hematopoietic cells	5
CD29; Integrin, beta 1	Widely expressed	10
CD44; Phagocytic glycoprotein I	Widely expressed	7

2.   MAD-NT monocytes secrete oncostatin-M

In a first set of functional studies, we tested whether MAD-NT-conditioned medium (MAD-CM) activated the oncogenic EGF receptor and STAT3 pathways in tumour cell lines. The panel of tumour lines included MDA-MB-231, T-47D, MCF7, MDA-MB-468 and MDA-MB-435S mammary carcinoma, as well as SCC-9 squamous cell carcinoma cell lines. EGFR family members were not activated by MAD-CM in any of the tested cell lines (data not shown). However, stimulation with MAD-CM resulted in strongly increased pSTAT3 levels in all tested cell lines (Figure 5A). We enriched the pSTAT3-inducing activity in the retentate of a 50 kDa cutoff filter by fractionation of serum-free (SF) MAD-CM (50 kDa$^+$, Figure 5B). This fraction was subjected to mass spectrometric analysis.
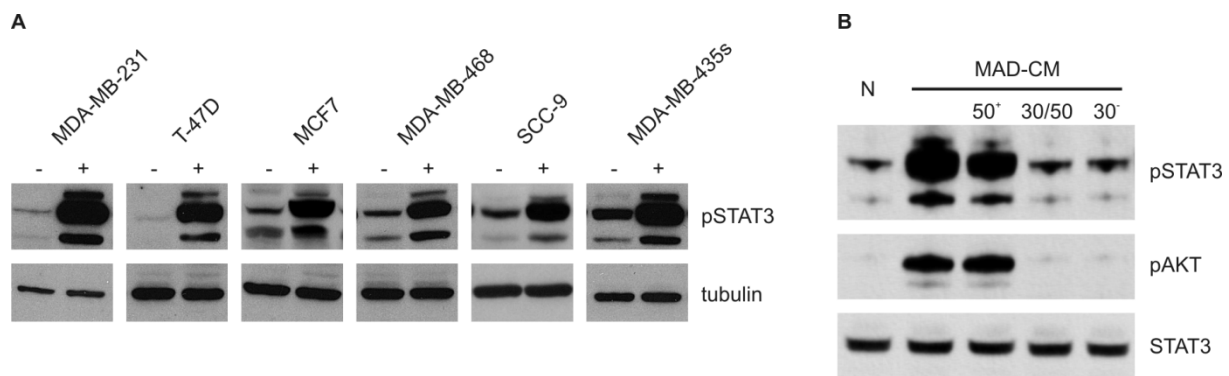

FIGURE 5. MAD-NT supernatant activates STAT3 in carcinoma cells. (A) Tumour cell lines were stimulated with control (-) or MAD-NT-conditioned medium (+). Cell lysates were immunoblotted using antibodies against pSTAT3 and tubulin. **(B)** A pSTAT3 and pAKT inducing activity is enriched in the 50 kDa$^+$ fraction of serum-free MAD-CM. Serum-free MAD-CM was fractionated using 50 kDa and 30 kDa cutoff filters. MDA-MB-231 cells were stimulated with the indicated fractions, and pSTAT3, pAKT and STAT3 levels were visualised. N: culture medium; 50$^+$: retentate of the 50 kDa cutoff filter, 30-50: 30 kDa – 50 kDa fraction, obtained after fractionation of the 50 kDa flowthrough using a 30 kDa cutoff filter; 30$^-$: flowthrough of the 30 kDa cutoff filter.

Hepatocyte growth factor was identified as one of the 22 secreted signalling molecules (Table 2), already shown to be released by the parental HL-60 cells (Nishino et al., 1991). Apart from HGF, we identified a set of proteins whose secretion by human monocytes had not been described yet. These include hepatoma-derived growth factor (HDGF), the secreted metalloprotease ADAMTS-1 and the proangiogenic factor CYR61. As possible STAT3 activator in our system we identified oncostatin-M, a member of the IL-6 family (Rose and Bruce, 1991; Zarling et al., 1986).

TABLE 2. Proteins identified by mass spectrometric analysis of MAD-NT supernatant (50 kDa⁺ fraction).

Gene	Protein name	Unique peptides
HGF	Hepatocyte growth factor precursor	47
OSM	Oncostatin-M precursor	2
HDGF	Hepatoma-derived growth factor	10
CYR61	Cysteine-rich angiogenic inducer 61	2
ADAMTS1	A disintegrin and metalloproteinase with thrombospondin motifs 1	2
TGFB1	Transforming growth factor beta-1 precursor	3
STC2	Stanniocalcin-2 precursor	3
CCL5	C-C motif chemokine 5 precursor	3
SCG2	Secretogranin-2 precursor	2
IL12B	Interleukin-12 subunit beta precursor	8
BMP11	Bone morphogenetic protein 11	2
TNFSF13B	Tumor necrosis factor ligand superfamily member 13B	2
IL25	Interleukin-25	4
IGF2	Insulin-like growth factor II precursor	2
IL18	Interleukin-18 precursor	3
SDF2	Stromal cell-derived factor 2 precursor	2
MIF	Macrophage migration inhibitory factor	4
GRN	Granulins precursor	4
SPINT1	Hepatocyte growth factor activator inhibitor type 1	3
CCL4	C-C motif chemokine 4 precursor	2
SCYE1	Endothelial monocyte-activating polypeptide 2	9
CXCL10	C-X-C motif chemokine 10 precursor	2

Next, we assessed the presence of IL-6 family ligand and receptor transcripts in a variety of epithelial and mononuclear cells. The ligand we had identified by mass spectrometric analysis of MAD-NT supernatants, oncostatin-M, was exclusively expressed by mononuclear cells, namely primary macrophages and MAD-NT cells. In contrast, *IL6* expression was restricted to cells of epithelial origin, here MDA-MB-231 breast carcinoma and SCC-9 squamous cell carcinoma lines. *LIF* was expressed by epithelial as well as mononuclear cells. Transcripts for both OSM specific receptors, *OSMRβ* and *LIFR*, were exclusively expressed by epithelial cells, while *IL6R* transcripts were predominantly expressed by mononuclear cells. As expected, *GP130*, the common signal transducing unit of the IL-6 family receptors, was ubiquitously expressed in the panel of tumour cell lines. In addition, we detected *GP130* transcripts in MCF 10A mammary hyperplastic cells, primary human

mammary epithelial cells (HMEC), *in vitro* differentiated primary human macrophages and MAD-NT cells (Figure 6).
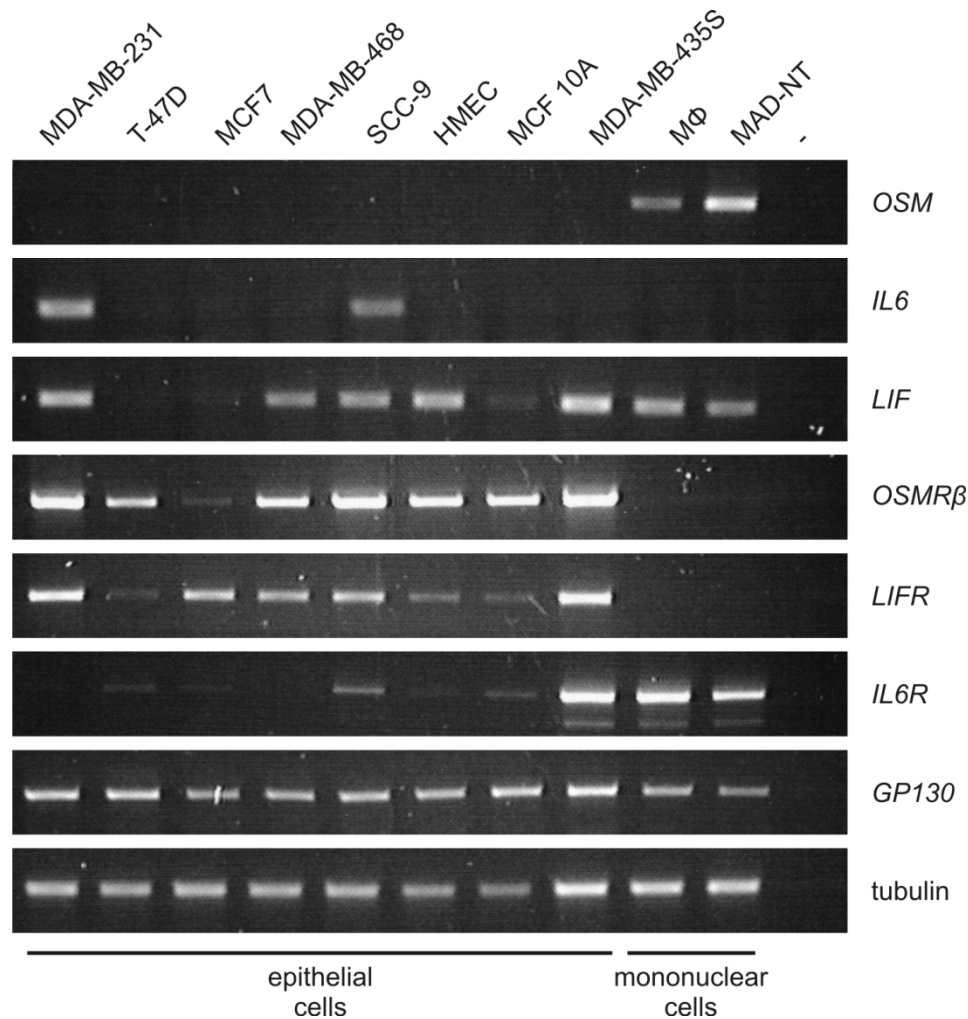

FIGURE 6. Ligands and receptors of the IL-6 family are differentially expressed in epithelial and mononuclear cells. *OSM* is exclusively expressed by mononuclear cells, while expression of both OSM specific receptors, *OSMRβ* and *LIFR*, is restricted to cells of epithelial origin. RT-PCR of IL-6 family ligands and receptors. -: water control.

Next, we validated proteins identified by mass spectrometric analysis of MAD-NT supernatants. The soluble metalloprotease ADAMTS-1 is being reviewed as metastasis promoter (Liu et al., 2006; Lu et al., 2009). We immunoprecipitated full-length ADAMTS-1 protein from MAD-NT supernatant, confirming its secretion by our monocytic cell model (Figure 7A). To test whether MAD-NT cells secrete an active form of HGF, we stimulated MDA-MB-231 cells with MAD-CM and immunoprecipitated the hepatocyte growth factor receptor (HGFR). Incubation with MAD-CM leads to strongly increased levels of tyrosine-phosphorylated HGFR, which were abrogated by an antibody blocking HGF function. Analysis of MDA-MB-231 cell lysates revealed that MAD-CM also increased pAKT and pSTAT3 levels. Neutralisation of HGF function abrogated AKT phosphorylation, but had no effect on pSTAT3 levels. These findings indicate that MAD-NT secrete relevant amounts of

active HGF, which induces phosphorylation of HGFR and AKT in MDA-MB-231 cells. However, the phosphorylation of STAT3 elicited by MAD-CM is not caused by MAD-NT-secreted HGF (Figure 7B).

The presence of OSM protein in the MAD-NT secretome and the observed transcription profiles point to MAD-NT-secreted oncostatin-M as the relevant STAT3 activator in the tested tumour cell lines. MAD-NT supernatants contained considerable amounts of OSM (Figure 7C). Like MAD-CM, culture medium supplemented with recombinant OSM induced STAT3 phosphorylation in MDA-MB-231 cells. In either assay, STAT3 phosphorylation was completely abrogated by an antibody blocking OSM function (Figure 7D).
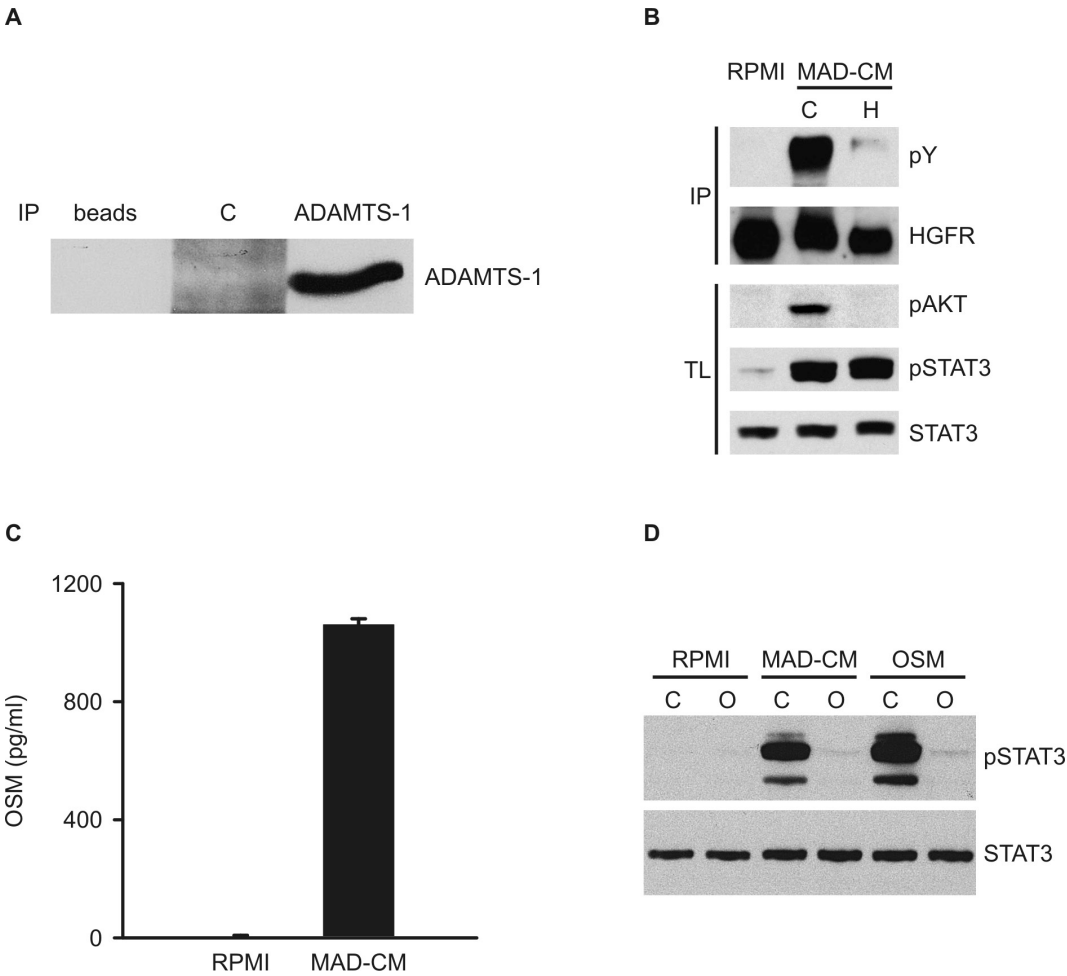

FIGURE 7. Oncostatin-M secreted by MAD-NT monocytes activates STAT3 in MDA-MB-231 cells. (A) MAD-NT cells secrete the soluble metalloprotease ADAMTS-1. Immunoprecipitation (IP) of MAD-CM was performed with control beads, a control antibody (C) or an antibody specific for ADAMTS-1, followed by Western blot analysis. **(B)** MAD-NT-secreted HGF induces phosphorylation of HGFR and AKT in MDA-MB-231 cells. Cells were stimulated with RPMI or MAD-CM, after preincubation with an HGF blocking antibody (H) or a control Ig (C). Following cell stimulation and lysis, HGFR was immunoprecipitated with a specific antibody. Phosphotyrosines (pY), HGFR, pAKT, pSTAT3 and STAT3 were visualised in immunoprecipitates (IP) and total cell lysates (TL). **(C)** MAD-NT monocytes secrete OSM (ELISA). **(D)** OSM is the relevant STAT3 activator secreted by MAD-NT monocytes. MDA-MB-231 cells were stimulated with RPMI, MAD-CM or 1 ng/ml recombinant OSM, after preincubation with an OSM blocking antibody (O) or control Ig (C). pSTAT3 and STAT3 levels were examined by immunoblot analysis of cell lysates.
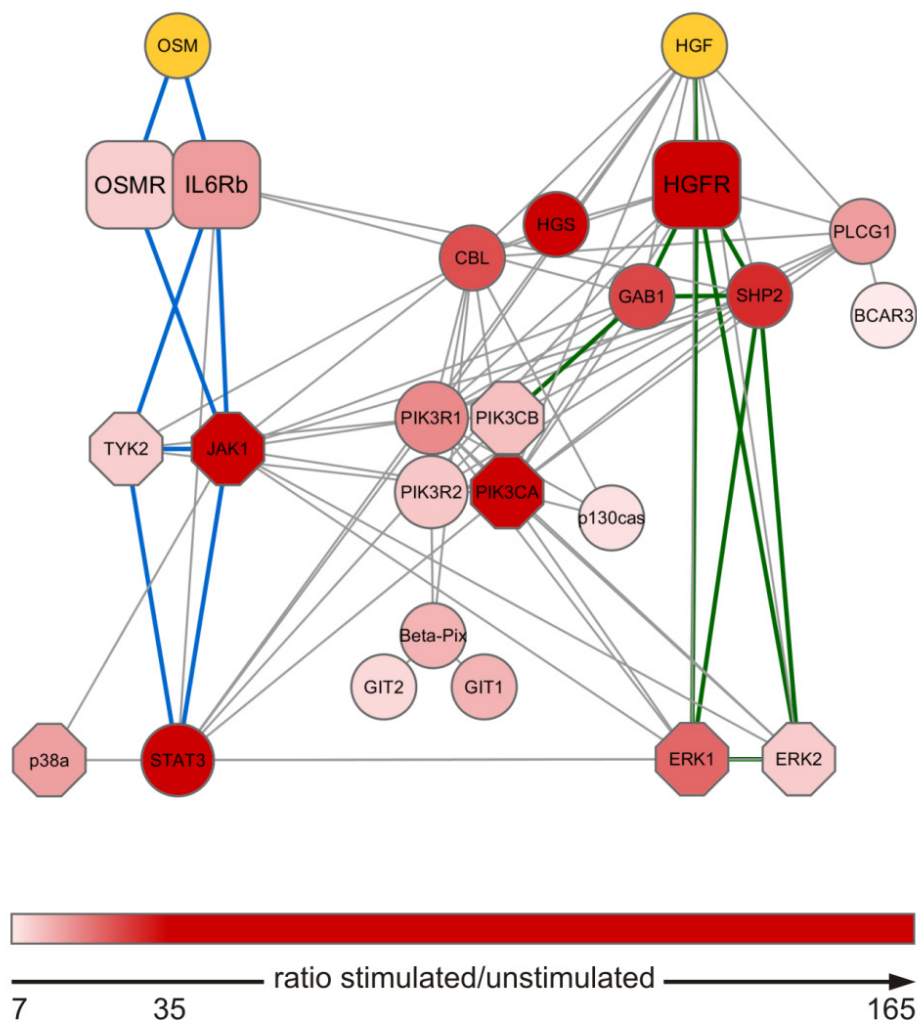
FIGURE 8. MAD-NT supernatant activates the OSMRβ-gp130 and HGF receptor pathways in MDA-MB-231 cells. Interaction network of proteins quantified by mass spectrometric phospho-proteome analysis. SILAC-labelled MDA-MB-231 cells were treated either with serum-free MAD-CM (50 kDa+ fraction) or control medium. Phosphotyrosine proteins were enriched and analysed in a mass spectrometer. Colour coding indicates the ratio of stimulated vs. control cells. In MAD-CM treated MDA-MB-231 cells, phosphorylated OSMRβ and gp130 were enriched by 10.7-fold and 16.5-fold, respectively. Downstream, pSTAT3 was enriched by 36.5-fold and the signal mediating kinases pTYK2 and pJAK1 were enriched by 10.7-fold and 36.5-fold, respectively. HGF present in the MAD-NT supernatant increased phospho-HGFR by 35.3-fold. In yellow: proteins identified by qualitative mass spectrometric analysis of MAD-CM.

To gain a deeper insight into the impact of monocyte-secreted factors on tumour cell signalling pathways, we performed a quantitative mass spectrometric analysis of the phosphotyrosine-regulated proteome of MDA-MB-231 cells stimulated by MAD-CM. To this end, isotope-labelled MDA-MB-231 cells (Ong et al., 2002) were treated with either control medium or SF MAD-CM (50 kDa+ fraction). Phosphotyrosine proteins were enriched and subjected to mass spectrometric analysis according to Mann and colleagues (Blagoev et al., 2004). Data analysis revealed that the oncostatin-M receptor beta pathway and the hepatocyte growth factor receptor pathway were the main phosphotyrosine-regulated

signalling pathways activated in MDA-MB-231 cells upon stimulation with the MAD-CM 50 kDa⁺ fraction (Figure 8). In detail, phosphorylated OSMRβ and gp130 were enriched 10.7-fold and 16.5-fold, respectively. Downstream, we detected enrichment of pSTAT3 (36.5-fold) and of the signal mediating kinases pTYK2 (10.7-fold) and pJAK1 (36.5-fold). HGF present in the MAD-NT supernatant led to a 35.3-fold enrichment of tyrosine-phosphorylated HGFR. These findings demonstrate that MAD-NT cells secrete OSM, which in turn induces STAT3 phosphorylation in the reporter cell line MDA-MB-231. OSM signalling is mediated via activation of the type II OSM receptor complex comprised of OSMRβ and gp130, followed by downstream phosphorylation of JAK1 and TYK2. In conclusion, MAD-NT-derived oncostatin-M is a potent STAT3 activator in a variety of carcinoma cell lines.

3. *In vitro* interaction model between tumour cells and primary mononuclear cells

To validate our findings from the MAD-NT model system, we designed an experimental setup based on the priming of primary human mononuclear cells with conditioned media from a panel of human tumour and nontransformed cells. In contrast to direct coculture, such priming experiments permit a thorough analysis of factors secreted by both cell types, on protein and transcript level. Figure 9 provides our model of tumour cell/mononuclear cell interaction, based on mutually secreted factors.
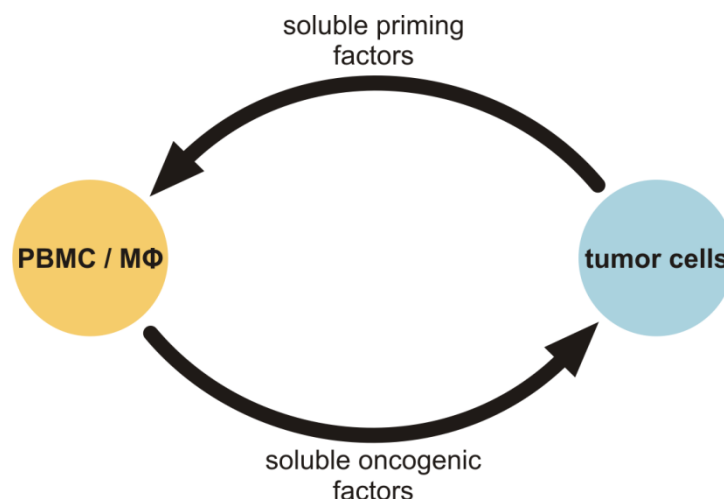

FIGURE 9. Interaction model between tumour cells and primary human mononuclear cells.

We assumed that, *in vivo*, chemotactic gradients of soluble, tumour-derived factors trigger the extravasation of PBMC in the vicinity of tumour cells, where they differentiate into TAM (Mantovani et al., 1995). This implies that tumour-primed PBMC already participate in the crosstalk between tumour cells and microenvironment. Following differentiation, TAM are

subject to long-term exposure to tumour-derived priming factors, and respond by releasing soluble oncogenic factors. To study the crosstalk mechanisms between tumour cells and mononuclear cells *in vitro*, we pursued three priming strategies: a) short-time priming of PBMC for 24 hrs to explore the effects of tumour-secreted factors on monocytes; b) short-time priming of *in vitro* differentiated macrophages for 24 hrs; c) to mimic long-time effects of tumours on TAM, we primed *in vitro* differentiated primary macrophages for seven days. Subsequent to priming, PBMC- or MΦ-conditioned media were used to stimulate reporter cells. MDA-MB-231 served as indicator of STAT3 activators present in the supernatants. SCC-9 cells are an established model for EGFR activation studies (Gschwind et al., 2002) and were used as indicators of EGFR agonists secreted by PBMC/MΦ. Our experimental approach is outlined in Figure 10.
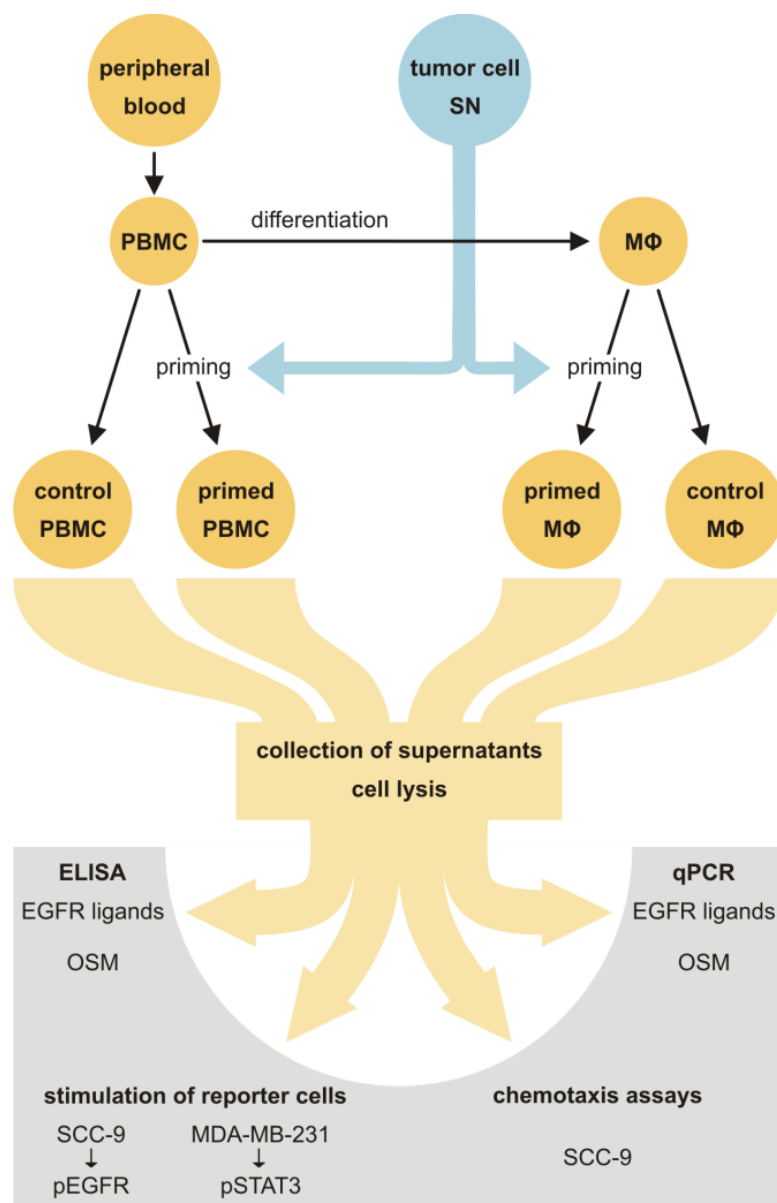

FIGURE 10. Experimental approach for the study of effects of tumour cell supernatants (SN) on primary human PBMC and *in vitro* differentiated MΦ.

In vitro, PBMC differentiate spontaneously to MΦ in the presence of human serum. We monitored scatter properties and expression of monocyte/macrophage markers CD64 and CD14 in PBMC and *in vitro* differentiated MΦ over a ten-day period. One day after isolation, the cell preparation contained 6-8 % lymphocytes and more than 90 % monocytes. At days seven and ten, the fraction of lymphocytes had decreased below 1 %. At day one, roughly 50 % of cells expressed CD64 and CD14. Upon differentiation, approximately 90 % of macrophages expressed CD64, irrespective of priming status. Priming with MDA-MB-231 cell supernatants induced higher levels of CD14 expression (Figure 11A).
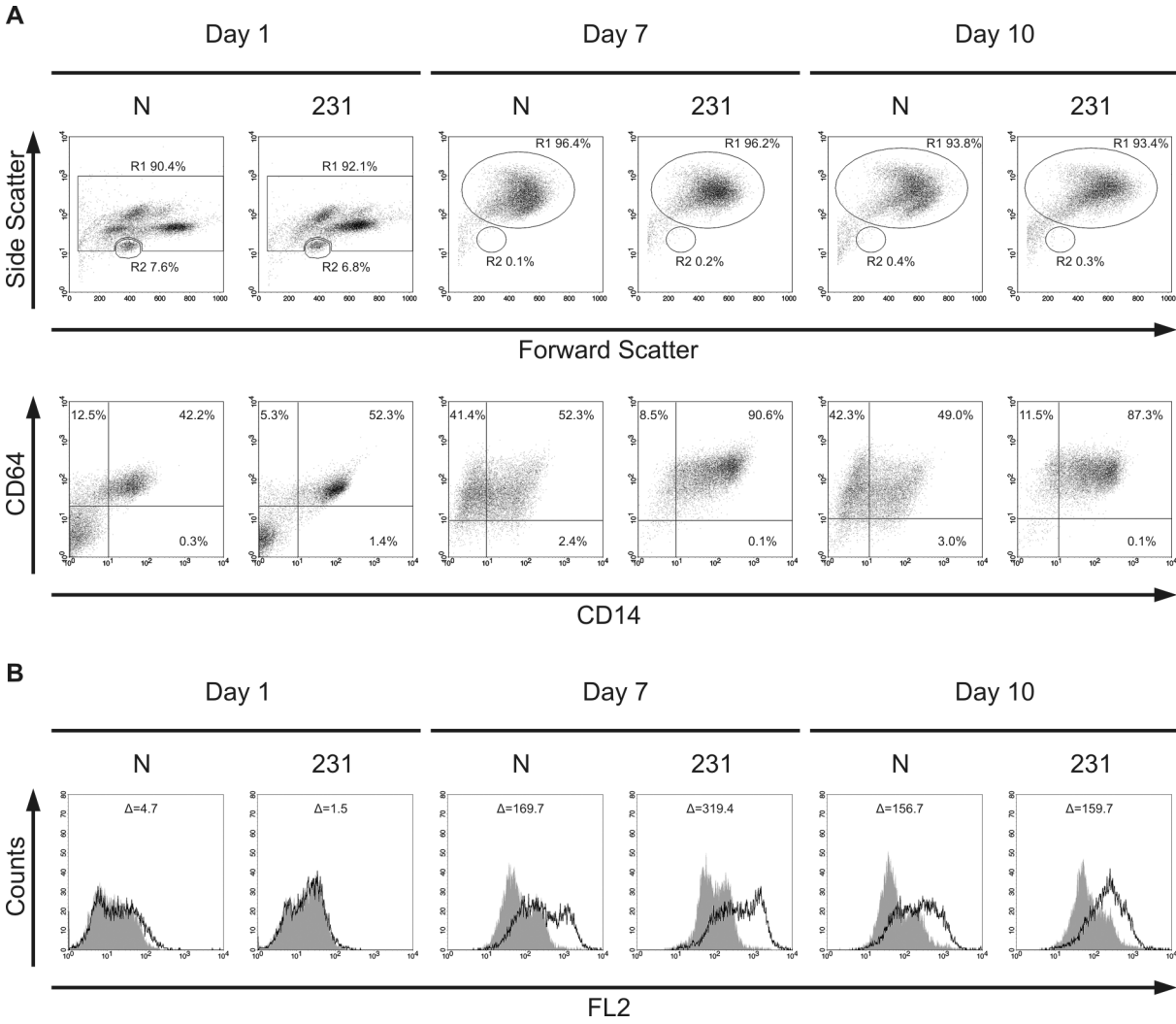

FIGURE 11. Human PBMC differentiate spontaneously to macrophages. (A) CD14 and CD64 expression patterns in PBMC and differentiated macrophages. Freshly isolated PBMC were treated with normal culture medium (N) or MDA-MB-231-conditioned medium (231) for 24 hrs. Alternatively, cells were allowed to differentiate in normal culture medium for 4 days, after which they received culture medium or MDA-MB-231-conditioned medium for 6 days. At the indicated timepoints, CD14 FITC/CD64 PE double-stained cells were analysed in a flow cytometer. R1: monocytic region; R2: lymphocytic region. **(B)** Scavenger receptor A 1 expression accompanies the differentiation of PBMC to macrophages *in vitro*. PBMC differentiated *in vitro* over a 10-day period as described in (A). At the indicated timepoints, SCARA1 expression was assayed in a flow cytometer. Δ: difference between the median fluorescence intensities of stained cells (black histogram) vs. cells treated with control Ig (gray histogram).

As expected, scavenger receptor A 1 (SCARA1) was not expressed by PBMC. Upon differentiation, however, cells expressed considerable levels of SCARA1, which did not further increase between days seven and ten. These data indicate that PBMC had differentiated to MΦ after seven days of culture (Figure 11B).

According to Condeelis and colleagues, TAM promote migration of mouse mammary carcinoma cells *in vivo* by activating tumour cell EGFR (Wyckoff et al., 2004). Although MAD-NT supernatants did not contain EGF-like ligands, we were interested in exploring whether primary human mononuclear cells release EGFR agonists. To gain a general view of the expressed EGF family ligands, we analysed transcript levels in primed and non-primed PBMC and MΦ. Our analysis revealed the presence of *OSM* and four of the seven possible EGFR agonists. In detail, we identified *AREG*, *EREG*, *HBEGF* and *TGFA* transcripts in all tested cell types. *BTC*, *EGF* and *EPGN* transcripts were not detected (Figure 12). Hepatocyte growth factor, which was abundantly expressed by MAD-NT cells, was not detected in primary mononuclear cells (data not shown). We studied the effects of tumour cell-secreted factors on primary human mononuclear cells by priming PBMC/MΦ with control medium or diluted MDA-MB-231 supernatants (1:1). Following priming, transcript and secreted protein levels of EGFR ligands and OSM were monitored.
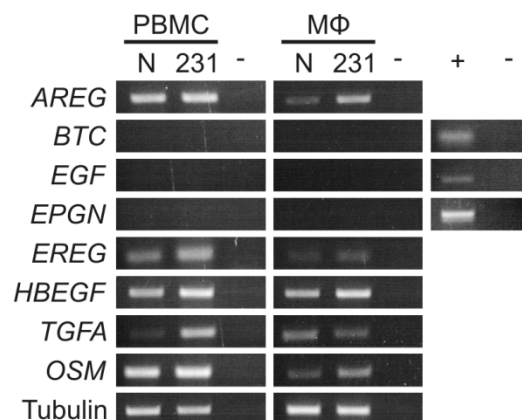

FIGURE 12. Primary human PBMC and MΦ express EGF family ligands and OSM. Freshly isolated PBMC and *in vitro* differentiated MΦ received normal culture medium (N) or MDA-MB-231-conditioned medium (231) for 24 hrs. PCR was performed on reverse-transcribed mRNA samples. -: water control; +: placenta cDNA positive control.

4. Tumour cell-derived factors trigger divergent patterns of transcriptional activity and ligand secretion in PBMC and MΦ

Within 24 hrs, priming of PBMC upregulates *EREG, TGFA* and *OSM* transcripts, as shown by qPCR analysis (Figure 13A). On protein level, primed PBMC significantly induced pEGFR levels in the reporter cell line. In order to identify the EGFR agonists secreted by primed PBMC, we tested neutralising antibodies directed against AREG, EREG, HB-EGF and TGFα. Epiregulin neutralisation by an inhibitory antibody reduced pEGFR to basal levels. Though

highly expressed at the transcript level, a TGFα blocking antibody had no effect (Figure 13B), and TGFα secretion was not detected in ELISA (data not shown). In contrast to TGFα, EREG plays a key role in EGFR activation *in vitro*. Flow cytometric analysis confirmed that pro-EREG was expressed by PBMC and not by lymphocytes (Figure 13D). In contrast to MAD-NT, non-primed PBMC secreted only marginal levels of OSM. After priming, however, highly elevated levels of OSM were detected in PBMC supernatants, while the protein was neither present in culture medium nor in medium used to prime PBMC (Figure 13C). Consequently, supernatants of primed PBMC significantly upregulated pSTAT3 levels in the reporter cell line, which were fully abrogated by OSM blockage (Figure 13B).
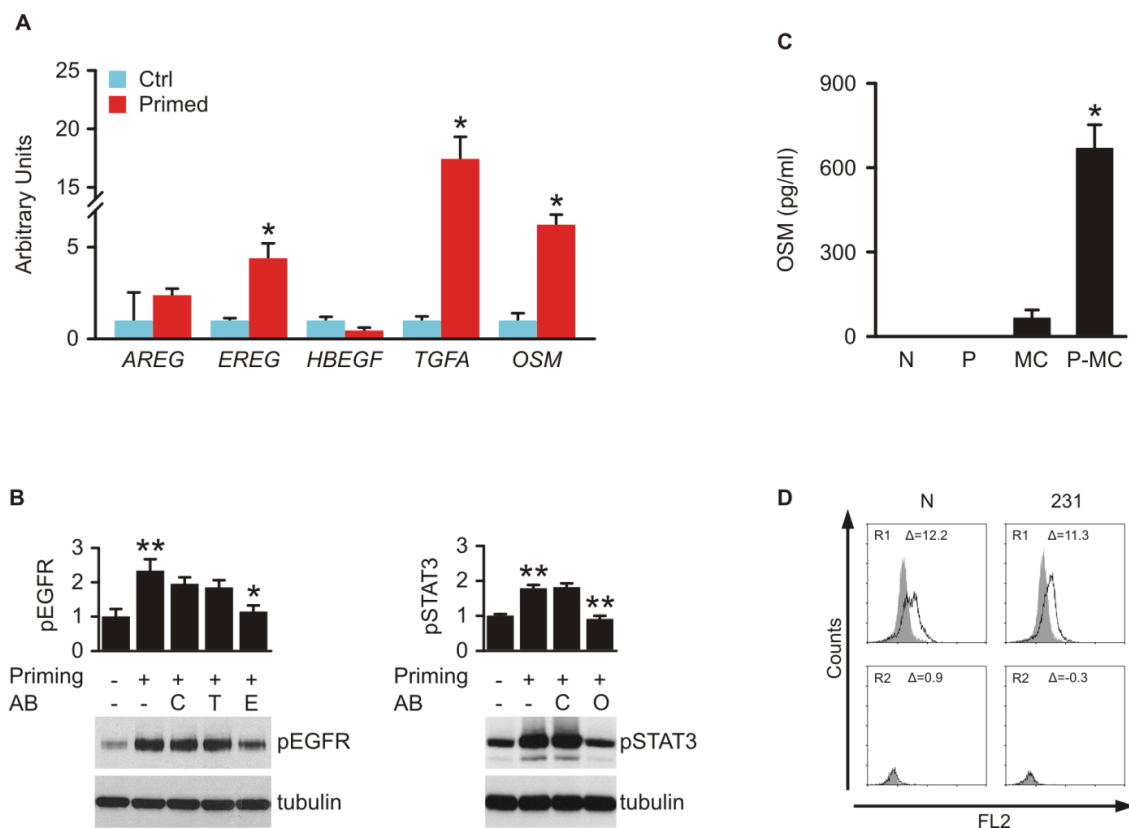

FIGURE 13. PBMC secrete EREG and OSM upon priming by MDA-MB-231 carcinoma cells. (A) Primed PBMC induce *EREG*, *TGFA* and *OSM* transcripts (qPCR). Freshly isolated PBMC were cultured in control medium (Ctrl) or MDA-MB-231-conditioned medium (Primed) for 24 hrs. mRNAs were reverse-transcribed and analysed by quantitative PCR. Representative experiment shows means ± 95 % confidence intervals; *p<0.05 by Mann-Whitney's U-Test; n=4. **(B)** Primed PBMC secrete EREG and OSM. PBMC were cultured in control medium or MDA-MB-231-conditioned medium for 24 hrs. PBMC supernatants were preincubated with control sera or blocking antibodies, then used to stimulate reporter cells in which pEGFR, pSTAT3 and tubulin levels were visualised. Lower panels: representative Western blot experiments. Upper panels: densitometric analysis showing means ± SEM; n=4; C: control Ig; T: TGFα blocking antibody; E: EREG blocking antibody; O: OSM blocking antibody; *p<0.02; **p<0.006 by Student's T-Test. **(C)** Primed PBMC secrete elevated OSM levels (ELISA). PBMC were incubated for 24 hrs in culture medium or MDA-MB-231-conditioned medium. N: culture medium; P: priming medium; MC: supernatant from control PBMC; P-MC: supernatant from primed PBMC. Results are means ± SEM; n=7; *p<0.002 by Mann-Whitney's U-Test. **(D)** Primary human PBMC express pro-EREG. PBMC received culture medium (N) or MDA-MB-231-conditioned medium (231) for 24 hrs. EREG expression levels were visualised via flow cytometry of cells stained with an epiregulin PE antibody. R1: monocytic region; R2: lymphocytic region.

Priming of PBMC isolated via adherence and priming of purified CD64⁺/CD14⁺ PBMC resulted in similar levels of secreted EREG and OSM, confirming that monocyte populations secrete these two factors (Figure 14). Together, these data indicate that priming of PBMC by MDA-MB-231 breast carcinoma cells induces *EREG*, *TGFA* and *OSM* transcription. However, primed PBMC only secrete functionally active EREG and OSM.
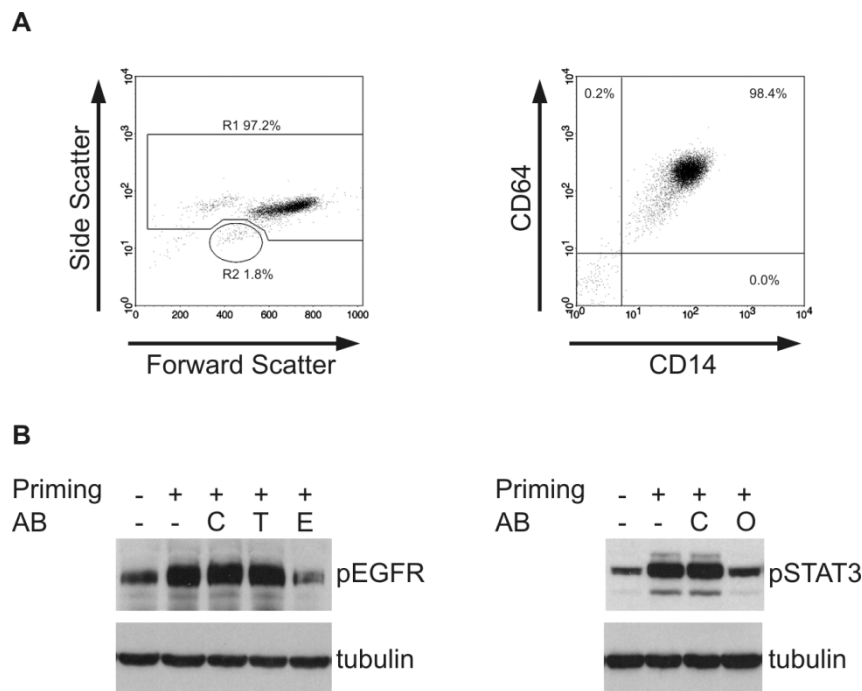

FIGURE 14. CD14⁺/CD64⁺ primary human PBMC secrete EREG and OSM upon priming by MDA-MB-231 cells. **(A)** PBMC isolated by CD14 positive selection express CD64 and CD14. Freshly isolated PBMC double-stained with CD14 FITC/CD64 PE antibodies were analysed in a flow cytometer. Left panel: forward and side scatter properties. R1: monocytic region; R2: lymphocytic region. Right panel: CD14/CD64 staining (gate = R1). **(B)** CD14⁺/CD64⁺ PBMC primed by tumour cells secrete EREG and OSM. PBMC isolated by CD14 positive selection received culture medium or MDA-MB-231-conditioned medium for 24 hrs. PBMC supernatants were preincubated with control Ig or blocking antibodies, then used to stimulate reporter cells in which pEGFR, pSTAT3 and tubulin levels were visualised. Representative Western blot experiment. C: control Ig; T: TGFα blocking antibody; E: EREG blocking antibody; O: OSM blocking antibody.

In comparison to PBMC, differentiated MΦ displayed significantly increased *HBEGF*, *AREG* and *OSM* transcript levels after short-time priming (24 hrs, Figure 15A). After seven days of priming, *HBEGF* and *OSM* transcripts were still significantly increased. However, *AREG* transcripts had decreased to basal levels (Figure 15B). Transcriptional profiling revealed that *EREG* levels, though upregulated in primed MΦ, remained low in this cell type (Figure 12). On the protein level, MΦ primed for 24 hrs upregulated pEGFR levels significantly in the reporter cell line, an effect which was completely blocked by an inhibitory antibody against HB-EGF. In line with this observation, a neutralising antibody directed against amphiregulin protein had no effect, even though *AREG*, like *HBEGF*, was highly upregulated on transcript level (Figure 15C).
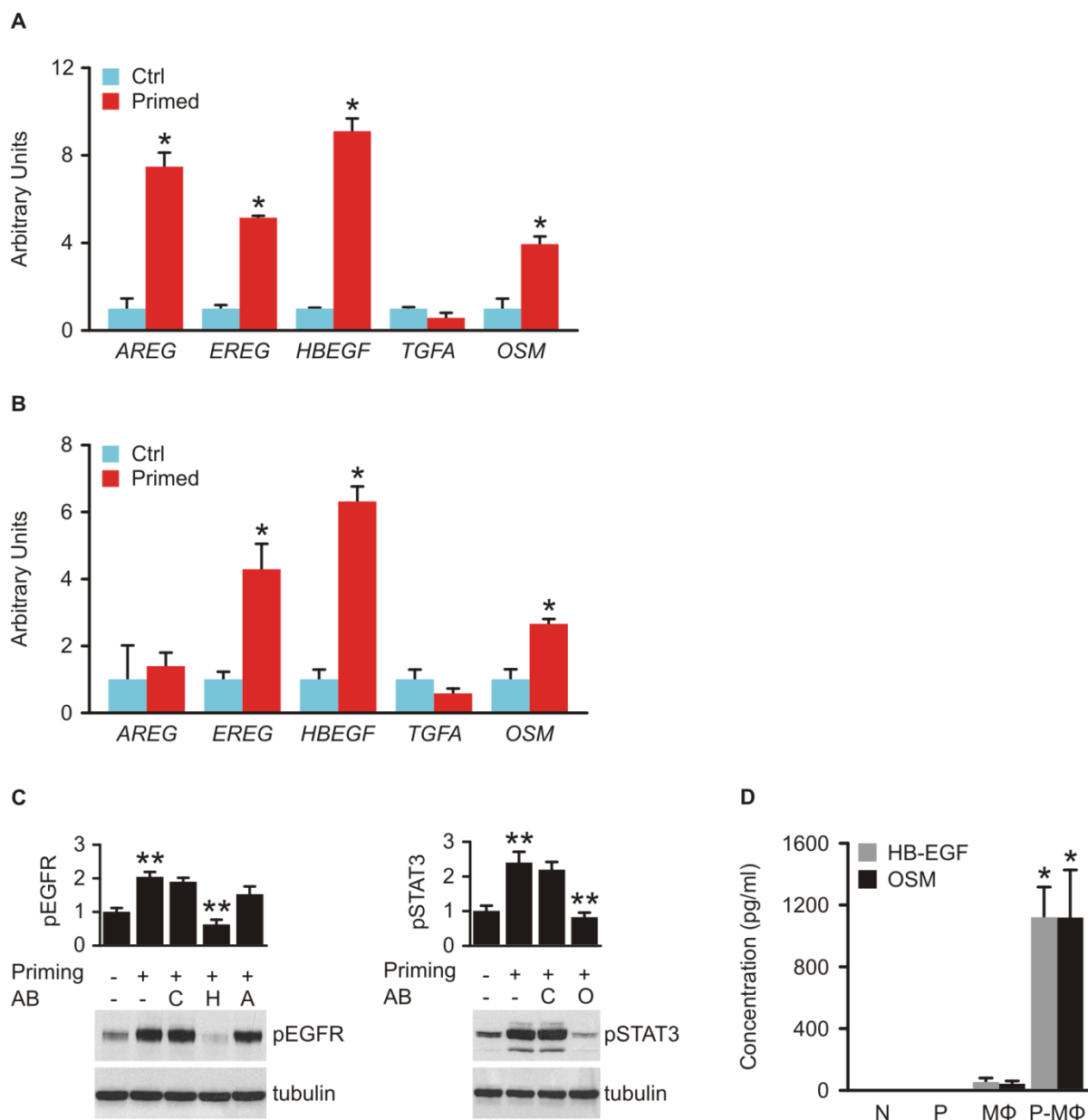
FIGURE 15. MΦ secrete HB-EGF and OSM upon priming by MDA-MB-231 carcinoma cells. (A) Short-time primed MΦ upregulate *AREG*, *EREG*, *HBEGF* and *OSM* transcription (qPCR). MΦ were cultured for 24 hrs in control medium (Ctrl) or MDA-MB-231-conditioned medium (Primed). mRNAs were reverse-transcribed and analysed by quantitative PCR. Representative experiment shows means ± 95 % confidence intervals; *p<0.02 by Mann-Whitney's U-Test; n=4. **(B)** Long-time primed MΦ display elevated *EREG*, *HBEGF* and *OSM* transcript levels (qPCR). MΦ were cultured for 7 days with control medium (Ctrl) or MDA-MB-231-conditioned medium (Primed). mRNAs were reverse-transcribed and analysed by quantitative PCR. Representative experiment shows means ± 95 % confidence intervals; *p<0.05 by Mann-Whitney's U-Test; n=3. **(C)** Primed MΦ secrete HB-EGF and OSM. MΦ were primed with control medium or MDA-MB-231-conditioned medium for 24 hrs. MΦ supernatants were preincubated with control sera or blocking antibodies, then used to stimulate reporter cells in which pEGFR, pSTAT3 and tubulin levels were visualised. Lower panels: representative Western blot experiments. Upper panels: densitometric analysis showing means ± SEM; pEGFR: n=6; pSTAT3: n=12; C: control Ig; H: HB-EGF blocking antibody; A: AREG blocking antibody; O: OSM blocking antibody. **p<0.00006 by Student's T-Test. **(D)** Primed MΦ secrete elevated HB-EGF and OSM levels (ELISA). MΦ were cultured for 24 hrs in control medium or MDA-MB-231-conditioned medium. N: culture medium; P: priming medium; MΦ: supernatant of control macrophages; P-MΦ: supernatant of primed macrophages. Results are means ± SEM; n=6; *p<0.004 by Mann-Whitney's U-Test.

Medium of primed MΦ significantly elevated pSTAT3 levels in the reporter cell line and an OSM blocking antibody neutralised this effect (Figure 15C). Short-time priming of differentiated MΦ activated the effector pathways for EGF family ligands and OSM to a similar extent as long-time priming (data not shown). Quantitation of secreted HB-EGF and OSM levels confirmed that priming significantly increased secretion (Figure 15D). In contrast, AREG was not secreted by primed MΦ (data not shown).

Taken together, these data indicate that, even though various EGFR ligands are transcriptionally induced, primed macrophages only secrete functionally active HB-EGF and OSM, irrespective of priming duration.

5.   Tumour-primed PBMC secrete epiregulin and oncostatin-M

The previous experiments show that tumour cell-derived factors prime PBMC and MΦ to secrete one specific EGFR agonist in combination with OSM, the relevant STAT3 activator. We next asked whether similar response patterns might be provoked in PBMC and MΦ upon priming with an expanded panel of tumour cell supernatants. The panel contained MDA-MB-231, T-47D, MCF7, MDA-MB-468 invasive mammary and SCC-9 squamous carcinoma cell lines. MCF 10A mammary epithelial cells used in this panel represent a benign breast lesion, and primary HMEC are derived from healthy breast epithelium. Stimulation with conditioned media from PBMC after priming with MDA-MB-231, T-47D, MDA-MB-468 and MCF 10A supernatants strongly increased pEGFR levels in reporter cells (Figure 16A, upper panels). The same conditioned media also increased pSTAT3 levels (Figure 16A, lower panels). Incubation with supernatants of non-primed PBMC induced only basal phosphorylation levels of EGFR and STAT3 in the reporter cell lines, as did control epithelial cell supernatants.

We next analysed whether PBMC secrete OSM as the functional STAT3 activating factor. Supernatants of primed PBMC that upregulated pSTAT3 contained considerable amounts of OSM. OSM was absent in PBMC supernatants that did not elicit STAT3 phosphorylation. OSM was neither detected in supernatants of non-primed PBMC nor in control epithelial cell supernatants (Figure 16B). Neutralisation of OSM in supernatants of PBMC abrogated pSTAT3 signals (Figure 16D). These data show that primed PBMC secrete OSM as the only relevant STAT3 activator in our system.

Supporting the finding that EREG is the EGFR agonist secreted by primed PBMC, an antibody blocking EREG function reduced EGFR phosphorylation to basal levels, while neutralisation of TGFα had no effect (Figure 16C). In line with our observations in PBMC primed by MDA-MB-231, blocking of AREG or HB-EGF did not reduce pEGFR levels (data not shown). Supernatants of non-primed PBMC induced only basal EGFR phosphorylation in reporter cells. Thus, upon priming with a variety of cell lines, PBMC again secrete EREG as the only functional EGFR agonist.

Our results show that a variety of tumour cell lines primes PBMC to co-secrete epiregulin and oncostatin-M, suggesting a uniform secretion pattern to be exploited for therapeutic purposes.
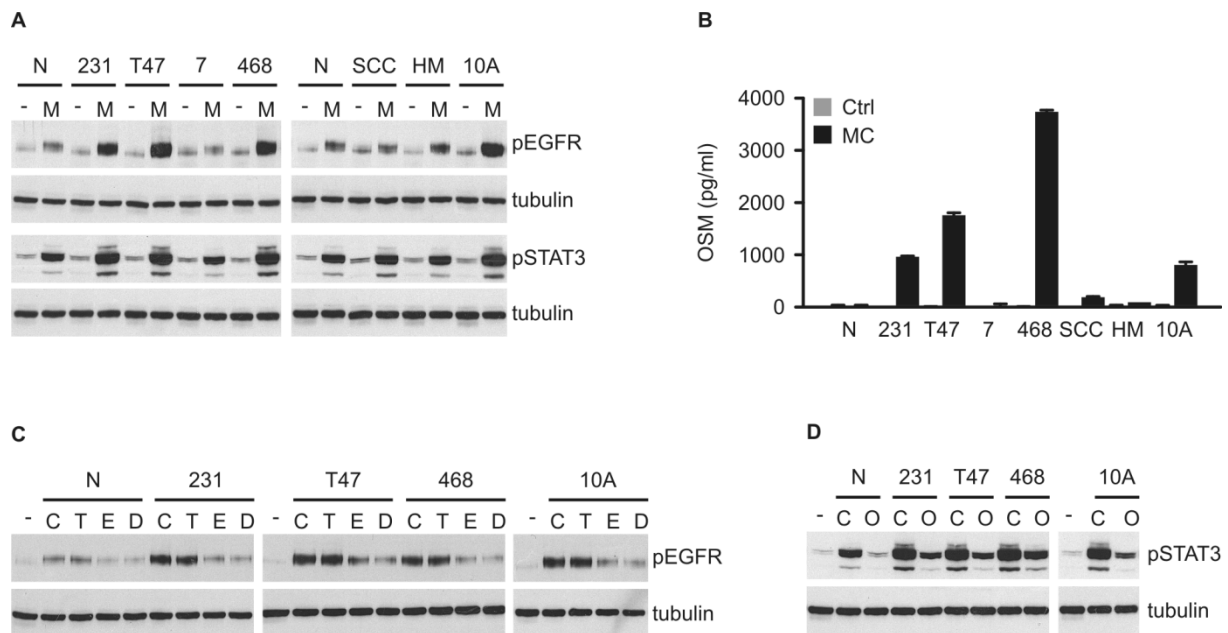

FIGURE 16. Tumour-primed PBMC secrete EREG and OSM. (A) Supernatants of primed PBMC contain EGFR and STAT3 activators. Freshly isolated PBMC were incubated for 24 hrs with culture medium (N) or conditioned media of MDA-MB-231 (231), T-47D (T47), MCF7 (7), MDA-MB-468 (468), SCC-9 (SCC), primary human mammary epithelial cells (HM) or MCF 10A (10A). Reporter cells were stimulated with PBMC supernatants and pEGFR, pSTAT3 and tubulin levels were visualised. M: medium conditioned by PBMC; -: priming media that were control-incubated for the same period. **(B)** Primed PBMC secrete OSM (ELISA). Ctrl: priming media that were not incubated with PBMC; MC: PBMC supernatants. **(C)** EREG is the relevant EGFR agonist secreted by primed PBMC. Reporter cells were stimulated with supernatants of PBMC primed by the indicated cell lines. pEGFR and tubulin levels were visualised. Where indicated, PBMC supernatants were preincubated with control Ig or blocking antibodies. -: culture medium; C: control Ig; T: TGFα blocking antibody; E: EREG blocking antibody; D: double treatment. **(D)** OSM is the relevant STAT3 activator secreted by primed PBMC. Reporter cells were stimulated with supernatants of PBMC primed by the indicated cell lines. pSTAT3 and tubulin levels were visualised. Where indicated, PBMC supernatants were preincubated with control Ig or blocking antibodies. -: culture medium; C: control Ig; O: OSM blocking antibody.

6. Tumour-primed macrophages secrete HB-EGF and oncostatin-M

We next asked whether priming by the presented tumour cell panel also elicits a similarly uniform secretory response in primary human macrophages. We primed MΦ differentiated *in vitro* for 7 days with our panel of conditioned media. Upon priming by a fraction of tumour cell lines (MDA-MB-231, T-47D, MCF7, SCC-9), MΦ supernatants indeed increased phosphorylation of EGFR in reporter cells (Figure 17A, upper panels) and equally induced increased pSTAT3 levels (Figure 17A, lower panels). The active MΦ supernatants contained considerable amounts of HB-EGF and OSM. Neither ligand, however, was secreted by

control MΦ nor by the priming cell panel (Figure 17B). The ligands were also absent in supernatants of MΦ primed by MDA-MB-468, MCF 10A and HMEC. Accordingly, supernatants devoid of HB-EGF and OSM induced only basal EGFR and STAT3 phosphorylation levels. An antibody blocking HB-EGF function abrogated EGFR phosphorylation elicited by active supernatants of primed MΦ (Figure 17C). An antibody specific to OSM neutralised pSTAT3 signals, confirming that OSM is the only relevant STAT3 activator secreted by primed MΦ.

Similar to PBMC priming, a number of tumour cell lines induces MΦ to co-secrete an EGFR agonist and a STAT3 activator. In contrast to PBMC, but confirming a uniform secretion pattern, MΦ release HB-EGF and OSM upon priming by tumour cells.
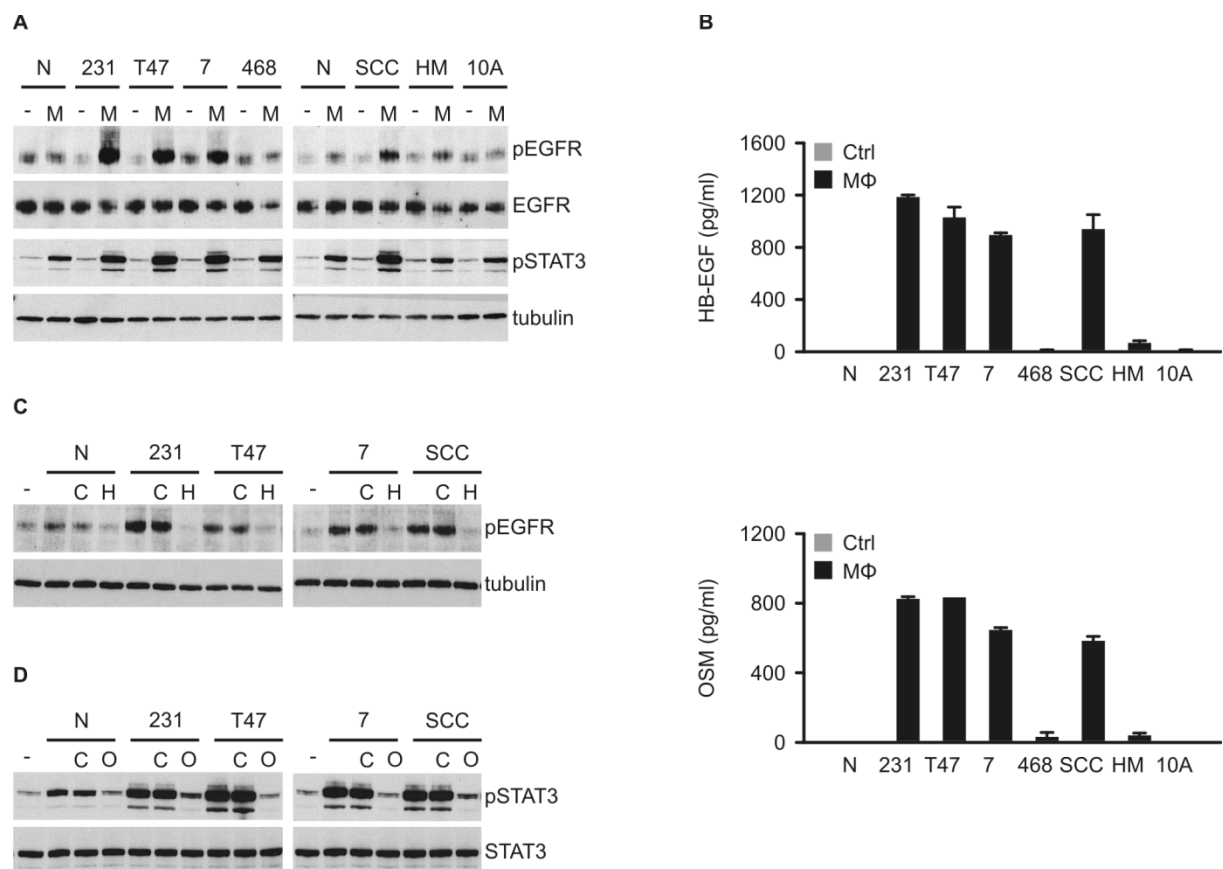

FIGURE 17. Tumour-primed macrophages secrete HB-EGF and OSM. (A) Supernatants of primed MΦ contain EGFR and STAT3 activators. Reporter cells were stimulated with supernatants of MΦ primed by the indicated cell lines. pEGFR, EGFR, pSTAT3 and tubulin levels were visualised. M: medium conditioned by MΦ; -: priming media that were control-incubated for the same period. **(B)** Primed MΦ secrete HB-EGF and OSM (ELISA). Ctrl: priming media that were not incubated with macrophages; MΦ: macrophage supernatants. **(C)** HB-EGF is the relevant EGFR agonist secreted by primed MΦ. Reporter cells were stimulated with supernatants of MΦ primed by the indicated media and pEGFR and tubulin levels were visualised. Where indicated, MΦ supernatants were preincubated with control Ig or blocking antibodies. -: culture medium; C: control Ig; H: HB-EGF blocking antibody. **(D)** OSM is the relevant STAT3 activator secreted by primed MΦ. Reporter cells were stimulated with supernatants of MΦ primed by the indicated media and pSTAT3 and STAT3 levels were visualised. Where indicated, MΦ supernatants were preincubated with control Ig or blocking antibodies. -: culture medium; C: control Ig; O: OSM blocking antibody.

7.   Tumour cells specifically prime PBMC, MΦ, or both

We observed a clear distinction in priming capacities of tumour cell lines on primary mononuclear cells: primary breast epithelial cells (HMEC) derived from healthy donors neither convey a secretory response in PBMC nor in MΦ. Selective PBMC priming was achieved by MCF 10A and MDA-MB-468 cells, while MCF7 and SCC-9 cells exclusively primed MΦ. MDA-MB-231 and T-47D breast carcinoma cells primed PBMC as well as MΦ (Figure 16 and 17). A correlation between preferential priming of PBMC versus MΦ and mesenchymal dedifferentiation of carcinoma cells was not supported by our data. However, preferential priming of mononuclear cells suggests that tumour cells produce distinct activities that in turn trigger defined secretory responses in PBMC and differentiated MΦ.

8.   Tumour cell-derived IL-6 activates STAT3 in mononuclear cells

Our data show that mononuclear cell-derived OSM activates STAT3 in carcinoma cells. However, in human tumours, constitutive STAT3 activity extends beyond the cancer cell subset, and is also common in tumour-associated myeloid cells (Yu et al., 2007). There, phosphorylation of STAT3 is instrumental in suppressing antitumour immune reactions (Cheng et al., 2008).

Next, we explored whether tumour cell-derived factors trigger the paracrine activation of STAT3 in mononuclear cells. We used our panel of tumour- and nontransformed cell supernatants to stimulate mononuclear cells. MAD-NT cells and MΦ that received culture medium or supernatants of nontransformed MCF 10A and HMEC cells displayed only marginal pSTAT3 levels. However, stimulation with MDA-MB-231 and SCC-9 carcinoma cell supernatants strongly upregulated pSTAT3 levels in MAD-NT and primary macrophages (Figure 18A). Mononuclear cells express both IL-6 receptor subunits, *GP130* and *IL6R*, whereas MDA-MB-231 and SCC-9 cells express *IL6* (Figure 6). This points to a possible role of tumour cell-derived IL-6 in the paracrine activation of STAT3 in mononuclear cells. In agreement with this hypothesis, MAD-NT and MΦ displayed a dose-dependent increase in pSTAT3 levels upon stimulation with recombinant IL-6 (Figure 18A). A neutralising antibody directed against IL-6 abrogated pSTAT3 levels induced by MDA-MB-231 supernatants or recombinant IL-6 in MAD-NT cells (Figure 18B). Taken together, the mutual exchange of IL-6 family ligands between carcinoma cells and mononuclear cells persistently activates STAT3 transcription factors in both cell types. While mononuclear cell-secreted OSM activates STAT3 in cancer cells, tumour cell-derived IL-6 is a STAT3 activator in mononuclear cells.
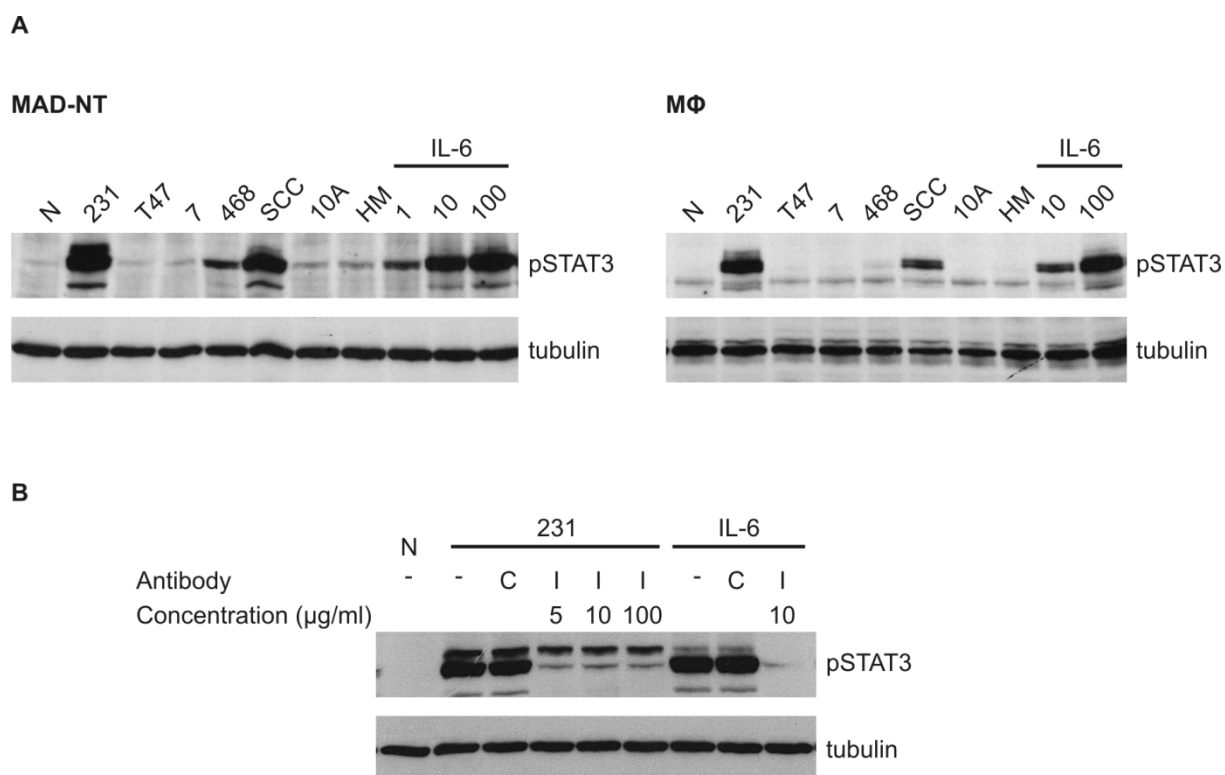
A

MAD-NT   MΦ

IL-6

N 231 T47 7 468 SCC 10A HM 1 10 100 — pSTAT3

tubulin

IL-6

N 231 T47 7 468 SCC 10A HM 10 100 — pSTAT3

tubulin

B

	N	231					IL-6		
Antibody	-	-	C	I	I	I	-	C	I
Concentration (µg/ml)				5	10	100			10

pSTAT3

tubulin

FIGURE 18. Tumour cell-derived IL-6 activates STAT3 in mononuclear cells. (A) Supernatants of MDA-MB-231 and SCC-9 carcinoma cells activate STAT3 in MAD-NT monocytes (left panels) and primary human MΦ (right panels). MAD-NT cells and *in vitro* differentiated MΦ received either culture medium (N) or supernatants of MDA-MB-231 (231), T-47D (T47), MCF7 (7), SCC-9 (SCC), MCF 10A (10A) or HMEC (HM) cells. Alternatively, MAD-NT cells and MΦ were stimulated with 1, 10 or 100 ng/ml recombinant IL-6. pSTAT3 and tubulin levels were visualised. **(B)** MDA-MB-231 cell-derived IL-6 is the main STAT3 activator in MAD-NT monocytes. MAD-NT cells received culture medium (N), MDA-MB-231 supernatants (231) or 100 ng/ml recombinant IL-6. pSTAT3 and tubulin levels were visualised. Where indicated, media were preincubated with control Ig (C) or an antibody blocking IL-6 function (I) at 5, 10 or 100 µg/ml.

9.   HB-EGF and OSM are promigratory in epithelial cells

In the next set of experiments, we addressed functional aspects of MΦ-derived HB-EGF and OSM on tumour cells. Oncostatin-M was first described as a cytokine with antiproliferative properties in tumour cell lines from different organs, including T-47D and MDA-MB-231 breast carcinoma cells (Grant and Begley, 1999; Underhill-Day and Heath, 2006; Zarling et al., 1986). We tested the effects of recombinant OSM on the growth rate of MDA-MB-231, T-47D, MCF7, MDA-MB-468, MDA-MB-435S breast carcinoma cells and MCF 10A breast hyperplasia cells. Although all tested cell lines expressed at least one OSM receptor (Figure 6), administration of OSM showed no antiproliferative effect, with the exception of MDA-MB-231 cells (Figure 19). This indicates that OSM lacks potent antiproliferative activity in breast cancer cells.
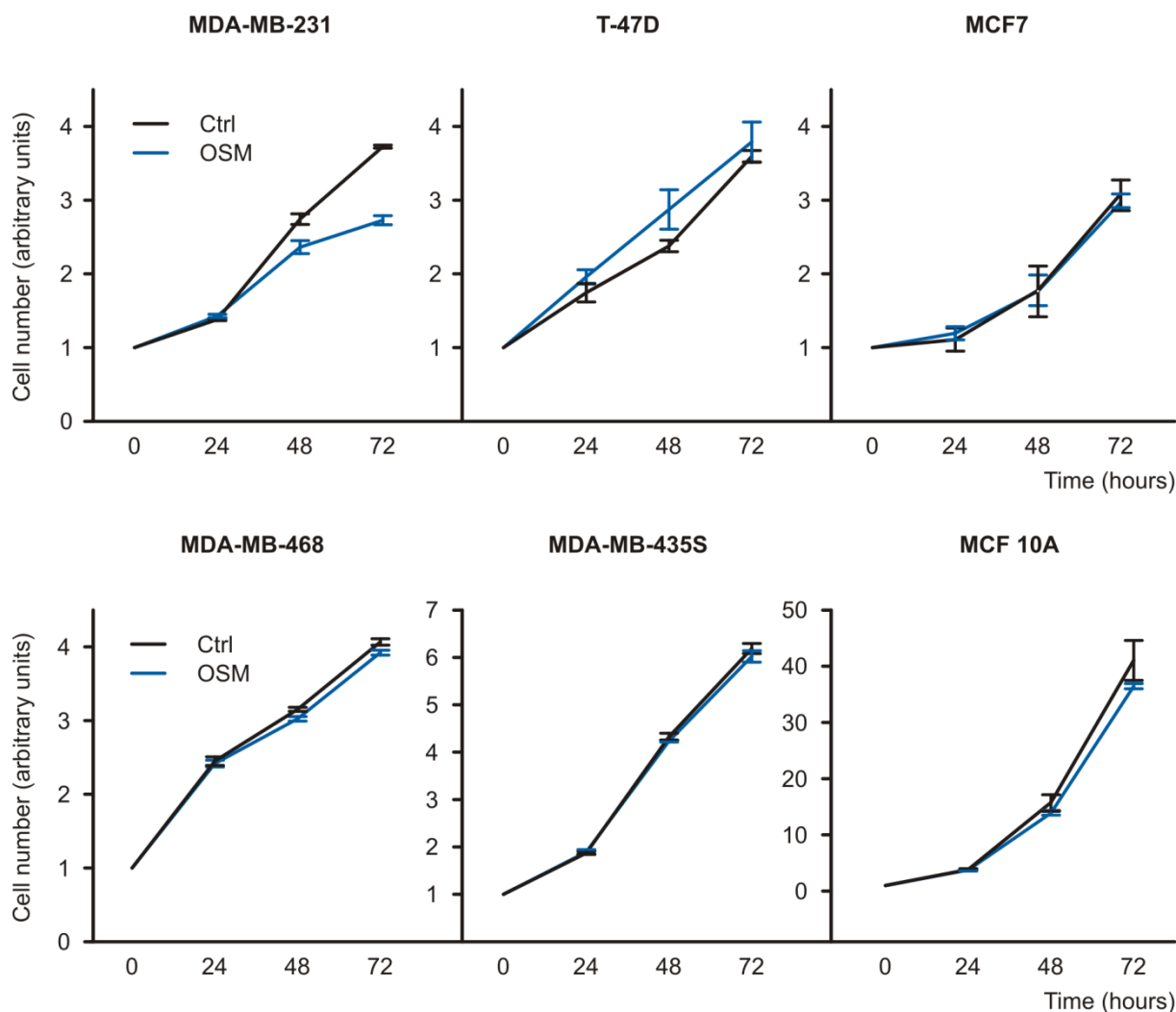
FIGURE 19. Oncostatin-M does not inhibit the proliferation of breast tumour cells. Cells were cultured in their respective culture media, with or without 20 ng/ml recombinant OSM. At the indicated timepoints, cells were detached and counted.

HB-EGF is a well-described EGFR agonist with profound implications in cell behaviour during development, homeostasis and disease. HB-EGF promotes cell migration, invasion, proliferation and survival (Higashiyama et al., 1991; Nishi and Klagsbrun, 2004). Clinical and *in vivo* mouse data indicate that HB-EGF drives tumour progression (Miyamoto et al., 2004; Tanaka et al., 2005; Thogersen et al., 2001). We studied the effects of HB-EGF on proliferation and migration of epithelial cells *in vitro*. Recombinant HB-EGF was a potent mitogen in MCF 10A cells (Figure 20A). In head and neck squamous carcinoma cell line SCC-9, HB-EGF induced a strong chemotactic response (Figure 20B). These findings suggest that macrophage-derived HB-EGF might promote proliferation and migration of carcinoma cells.
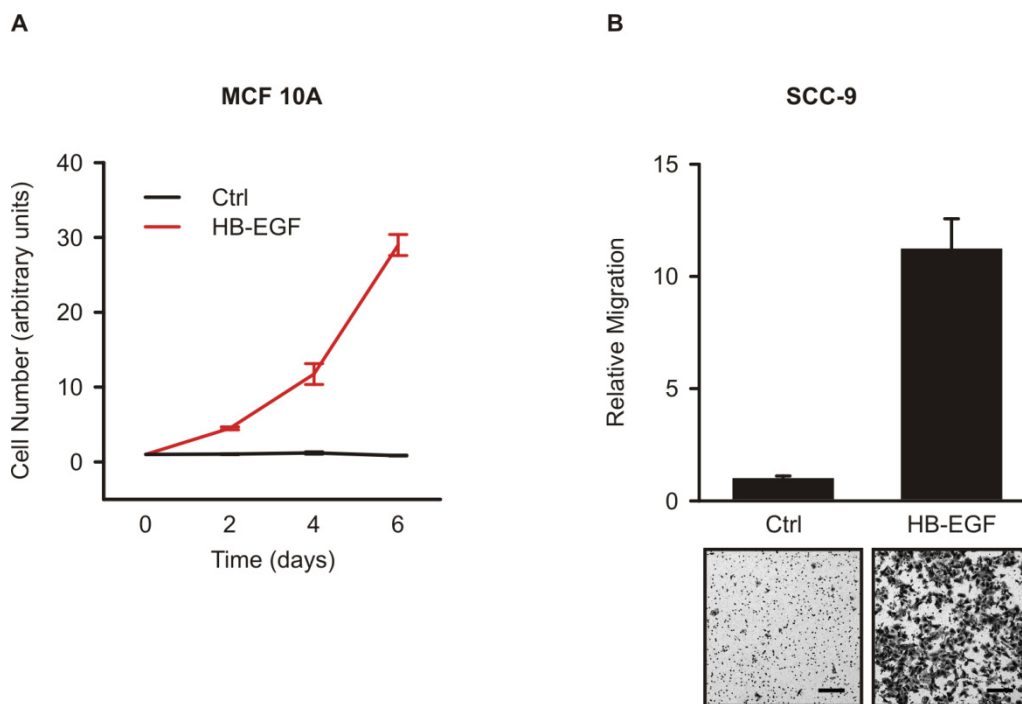
FIGURE 20. HB-EGF induces proliferation and chemotaxis of epithelial cells *in vitro*. (A) HB-EGF induces proliferation of MCF 10A cells. Cells were cultured in serum-free medium, with or without 40 ng/ml recombinant HB-EGF. At the indicated timepoints, cells were detached and counted. **(B)** HB-EGF induces chemotaxis of SCC-9 cells. Cells were plated into Boyden chambers, with and without 20 ng/ml recombinant HB-EGF in the lower compartment. Representative experiment with corresponding micrographs. Scale bar: 200 μm.

To test the influence of MΦ-secreted factors on SCC-9 chemotaxis, we collected serum-free supernatants from control and tumour-primed MΦ and used them as chemoattractants in Boyden chamber assays. Supernatants of tumour-primed MΦ increased SCC-9 chemotaxis by 3.8-fold compared to supernatants of control MΦ or priming medium alone. An HB-EGF neutralising antibody or the EGFR inhibitor AG1478 reduced migration to basal levels (Figure 21). Thus, priming of MΦ by tumour cells results in HB-EGF secretion at levels sufficient to drive cell migration, and HB-EGF is the relevant chemotactic factor for SCC-9 cells secreted by primed MΦ.

Liu and colleagues reported that OSM induces the undirected motility of MCF7 cells (Zhang et al., 2003). We incubated MCF7 cells for five days at increasing doses of recombinant OSM. Analysis of cell motility in the Boyden chamber assay confirmed a dose-dependent increase in scattering of MCF7 cells (Figure 22A). Similarly, we observed 2.6-fold increase in scattering of SCC-9 cells (Figure 22B). However, OSM had no effect on cells with mesenchymal morphology (MDA-MB-231, MDA-MB-435S; data not shown).
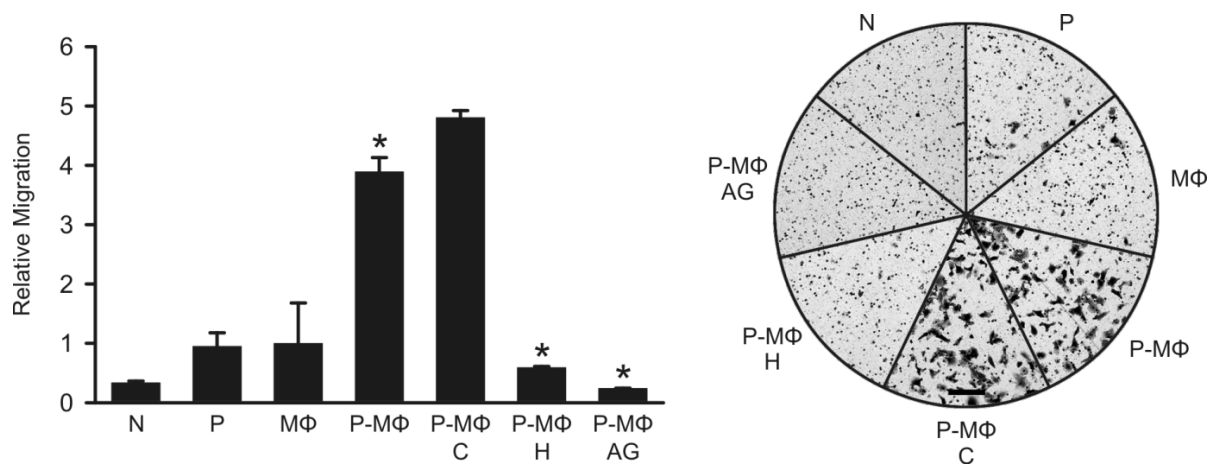
FIGURE 21. HB-EGF secreted by tumour-primed MΦ induces chemotaxis of SCC-9 cells. MΦ were cultured for 6 days in either control medium or 50 % MDA-MB-231-conditioned medium. Subsequently, cells received 50 % MDA-MB-231-conditioned serum-free medium or RPMI for 24 hrs. MΦ supernatants were collected and used as chemoattractants for SCC-9 cells in Boyden chamber assays. Where indicated, media were preincubated with control Ig (C), an HB-EGF blocking antibody (H) or 250 nM EGFR kinase inhibitor AG1478 (AG). Representative experiment with corresponding micrographs. N: culture medium; P: priming medium; MΦ: supernatant of control macrophages; P-MΦ: supernatant of primed macrophages; scale bar: 200 µm; n=3; *p<0.05 by Student's T-Test.
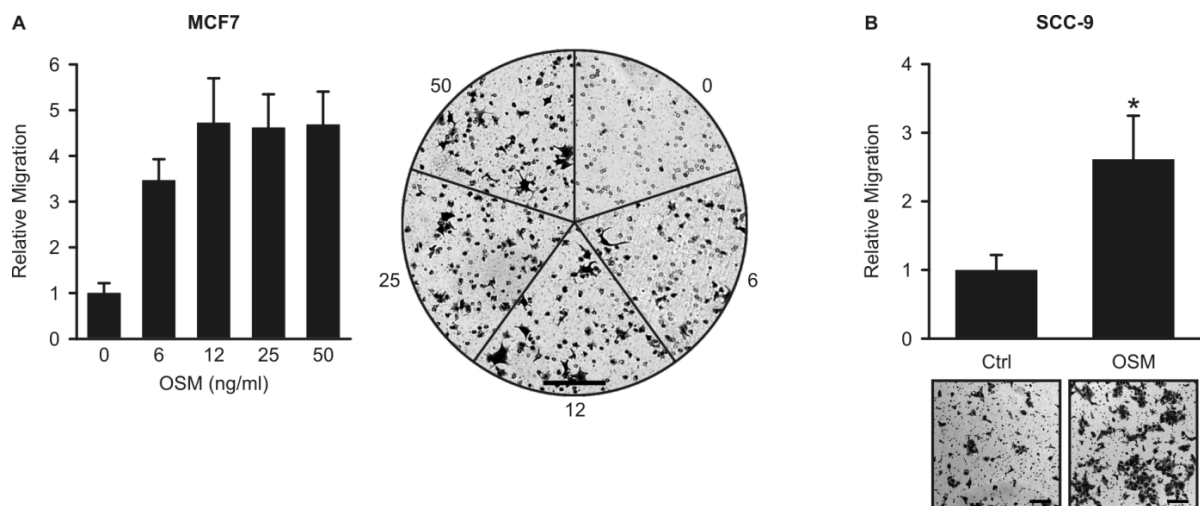
FIGURE 22. OSM promotes motility of MCF7 and SCC-9 cells. (A) OSM promotes motility of MCF7 cells. Cells were incubated for 5 days with or without the indicated concentrations of recombinant OSM. Subsequently, cells were plated into Boyden chambers, using the same dose of OSM in RPMI + 2 % FCS in the upper and lower compartments. Representative experiment with corresponding micrographs. Scale bar: 200 µm. **(B)** OSM upregulates the intrinsic motility of SCC-9 cells. Cells were incubated for 48 hrs with or without 10 ng/ml recombinant OSM, and were subsequently plated into Boyden chambers, using the same dose of OSM in RPMI in the upper and lower compartments. Results are means ± SEM; n=4; *p<0.05 by Student's T-Test. Micrographs show a representative experiment. Scale bar: 200 µm.

MCF 10A cells represent a benign breast epithelial model cell line that is barely migratory under most assay conditions. OSM treatment of MCF 10A did not significantly induce motility. A close examination of the Boyden chamber membranes, however, revealed that OSM treated cells had extended protrusions into the membrane pores (Figure 23A). This indicates that OSM alone upregulates the intrinsic motility of MCF 10A cells, but does not confer the ability to penetrate through the membrane pores. However, when HB-EGF was added to the lower chamber, OSM treated cells migrated two to three times faster along the HB-EGF gradient (Figure 23B). Taken together, prolonged treatment of MCF7 and SCC-9 cells with recombinant OSM induces undirected motility in these tumour cells. OSM and HB-EGF cooperate in promoting chemotaxis of MCF 10A epithelial cells.
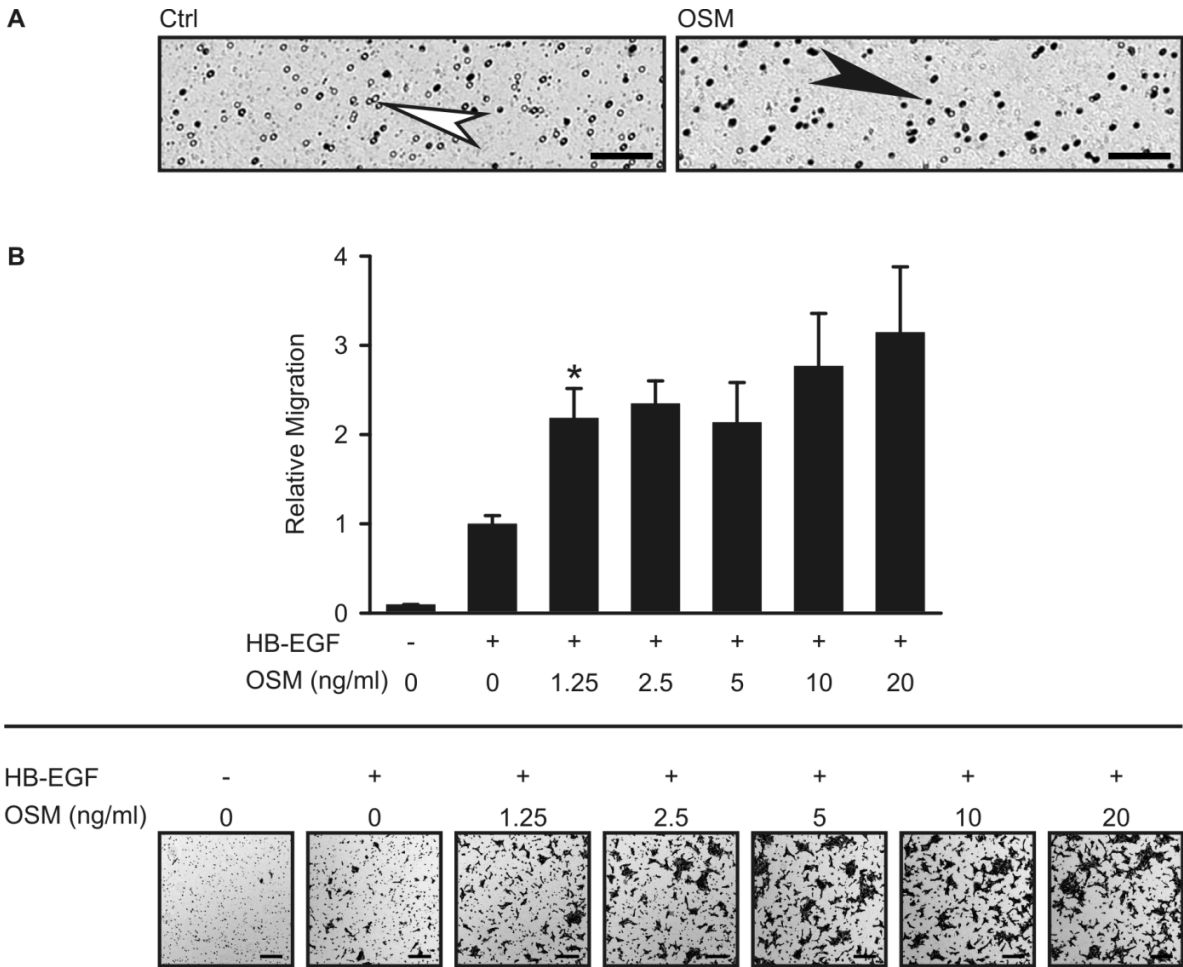

FIGURE 23. HB-EGF and OSM cooperate in promoting chemotaxis of MCF 10A cells. (A) MCF 10A cells treated with OSM alone extend protrusions into the pores, but cannot penetrate the Boyden chamber membrane. Cells were cultured for 48 hrs with or without 20 ng/ml recombinant OSM. Subsequently, cells were plated into Boyden chambers, using the same concentration of OSM in RPMI in the upper and lower compartments. White arrow: empty pore; black arrow: filled pore; scale bar: 100 μm. **(B)** OSM treated cells migrate faster into an HB-EGF gradient. Cells were cultured for 48 hrs with or without the indicated concentrations of recombinant OSM. Subsequently, cells were plated into Boyden chambers, using the same concentration of OSM in RPMI in the upper and lower compartments. Where indicated, 2 ng/ml recombinant HB-EGF was used as a chemoattractant in the lower compartment. Results are means ± SEM; n=3; *$p<0.05$ by Student's T-Test; micrographs show a representative experiment; scale bar: 200 μm.

10. EGFR agonists and IL-6 family ligands are frequently co-expressed with HB-EGF in human tumours

The data obtained from our priming experiments indicates that tumour-associated mononuclear cells co-secrete OSM, together with HB-EGF or EREG. *In vitro*, the underlying transcriptional induction patterns for EGFR ligands and OSM are complex and involve the upregulation of at least one additional EGFR ligand. We reasoned that co-expression patterns of certain EGFR ligands, IL-6 family ligands and myeloid markers might provide clues whether tumour-associated mononuclear cell subsets are a source of EGFR ligands and OSM *in vivo*. To test this hypothesis, we conducted a co-expression analysis of several microarray datasets of clinical tumour samples available at Oncomine™. Our analysis of the Nakagawa prostate (Nakagawa et al., 2008), Stransky bladder (Stransky et al., 2006) and Boersma breast (Boersma et al., 2008) datasets revealed that *HBEGF* was co-expressed with other *EGF* and *IL6* family members. *AREG*, *EREG*, *OSM*, *IL6* and *LIF* were frequently co-expressed with *HBEGF*. Moreover, *HBEGF* expression in tumours is accompanied by the expression of myeloid markers like *CD16b* and *CD1C* (Table 3). These co-expression patterns are similar to those of tumour-primed PBMC and MΦ (Figure 13 and 15) and indicate that, indeed, tumour-associated mononuclear cells might be a source of EGF and IL-6 family ligands *in vivo*.

TABLE 3. EGFR agonists, IL-6 family ligands and myeloid markers are frequently co-expressed with *HBEGF* in human tumours. Co-expression analysis of microarray datasets available at Oncomine™. n: number of samples.

Dataset	n	Genes co-expressed with *HBEGF*	Correlation value
Nakagawa prostate	596	*IL6*; interleukin 6	0.660
		AREG; amphiregulin	0.596
		LIF; leukemia inhibitory factor	0.465
		OSM; oncostatin M	0.319
Stransky bladder	57	*AREG*; amphiregulin	0.464
		EREG; epiregulin	0.464
		CD16b; Fc fragment of IgG, low affinity IIIb, receptor	0.464
Boersma breast	95	*IL6*; interleukin 6	0.748
		LIF; leukemia inhibitory factor	0.423
		CD1C; CD1c molecule	0.359

11.   HB-EGF plasma levels correlate with primary tumour growth and lymph node involvement in patients with invasive breast carcinoma

According to our TAM-tumour cell interaction model, we reasoned that in cancer patients, TAM-secreted factors would not only act locally within the tumour but also diffuse into the bloodstream. Thus, detection of elevated plasma levels of TAM-secreted factors might provide information on the patient's tumour status. To this end, we determined HB-EGF and OSM plasma levels in mammary carcinoma patients. Plasma samples from 102 female patients with ductal carcinoma *in situ* (DCIS) or invasive breast carcinoma were analysed. 26 healthy female donors, two donors with fibroadenoma and one donor with Crohn's disease served as controls. The detected HB-EGF and OSM protein levels displayed a highly significant correlation, as determined by two different correlation tests (Figure 24 and Table 4). In healthy donors, HB-EGF and OSM concentrations were constitutively low (mean HB-EGF concentration: 21.2 pg/ml; mean OSM concentration: 13.8 pg/ml). In disease, however, the concerted secretion of both ligands extended beyond the tumour patient set and was also detected in the two fibroadenoma patients and the patient with Crohn's disease.
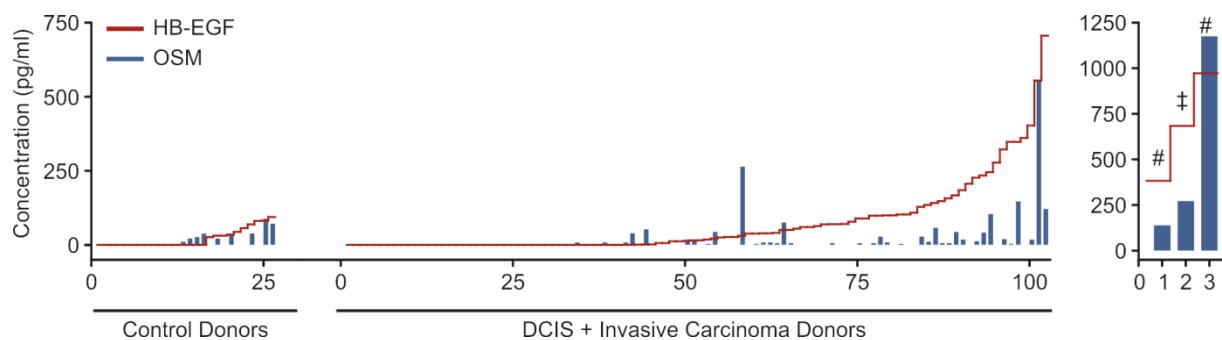
FIGURE 24. HB-EGF and OSM plasma protein levels correlate in human donors. Plasma from 26 control donors, 102 breast carcinoma patients, and 3 donors with fibroadenoma (#) or Crohn's disease (‡) was analysed.

TABLE 4. Correlation between HB-EGF and OSM protein plasma levels in human donors.

Method	Correlation value	95 % confidence interval	p-Value
Pearson's product-moment correlation	0.722	0.628 – 0.795	<2.2e-16
Kendall's rank correlation tau	0.437	N.D.	4.4e-10

Given that HB-EGF levels were elevated in a large proportion of patients' plasma samples, we reasoned that HB-EGF plasma levels might correlate with growth and/or progression of mammary carcinomas. Mean plasma concentrations of HB-EGF reflect primary tumour size: for small tumours (pT1; 23 patients) we detected 29.6 pg/ml, medium sized tumours (pT2;

13 patients) displayed 62.1 pg/ml and large tumours (pT3; 9 patients) 131.8 pg/ml. In conclusion, HB-EGF plasma levels correlated with primary tumour sizes (Figure 25A). P-values by Mann-Whitney's U-Test are: Ctrl-pT2: 0.0058; Ctrl-pT3: 0.0003; pT1-pT2: 0.0017; pT1-pT3: 0.0008. In addition, elevated HB-EGF plasma levels also correlate with lymph node dissemination of mammary breast carcinomas: healthy donors (Ctrl; n=26) and lymph node negative invasive mammary carcinoma patients (pN0; n=26) displayed mean HB-EGF plasma concentrations of 21.2 pg/ml and 24.6 pg/ml, respectively, whereas in patients with disseminated tumours significantly elevated HB-EGF levels were detected (pN>0; 97.5 pg/ml; n=28). P-values by Mann-Whitney's U-Test are: Ctrl-pN>0: 0.0034; pN0-pN>0: 0.0063; Figure 25B).
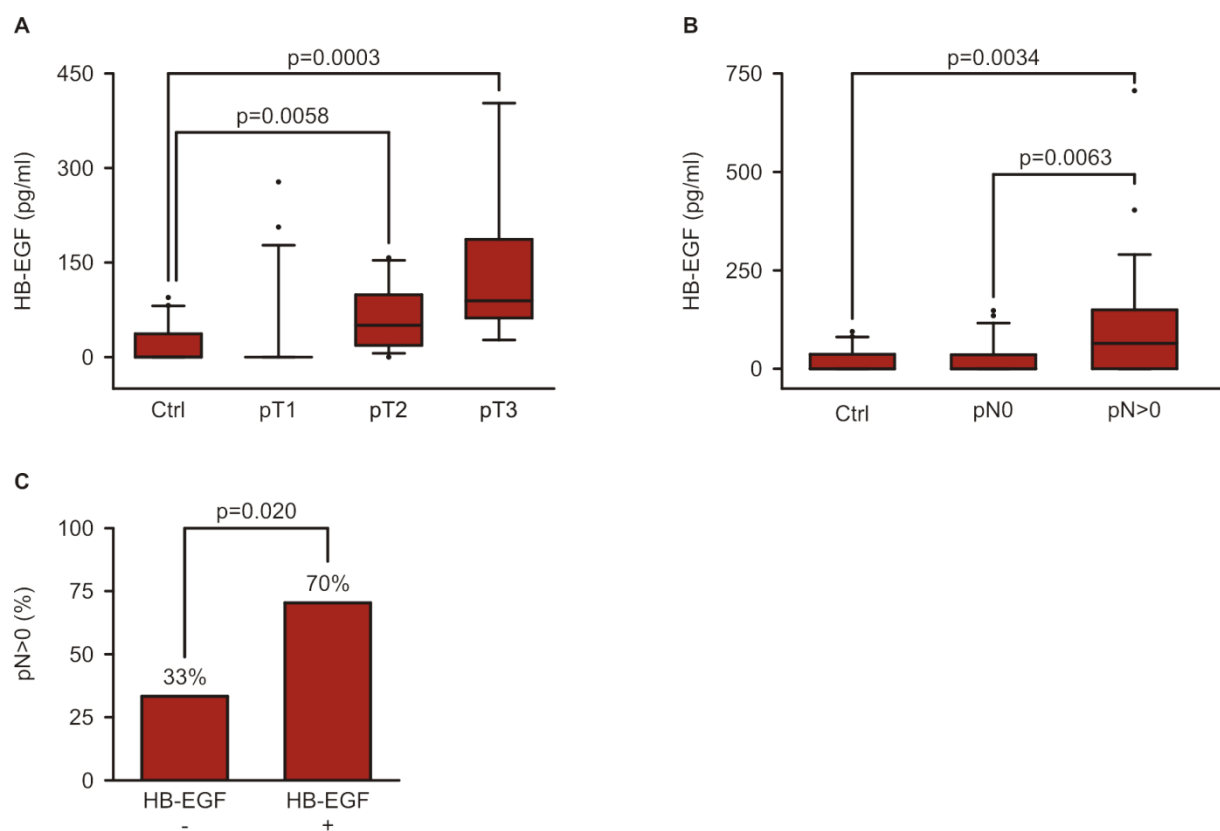

FIGURE 25. Elevated HB-EGF plasma protein levels accompany growth and dissemination of invasive breast carcinoma. (A) HB-EGF plasma protein levels correlate with primary tumour size. Box plots show HB-EGF plasma levels of 26 control donors, 23 pT1 donors, 13 pT2 donors and 9 pT3 donors. P-values by Mann-Whitney's U-Test are: Ctrl-pT2: 0.0058; Ctrl-pT3: 0.0003; pT1-pT2: 0.0017; pT1-pT3: 0.0008. **(B)** HB-EGF plasma protein levels correlate with lymph node dissemination of invasive breast carcinoma. Box plots depict HB-EGF levels of control donors (Ctrl; n=26), donors with nodal negative (pN0; n=26) and with nodal positive disease (pN>0; n=28). **(C)** Elevated HB-EGF plasma levels are indicative of disseminating breast carcinomas. Invasive breast carcinoma patients (n=54) were grouped into an HB-EGF negative (-; n=27) and HB-EGF positive (+; n=27) cohort, using the mean plasma HB-EGF concentration of control donors (21.2 pg/ml; n=26) as a threshold. 70 % (19/27) of HB-EGF positive patients had disseminated tumours, whereas only 33 % (9/27) of HB-EGF negative patients were lymph node positive. p=0.020 by Mann Whitney's U-Test. Conditional probabilities: P(pN>0 | HB-EGF[+])=0.704 and P(pN>0 | HB-EGF[-])=0.333.

To verify whether elevated HB-EGF plasma levels identify patients with lymph node involvement, we defined the mean plasma HB-EGF concentration of healthy donors (21.2 pg/ml; Figure 23) as a threshold to separate invasive breast carcinoma patients into an HB-EGF negative and positive cohort. In this scoring, 50% (27 of 54) of the patients were determined HB-EGF positive, and tumour cell positive lymph nodes were detected in 52% (28 of 54) of the patients. However, the fraction of disseminated breast carcinomas exceeds 70% (19 of 27) among HB-EGF positive patients, whereas only 33% (9 of 27) of the HB-EGF negative cohort are lymph node positive (Figure 25C).

These data show a strong and highly significant correlation between the protein levels of HB-EGF and OSM in plasma samples of human donors. Our patient data combined with the *in vitro* experiments suggest tumour-primed macrophages to be the source of both ligands *in vivo*. In addition, HB-EGF plasma levels correlate significantly with primary tumour size and the dissemination of tumour cells to lymph nodes.

12.   Tumour *HBEGF* expression is predominantly localised in the stromal compartment

To further substantiate our clinical data, we analysed tumour microarray datasets available at Oncomine™. The breast carcinoma microarray dataset by Ambs and colleagues distinguished between genes expressed by tumour cells on one hand versus stromal cells on the other (Boersma et al., 2008). Our analysis of this dataset revealed considerably elevated levels of *HBEGF* and of the monocytic marker *CD64* in the stromal compartment (Figure 26A), suggesting that tumour-associated mononuclear cells express this EGF family member.

In our *in vitro* experiments, priming of differentiated MΦ was not only achieved by mammary carcinoma cell lines and MΦ-derived factors are functional in other carcinoma cells. Analysis of the bladder carcinoma microarray dataset published by Radvanyi and colleagues (Stransky et al., 2006) showed *HBEGF* to be overrepresented in infiltrating carcinoma samples (Figure 26B). Furthermore, *HBEGF* expression levels increased with tumour grade in this dataset (Figure 26C). These data corroborate our *in vitro* findings that HB-EGF is involved in the progression of a variety of carcinomas.
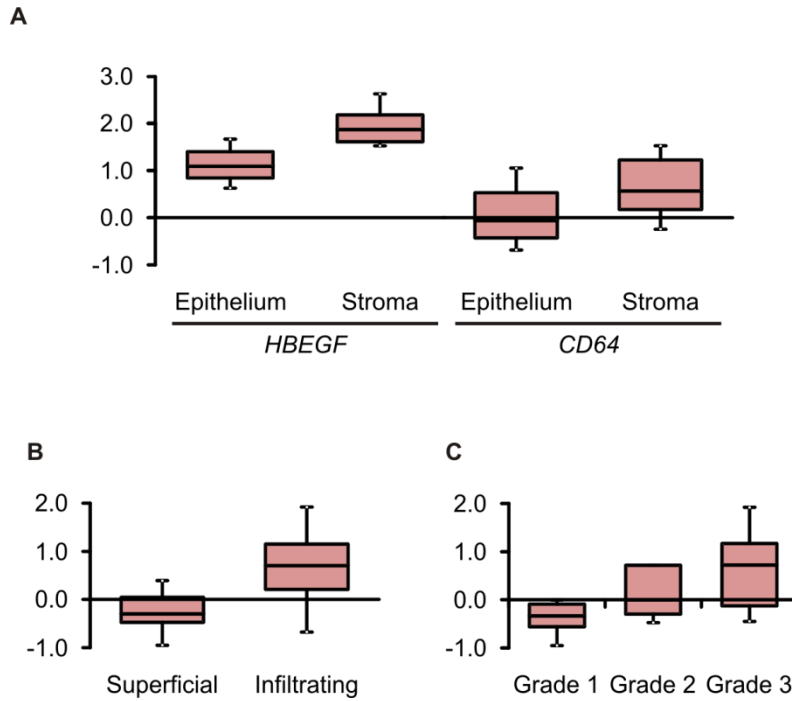
FIGURE 26. *HBEGF* expression in breast and bladder carcinoma. (A) *HBEGF* and the myeloid marker *CD64* are predominantly expressed in the stromal compartment of breast carcinomas. Boxplots show Oncomine™ data analysis of the Boersma breast microarray dataset. Tumour samples were subjected to laser capture microdissection and differential microarray analysis was performed on epithelium (n=48) versus stroma (n=47). **(B)** *HBEGF* is predominantly expressed in infiltrating bladder carcinoma. Oncomine™ data analysis of the Stransky bladder microarray dataset shows the expression of *HBEGF* in infiltrating bladder carcinoma (n=32) versus superficial carcinomas (n=25). **(C)** *HBEGF* expression increases with tumour grade in bladder carcinomas. Oncomine™ data analysis of the Stransky bladder microarray dataset shows the expression of *HBEGF* in grade 1 (n=12), grade 2 (n=11) and grade 3 (n=31) tumours.

V.   DISCUSSION

Tumour cells and associated macrophages engage in an intricate crosstalk which is yet poorly understood at the molecular level. Based on a model that both cell types communicate via secreted factors, we have used cell supernatants to study the reciprocal influence of tumour cells and mononuclear cells. Our main focus was the paracrine signalling of monocytes and macrophages to tumour cells (Pollard, 2004).

By establishing MAD-NT as a new model of spontaneously differentiating monocytes we developed an unbiased screening approach to identify less characterized monocyte-secreted ligands acting on tumour cells. Mass spectrometric analysis of the MAD-NT secretome identified tumour-promoting factors whose secretion by human monocytes had not been described yet, including hepatoma-derived growth factor (HDGF), the soluble metallo-protease ADAMTS-1 and the proangiogenic factor CYR61.

MAD-NT cells secrete an activity that stimulates phosphorylation of STAT3 in a variety of tumour cell lines. Constitutive activation of STAT3 is common in melanoma, breast, head and neck, lung, pancreatic and prostate cancer (Yu and Jove, 2004). We identified oncostatin-M as the STAT3 stimulating factor secreted by MAD-NT monocytes. Oncostatin-M receptors consist of two subunits: gp130, the signalling subunit, is ubiquitously expressed in monocytes and tumour cells. We found the specific ligand binding subunits, OSMRβ and LIFR, to be exclusively expressed in epithelial and carcinoma cells. This indicates that OSM, although constitutively secreted, does not play a role as an autocrine factor in leukemic MAD-NT cells. In addition to MAD-NT, tumour-primed primary PBMC and MΦ secrete OSM, and only mononuclear cell-secreted OSM activates STAT3 in our reporter tumour cell line. This underscores the unique paracrine role of monocyte-derived oncostatin-M acting on tumour cells and confirms MAD-NT cells as a valuable screening model for the identification of monocyte-secreted ligands with a role in the tumour microenvironment. Secretion of OSM has been reported for neutrophils (Queen et al., 2005), T lymphocytes (Boniface et al., 2007) and phorbol esther-activated myeloid leukemia cell lines (Malik et al., 1989).

While MAD-NT cells constitutively secrete large amounts of OSM, we detected only basal levels of OSM to be secreted by freshly isolated PBMC and derived MΦ. Prior incubation with tumour cell supernatants dramatically enhanced secretion of OSM by PBMC and MΦ. This is the first report that shows tumour cell-derived activities to induce OSM secretion by primary human PBMC and MΦ, supporting a paracrine interaction model.

Human PBMC and/or differentiated MΦ were effectively primed by all of the tested tumour cell lines. Priming results in co-secretion of EREG and OSM by PBMC, while tumour-primed MΦ co-secrete HB-EGF and OSM. Priming results in rather complex transcriptional induction profiles of EGFR ligands in PBMC versus MΦ and depends on the primed cell type and priming duration. We observed three distinct transcript induction patterns, each

involving at least one additional EGFR ligand that was induced transcriptionally but not shed in soluble form. Primed PBMC did not shed soluble TGFα, while primed MΦ did not shed EREG or AREG. However, this transcriptional complexity is lost at the secretory level, and only PBMC-derived EREG and MΦ-produced HB-EGF stand out as functionally relevant EGFR ligands. Thus, transcriptional regulation plus posttranslational modification mechanisms select the functionally active EGFR ligands secreted by mononuclear cells upon priming. Our comparative analysis indicates that tumour-associated mononuclear cell types are characterized by the EGFR ligand they secrete.

However, the fact that mononuclear cells upregulate several EGF family transcripts in response to tumour cells might have further implications. EGFR ligand secretion is controlled by post-transcriptional mechanisms, e.g. by translational regulation of the ligands or expression and activation of shedding enzymes that liberate membrane-bound EGFR proligands. Primed tumour-associated monocytes/MΦ presenting several EGFR proligands on their plasma membrane might serve as stores from which soluble ligands can be mobilised in a paracrine fashion. One such pathway is the EGFR transactivation, a process during which several stimuli, from GPCR ligands to cytokines and cellular stress, lead to ADAM-mediated shedding of soluble EGFR ligands (Gschwind et al., 2001). OSM transcripts were readily detectable in control PBMC and MΦ, and were upregulated 3- to 7-fold upon priming. By comparison, levels of secreted OSM were very low to undetectable in supernatants from control PBMC/MΦ, and were increased 12- to 28-fold upon priming. This indicates that OSM secretion, which follows the classical secretory pathway, is also subject to posttranscriptional regulation.

Recently, Wongkham and colleagues performed a transcriptional analysis of PBMC from patients with cholangiocarcinoma. Although *EREG* transcript levels were elevated in these patients, no correlation to clinical parameters was found. This indicates that transcriptional analysis alone cannot predict the functionally relevant EGFR agonist released by tumour-primed mononuclear cells (Subimerb et al., 2010).

In summary, two secretory patterns emerge in PBMC and MΦ in response to interaction with tumour cells. In contrast to genomically variable cancer cells, genetically stable mononuclear cells respond to tumour cells by the stereotype secretion of a specific EGFR ligand in combination with OSM.

Our model further shows that the mutual exchange of two IL-6 family ligands leads to the activation of STAT3 transcription factors in carcinoma cells and mononuclear cells. Mononuclear cell-secreted OSM is exclusively active in epithelial cells and derived tumour cells, while two of the five tested carcinoma cells express IL-6, which activates STAT3 in mononuclear cells. A series of reports have shown that persistent STAT3 activity in tumour-infiltrating immune cells is essential in abrogating antitumour immune responses (Cheng et al., 2003; Cheng et al., 2008; Kortylewski et al., 2005; Wang et al., 2004). Our findings indicate that tumour cell-derived IL-6 might be primarily important in suppressing immunosurveillance mechanisms in tumour-associated mononuclear cells. Recently, a

monoclonal antibody targeting IL-6 was tested in phase II clinical trials in prostate and metastatic renal cancer patients. The obtained results were rather disappointing, perhaps illustrating that a monotherapy directed against a factor that is predominantly active in stromal cells is not beneficial in patients with advanced tumours (Dorff et al., 2010; Rossi et al., 2010). Yet, at the same time an antibody targeting the IL-6 receptor is being successfully used to treat rheumatoid arthritis patients, confirming that patients with inflammatory disorders benefit from IL-6 pathway inhibition (Jones and Ding, 2010).

On the biological level, recombinant OSM and HB-EGF strongly cooperate in inducing chemotaxis of benign breast cells. For this cell type, HB-EGF acts as a strong mitogen. Contradicting previous reports (Grant and Begley, 1999; Underhill-Day and Heath, 2006; Zarling et al., 1986), OSM alone shows antiproliferative activity in only one out of the six breast tumour cell lines tested. However, recent studies have revealed that OSM stimulates cell motility and detachment from substratum (Holzer et al., 2004; Jorcyk et al., 2006). Thus, OSM-mediated cell detachment might have contributed to the lower numbers of adherent cells recorded upon OSM treatment in previous reports. Importantly, OSM is increasing the intrinsic motility of carcinoma cells, while macrophage-secreted HB-EGF is the key chemotactic factor for squamous cell carcinoma cells. In addition, HB-EGF influences tumour cell proliferation. Our *in vitro* data suggest that the combination of TAM-derived OSM and HB-EGF furthermore enhances migratory processes of cancer cells.

Identifying expression patterns that are specific for tumour-associated mononuclear cells in cancer patient microarray datasets is a difficult undertaking. On the one hand, as indicated by our *in vitro* data, tumour cells differ in their ability to provoke priming responses in infiltrating mononuclear cells. On the other hand, the vast majority of microarray expression profiles were gathered from whole tumour samples and do not distinguish between genes expressed by tumour or stromal cells. Data that do allow for this distinction, like the Boersma breast set, are based on laser capture microdissection, a laborious method that can only be performed on a small number of samples. Analysis of these datasets reveals that in prostate, bladder and breast tumours, *HBEGF* is co-expressed with other *EGF* family and *IL6* family ligands. This co-expression is predominantly accompanied by myeloid markers and underscores transcript induction profiles we observed in tumour-primed mononuclear cells *in vitro*. These patterns indicate that myeloid cells in the tumour environment express *EGF* and *IL6* family ligands in primary tumours of different origin, *in vitro* and *in vivo*.

Supporting our hypothesis that TAM-derived HB-EGF and OSM act on tumour cells *in vivo*, systemic HB-EGF protein levels are strongly associated with primary tumour growth in invasive breast cancer patients. In particular, lymph node dissemination is accompanied by increased HB-EGF levels, as the majority of lymph node positive patients displays elevated HB-EGF plasma levels. In general, elevated HB-EGF concentrations strongly correlate with increased OSM plasma protein levels.

Elevated HB-EGF and OSM concentrations in plasma samples of breast cancer patients suggest a major contribution of TAM to tumour growth and metastasis *in vivo*. *HBEGF* transcripts are mainly detected in the stroma of mammary carcinomas and correlate with the myeloid marker *CD64*, further supporting the assumption that TAM account for the expression of *HBEGF* in the tumour microenvironment.

The involvement of OSM in tumorigenesis and tumour progression has not been extensively studied. However, increased phosphorylation of its downstream effector, STAT3, is common in human breast carcinomas and relates to tumour size (Yeh et al., 2006) and lymph node dissemination (Hsieh et al., 2005). In a mouse model of activated *neu*-driven mammary carcinoma formation, conditional ablation of STAT3 in tumour cells reduced tumour growth and minimised metastasis formation to the lungs. These data reveal a degree of convergence between EGFR-like downstream signals and STAT3 activity in tumour growth and dissemination. Moreover, STAT3 depletion is accompanied by downregulation of a number of inflammatory mediators and *osmrß* in particular in primary tumours (Ranger et al., 2009).

Several *in vivo* models have shown that EGFR ligand overexpression in mouse mammary glands results in lesions ranging from benign hyperplasia to invasive, metastatic carcinoma (Schroeder and Lee, 1997; Seitzer et al., 2010). In patients, EREG and HB-EGF expression are well studied particularly in bladder carcinomas, where transcript levels inversely correlate with patients' survival (Thogersen et al., 2001). Our analysis of the Stransky bladder carcinoma microarray dataset (Stransky et al., 2006) corroborated these findings inasmuch as *HBEGF* transcript levels increase in infiltrating tumours with respect to superficially growing lesions. This and the positive correlation between *HBEGF* expression and tumour grade indicates that *HBEGF* promotes tumour progression in these patients. *HBEGF* sustains the specific dissemination of human mammary tumour cells to the brain, whereas dissemination to the lung is promoted by *EREG* expression, as Massagué and co-workers have shown in mouse xenograft models (Bos et al., 2009; Minn et al., 2005). Our data on differential priming capacities of tumour cells towards PBMC versus MΦ implicate that specific subsets of mononuclear cells might be involved in organ-specific metastatic processes. Figure 27 illustrates our model for the interaction between carcinoma cells and mononuclear cells.

The detection of HB-EGF and OSM proteins in plasma of two patients with fibroadenomas indicates that the secretion of these ligands is not restricted to malignant tumours. PBMC isolated from patients with fibroadenoma and fibroadenosis display decreased phagocytosis and chemotaxis, revealing an interaction of myeloid and tumour cells even in benign lesions (Al-Sumidaie et al., 1987). Apart from tumorigenesis, the cooperative emergence of HB-EGF and OSM even in inflammatory situations is apparent in one patient with Crohn's disease. For these patients, so far only elevated plasma levels of IL-6 have been reported (Gross et al., 1992).
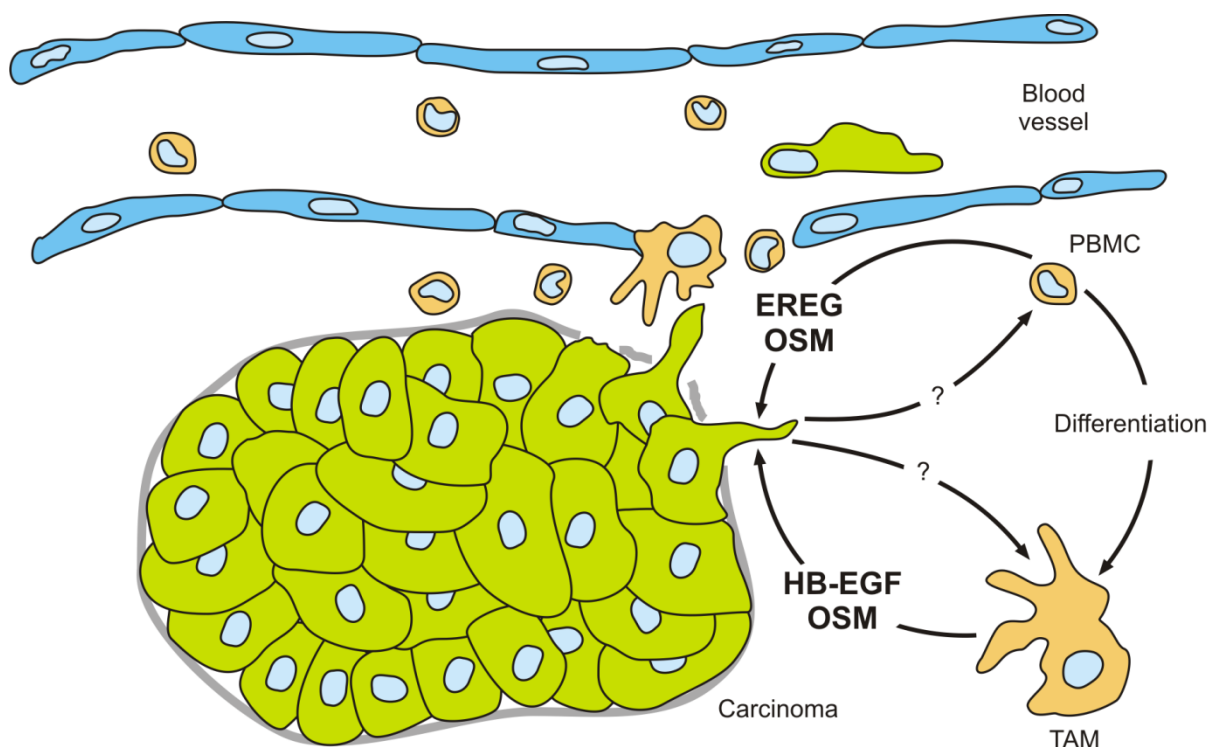
FIGURE 27. Paracrine interaction model between tumour cells and associated monocytes/macrophages. PBMC extravasate in the vicinity of a developing tumour and respond to tumour-derived soluble factors by co-secreting EREG and OSM. After differentiation, TAM secrete HB-EGF and OSM. EREG, HB-EGF and OSM secreted by infiltrating mononuclear cells act on tumour cells, activating EGFR and STAT3 pathways, ultimately accelerating tumour progression. Figure adapted from Condeelis and colleagues (Wang et al., 2005).

The co-secretion of EREG/HB-EGF and OSM by mononuclear cells raises questions about the role these secretory pathways might play under normal or pathological conditions. One possibility is that tumour cells exploit functions exerted by mononuclear cells during organogenesis and in homeostasis. HB-EGF-null mice are characterized by severely impaired heart development and a mouse model overexpressing soluble HB-EGF displays heart and skin hyperplasia (Iwamoto et al., 2003; Yamazaki et al., 2003). These data point out that controlled HB-EGF expression is crucial for development and homeostasis of heart and skin. Similarly, EREG-null mice suffer from chronic dermatitis (Shirasawa et al., 2004). While no data are published on OSM ablation, STAT3-null mice are embryonic lethal, underlining the pivotal role of this transcription factor during development (Takeda et al., 1997).

Conversely, the observed mononuclear priming mechanisms might be relevant for wound healing processes. Until lately, the exact role of MΦ infiltrating skin wounds has been a matter of debate. Eming and colleagues have recently developed a mouse model of selective MΦ depletion during distinct stages of skin repair (Lucas et al., 2010). Early-stage MΦ depletion hampered wound contraction, keratinocyte proliferation and granulation tissue formation, while mid-stage depletion resulted in impaired angiogenesis, severe bleeding and the abrogation of the repair cycle. Infiltrating MΦ of wild-type mice were identified as alternatively activated (M2), a phenotype that has previously been attributed to tumour-

associated macrophages (Sica et al., 2006). It is not yet known how monocytes are recruited into wounds and how their activation is directed. However, macrophage chemoattractants like MCP-1 are found in wounds and in the tumour microenvironment, where they serve as prognostic factors for cancer patient survival (Engelhardt et al., 1998; Ueno et al., 2000). However, there is indirect evidence pointing to possible roles of HB-EGF and OSM in wound healing. Klagsbrun and colleagues have described the secretion of HB-EGF in porcine wounds (Marikovsky et al., 1993). The keratinocyte-specific knockout of HB-EGF impaired epithelialisation in a mouse model of cutaneous wound healing (Shirakata et al., 2005). OSM secretion in wounds is so far only described for polymorphonuclear neutrophils (Goren et al., 2006). The mitogenic action of HB-EGF and the promigratory actions of HB-EGF and OSM point to a possible role of MΦ-secreted HB-EGF and OSM in early wound repair, which requires cells to detach from the epithelial monolayer and close the wound through migration and proliferation.

A recent report speculates on a paracrine loop involving HB-EGF secretion by macrophages (Rigo et al., 2010). The authors describe moderate induction levels of HB-EGF in their *in vitro* system. The mode of preparation of the phagocytic population, however, suggests that in fact PBMC were studied. Although an interesting aspect of the priming process of mononuclear cells is presented, strongly elevated HB-EGF plasma concentrations we observed in cancer patient samples are hardly explained by the model these authors propose.

Recent scientific advances have established that monocytes and macrophages are not only critically involved in inflammatory processes such as pathogen defence and wound healing, but also play an active role in cancer development. Their functions are modulated by tumour cells, resulting in tolerant, trophic phenotypes that are indispensable for tumour progression, but that are yet poorly understood (Pollard, 2004).

We show that tumour cell-secreted factors act on human peripheral blood monocytes and differentiated macrophages, where they induce secretory patterns that consistently lead to the paracrine activation of oncogenic EGFR- and STAT3 pathways in tumour cells. We identify HB-EGF and OSM as the key EGFR and STAT3 activators secreted by tumour-primed MΦ, and EREG and OSM as the key activating factors secreted by tumour-primed PBMC. HB-EGF and OSM profoundly influence tumour cell behaviour and cooperatively promote cell motility. Our work identifies HB-EGF, EREG and OSM as potential blood-bound markers that indicate pro-tumorigenic actions of tumour-associated monocytes and macrophages. Moreover, our results obtained *in vitro* indicate that these three proteins effectively mediate mononuclear cell-assisted cancer progression. We identified stereotype secretion patterns which are elementary for the development of specific ablation strategies designed to interfere with pro-tumorigenic mononuclear functions by inhibition of HB-EGF, EREG and OSM. The presented data suggest that HB-EGF in particular is functionally connected to tumour growth and dissemination. But prior to therapeutic approaches, a clear clinical characterization of the subset of tumours infiltrated by pro-tumorigenic

mononuclear cells is essential. The secretory patterns described here not only allow for the minimally invasive identification of the cohort of tumours supported by TAM and tumour-associated monocytes. Additionally, the detection of these patterns discriminates between subtypes of mononuclear cells involved in tumour progression. As such, the combination of elevated levels of HB-EGF and OSM specifies TAM, while monocytes are characterized by increased EREG plus OSM levels. Our work describes protumorigenic marker proteins that identify tumour-supportive mononuclear cells, thus establishing a basis for therapeutic intervention aimed at neutralising these STAT3 and EGFR activators at the molecular level.

VI. SUMMARY

Tumour-associated macrophages (TAM) promote malignant progression, yet the repertoire of tumour-promoting ligands they secrete is poorly characterized. In a two-step approach, we investigated pro-tumour factors secreted by mononuclear cells that activate two of the most important oncogenic pathways: EGFR and STAT3.

In a first step, we analysed MAD-NT, a spontaneously differentiating monocytic cell line. MAD-NT supernatant strongly activates STAT3 transcription factors in a variety of carcinoma cell lines. Mass spectrometric analysis of MAD-NT supernatants revealed oncostatin-M (OSM), a ligand of the IL-6 family, which activates STAT3 in several tumour cell lines.

In a second step, we validated our findings from the MAD-NT model system by analysing primary human mononuclear cells as well as plasma samples and microarray datasets of cancer patients. To explore the influence of tumour cell-secreted factors on the release of tumour-promoting factors by mononuclear cells, we performed priming experiments, exposing freshly isolated peripheral blood monocytes (PBMC) or *in vitro* differentiated primary macrophages (MΦ) to supernatants of various tumour and non-tumour cell lines. Only upon exposure to tumour cell-supernatants, peripheral blood monocytes and macrophages secrete one specific EGF family ligand each and OSM, a common STAT3 activator, triggering two of the pathways most frequently associated with tumour progression. Primed monocytes secrete epiregulin (EREG) and OSM, while macrophages secrete heparin-binding EGF-like growth factor (HB-EGF) and OSM.

At the cellular level, HB-EGF is a strong mitogen for breast-derived cells. Apart from that, HB-EGF potently induces chemotaxis of carcinoma and breast hyperplastic cells. HB-EGF secreted by tumour-primed MΦ is the main chemotactic ligand for SCC-9 squamous carcinoma cells. OSM strongly upregulates the undirected motility of tumour cells, and HB-EGF and OSM cooperatively induce chemotaxis of benign mammary cells.

Our analysis of microarray datasets from patients with prostate, bladder and breast tumours identified co-expression patterns that involve *HBEGF* and other *EGF* and *IL6* family ligands. In mammary carcinoma patients, elevated HB-EGF and OSM plasma protein levels correlate, and *HBEGF* is predominantly expressed in the tumour stroma. The observed co-expression and co-secretion patterns indicate that tumour-associated mononuclear cells secrete HB-EGF and OSM in cancer patients. Elevated HB-EGF plasma protein levels accompany tumour growth and dissemination in patients with invasive disease.

We identify monocyte/macrophage-secreted EREG, HB-EGF and OSM as potential targets for therapeutic intervention in the macrophage-assisted dissemination of tumours. Plasma levels of HB-EGF, EREG and OSM secreted by primed monocytes/macrophages of breast cancer patients could serve as novel markers indicating a pro-tumorigenic activation of mononuclear cells.

VII. ZUSAMMENFASSUNG

Tumorassoziierte Makrophagen (TAM) fördern die Progression von Tumoren. Das Repertoire tumorfördernder Liganden, die TAM sezernieren, ist unzureichend charakterisiert. In einem zweistufigen Ansatz wurden tumorfördernde Faktoren untersucht, die von mononukleären Zellen sezerniert werden und zwei der wichtigsten onkogenen Signalwege aktivieren: EGFR und STAT3.

Im ersten Schritt wurde das Sekretom von MAD-NT untersucht, einer spontan differenzierenden monozytischen Zelllinie. MAD-NT-Kulturüberstände aktivieren STAT3-Transkriptionsfaktoren in einer Reihe von Karzinomzelllinien. Die massenspektrometrische Untersuchung von MAD-NT Kulturüberständen identifizierte Oncostatin-M (OSM), einen Liganden der IL-6-Familie, welcher STAT3 in mehreren Tumorzelllinien aktiviert.

Die Validierung der Erkenntnisse aus dem MAD-NT-Modell erfolgte durch die Untersuchung primärer humaner mononukleärer Zellen sowie von Plasmaproben und Microarray-Datensätzen von Krebspatienten. Priming-Versuche charakterisierten den Einfluss Tumor-sezernierter Faktoren auf die Ausschüttung pro-tumorigener Faktoren durch mononukleäre Zellen. Dabei stellte sich heraus, dass primäre Blutmonozyten und Makrophagen erst nach Kontakt mit Tumorzellüberständen je einen spezifischen Liganden der EGF-Familie sowie einen gemeinsamen STAT3-Aktivator sezernieren. So vorbehandelte Monozyten sezernieren Epiregulin (EREG) und Oncostatin-M, während Makrophagen Heparin-binding EGF-like growth factor (HB-EGF) und OSM ausschütten.

HB-EGF wirkt stark mitogen auf hyperplastische Brustzellen und chemotaktisch in Karzinomzellen und hyperplastischen Zellen. So ist von Makrophagen im Tumor-Kontext sezerniertes HB-EGF der entscheidende chemotaktische Faktor in SCC-9 Karzinomzellen, während Oncostatin-M die ungerichtete Motilität von Tumorzellen erhöht. HB-EGF und OSM induzieren synergistisch die Chemotaxis benigner hyperplastischer Brustepithelzellen.

Bei der Analyse von Microarray-Datensätzen von Patienten mit Prostata-, Blasen- und Brusttumoren konnten Koexpressionsprofile von *HBEGF* mit weiteren Liganden der *EGF*- und *IL6*-Familie identifiziert werden. Plasmamengen von HB-EGF und OSM in Patienten mit Brustkarzinomen korrelieren, wobei *HBEGF* vorwiegend im Stroma exprimiert wird. Die in Krebspatienten beobachteten Expressions- und Sekretionsprofile weisen darauf hin, dass tumorassoziierte mononukleäre Zellen HB-EGF und OSM kosezernieren. Erhöhte HB-EGF Proteinmengen im Plasma von Brustkrebspatienten gehen einher mit stärkerem Tumorwachstum und Lymphknotenbefall.

Unsere Untersuchung hat EREG, HB-EGF und OSM als mögliche Ziele für die therapeutische Intervention gegen die Förderung der Tumormetastasierung durch mononukleäre Zellen identifiziert. Erhöhte Plasmamengen von HB-EGF, EREG und OSM in Brustkrebspatienten könnten als neue Marker dienen, die eine Pro-Tumorreaktion mononukleärer Zellen anzeigen.

VIII. REFERENCES

Al-Sumidaie, A. M., Leinster, S. J., and Jenkins, S. A. (1987). Altered monocyte function in patients with benign breast disease. Clin Exp Immunol *67*, 198-204.

Algarra, I., Cabrera, T., and Garrido, F. (2000). The HLA crossroad in tumor immunology. Hum Immunol *61*, 65-73.

Arredondo, J., Chernyavsky, A. I., Jolkovsky, D. L., Pinkerton, K. E., and Grando, S. A. (2006). Receptor-mediated tobacco toxicity: cooperation of the Ras/Raf-1/MEK1/ERK and JAK-2/STAT-3 pathways downstream of alpha7 nicotinic receptor in oral keratinocytes. FASEB J *20*, 2093-2101.

Banaei-Bouchareb, L., Gouon-Evans, V., Samara-Boustani, D., Castellotti, M. C., Czernichow, P., Pollard, J. W., and Polak, M. (2004). Insulin cell mass is altered in Csf1op/Csf1op macrophage-deficient mice. J Leukoc Biol *76*, 359-367.

Baud, V., and Karin, M. (2009). Is NF-kappaB a good target for cancer therapy? Hopes and pitfalls. Nat Rev Drug Discov *8*, 33-40.

Bingle, L., Brown, N. J., and Lewis, C. E. (2002). The role of tumour-associated macrophages in tumour progression: implications for new anticancer therapies. The Journal of Pathology *196*, 254-265.

Blagoev, B., Ong, S. E., Kratchmarova, I., and Mann, M. (2004). Temporal analysis of phosphotyrosine-dependent signaling networks by quantitative proteomics. Nat Biotechnol *22*, 1139-1145.

Boersma, B. J., Reimers, M., Yi, M., Ludwig, J. A., Luke, B. T., Stephens, R. M., Yfantis, H. G., Lee, D. H., Weinstein, J. N., and Ambs, S. (2008). A stromal gene signature associated with inflammatory breast cancer. Int J Cancer *122*, 1324-1332.

Bollrath, J., and Greten, F. R. (2009). IKK/NF-kappaB and STAT3 pathways: central signalling hubs in inflammation-mediated tumour promotion and metastasis. EMBO Rep *10*, 1314-1319.

Bollrath, J., Phesse, T. J., von Burstin, V. A., Putoczki, T., Bennecke, M., Bateman, T., Nebelsiek, T., Lundgren-May, T., Canli, O., Schwitalla, S., *et al.* (2009). gp130-mediated Stat3 activation in enterocytes regulates cell survival and cell-cycle progression during colitis-associated tumorigenesis. Cancer Cell *15*, 91-102.

Boniface, K., Diveu, C., Morel, F., Pedretti, N., Froger, J., Ravon, E., Garcia, M., Venereau, E., Preisser, L., Guignouard, E., *et al.* (2007). Oncostatin M secreted by skin infiltrating T lymphocytes is a potent keratinocyte activator involved in skin inflammation. J Immunol *178*, 4615-4622.

Bos, P. D., Zhang, X. H., Nadal, C., Shu, W., Gomis, R. R., Nguyen, D. X., Minn, A. J., van de Vijver, M. J., Gerald, W. L., Foekens, J. A., and Massague, J. (2009). Genes that mediate breast cancer metastasis to the brain. Nature *459*, 1005-1009.

Brechot, C. (2004). Pathogenesis of hepatitis B virus-related hepatocellular carcinoma: old and new paradigms. Gastroenterology *127*, S56-61.

Bromberg, J. F., Horvath, C. M., Besser, D., Lathem, W. W., and Darnell, J. E., Jr. (1998). Stat3 activation is required for cellular transformation by v-src. Mol Cell Biol *18*, 2553-2558.

Bromberg, J. F., Wrzeszczynska, M. H., Devgan, G., Zhao, Y., Pestell, R. G., Albanese, C., and Darnell, J. E., Jr. (1999). Stat3 as an oncogene. Cell *98*, 295-303.

Bronte-Tinkew, D. M., Terebiznik, M., Franco, A., Ang, M., Ahn, D., Mimuro, H., Sasakawa, C., Ropeleski, M. J., Peek, R. M., Jr., and Jones, N. L. (2009). Helicobacter pylori cytotoxin-associated gene A activates the signal transducer and activator of transcription 3 pathway in vitro and in vivo. Cancer Res *69*, 632-639.

Burnet, F. M. (1970). The concept of immunological surveillance. Prog Exp Tumor Res *13*, 1-27.

Cheng, F., Wang, H. W., Cuenca, A., Huang, M., Ghansah, T., Brayer, J., Kerr, W. G., Takeda, K., Akira, S., Schoenberger, S. P., *et al.* (2003). A critical role for Stat3 signaling in immune tolerance. Immunity *19*, 425-436.

Cheng, P., Corzo, C. A., Luetteke, N., Yu, B., Nagaraj, S., Bui, M. M., Ortiz, M., Nacken, W., Sorg, C., Vogl, T., *et al.* (2008). Inhibition of dendritic cell differentiation and accumulation of myeloid-derived suppressor cells in cancer is regulated by S100A9 protein. J Exp Med *205*, 2235-2249.

Choudhari, S. R., Khan, M. A., Harris, G., Picker, D., Jacob, G. S., Block, T., and Shailubhai, K. (2007). Deactivation of Akt and STAT3 signaling promotes apoptosis, inhibits proliferation, and enhances the sensitivity of hepatocellular carcinoma cells to an anticancer agent, Atiprimod. Mol Cancer Ther *6*, 112-121.

Coca, S., Perez-Piqueras, J., Martinez, D., Colmenarejo, A., Saez, M. A., Vallejo, C., Martos, J. A., and Moreno, M. (1997). The prognostic significance of intratumoral natural killer cells in patients with colorectal carcinoma. Cancer *79*, 2320-2328.

Collins, S. J. (1987). The HL-60 promyelocytic leukemia cell line: proliferation, differentiation, and cellular oncogene expression. Blood *70*, 1233-1244.

Coussens, L. M., and Werb, Z. (2002). Inflammation and cancer. Nature *420*, 860-867.

Cox, J., and Mann, M. (2008). MaxQuant enables high peptide identification rates, individualized p.p.b.-range mass accuracies and proteome-wide protein quantification. Nat Biotechnol *26*, 1367-1372.

Dannenberg, A. J., and Subbaramaiah, K. (2003). Targeting cyclooxygenase-2 in human neoplasia: rationale and promise. Cancer Cell *4*, 431-436.

De Luca, A., and Iaquinto, G. (2004). Helicobacter pylori and gastric diseases: a dangerous association. Cancer Lett *213*, 1-10.

De Palma, M., Venneri, M. A., Galli, R., Sergi Sergi, L., Politi, L. S., Sampaolesi, M., and Naldini, L. (2005). Tie2 identifies a hematopoietic lineage of proangiogenic monocytes required for tumor vessel formation and a mesenchymal population of pericyte progenitors. Cancer Cell *8*, 211-226.

De Wever, O., Nguyen, Q. D., Van Hoorde, L., Bracke, M., Bruyneel, E., Gespach, C., and Mareel, M. (2004). Tenascin-C and SF/HGF produced by myofibroblasts in vitro provide convergent pro-invasive signals to human colon cancer cells through RhoA and Rac. FASEB J *18*, 1016-1018.

Dennis, G., Jr., Sherman, B. T., Hosack, D. A., Yang, J., Gao, W., Lane, H. C., and Lempicki, R. A. (2003). DAVID: Database for Annotation, Visualization, and Integrated Discovery. Genome Biol *4*, P3.

Dorff, T. B., Goldman, B., Pinski, J. K., Mack, P. C., Lara, P. N., Jr., Van Veldhuizen, P. J., Jr., Quinn, D. I., Vogelzang, N. J., Thompson, I. M., Jr., and Hussain, M. H. (2010). Clinical and correlative results of SWOG S0354: a phase II trial of CNTO328 (siltuximab), a monoclonal antibody against interleukin-6, in chemotherapy-pretreated patients with castration-resistant prostate cancer. Clin Cancer Res *16*, 3028-3034.

Downward, J., Yarden, Y., Mayes, E., Scrace, G., Totty, N., Stockwell, P., Ullrich, A., Schlessinger, J., and Waterfield, M. D. (1984). Close similarity of epidermal growth factor receptor and v-erb-B oncogene protein sequences. Nature *307*, 521-527.

Dunn, G. P., Old, L. J., and Schreiber, R. D. (2004). The immunobiology of cancer immunosurveillance and immunoediting. Immunity *21*, 137-148.

Engelhardt, E., Toksoy, A., Goebeler, M., Debus, S., Brocker, E. B., and Gillitzer, R. (1998). Chemokines IL-8, GROalpha, MCP-1, IP-10, and Mig are sequentially and differentially expressed during phase-specific infiltration of leukocyte subsets in human wound healing. Am J Pathol *153*, 1849-1860.

Epling-Burnette, P. K., Liu, J. H., Catlett-Falcone, R., Turkson, J., Oshiro, M., Kothapalli, R., Li, Y., Wang, J. M., Yang-Yen, H. F., Karras, J., *et al.* (2001). Inhibition of STAT3 signaling leads to apoptosis of leukemic large granular lymphocytes and decreased Mcl-1 expression. J Clin Invest *107*, 351-362.

Fenner, F. (1982). A successful eradication campaign. Global eradication of smallpox. Rev Infect Dis *4*, 916-930.

Folkman, J. (2003). Fundamental concepts of the angiogenic process. Curr Mol Med *3*, 643-651.

Friedell, G. H., Betts, A., and Sommers, S. C. (1965). The Prognostic Value of Blood Vessel Invasion and Lymphocytic Infiltrates in Breast Carcinoma. Cancer *18*, 164-166.

Gallagher, R., Collins, S., Trujillo, J., McCredie, K., Ahearn, M., Tsai, S., Metzgar, R., Aulakh, G., Ting, R., Ruscetti, F., and Gallo, R. (1979). Characterization of the continuous, differentiating myeloid cell line (HL-60) from a patient with acute promyelocytic leukemia. Blood *54*, 713-733.

Garcia, R., Bowman, T. L., Niu, G., Yu, H., Minton, S., Muro-Cacho, C. A., Cox, C. E., Falcone, R., Fairclough, R., Parsons, S.*, et al.* (2001). Constitutive activation of Stat3 by the Src and JAK tyrosine kinases participates in growth regulation of human breast carcinoma cells. Oncogene *20*, 2499-2513.

Garcia, R., Yu, C. L., Hudnall, A., Catlett, R., Nelson, K. L., Smithgall, T., Fujita, D. J., Ethier, S. P., and Jove, R. (1997). Constitutive activation of Stat3 in fibroblasts transformed by diverse oncoproteins and in breast carcinoma cells. Cell Growth Differ *8*, 1267-1276.

Gershoni, J. M., and Palade, G. E. (1982). Electrophoretic transfer of proteins from sodium dodecyl sulfate-polyacrylamide gels to a positively charged membrane filter. Anal Biochem *124*, 396-405.

Goren, I., Kampfer, H., Muller, E., Schiefelbein, D., Pfeilschifter, J., and Frank, S. (2006). Oncostatin M expression is functionally connected to neutrophils in the early inflammatory phase of skin repair: implications for normal and diabetes-impaired wounds. J Invest Dermatol *126*, 628-637.

Gouon-Evans, V., Rothenberg, M. E., and Pollard, J. W. (2000). Postnatal mammary gland development requires macrophages and eosinophils. Development *127*, 2269-2282.

Grandis, J. R., Drenning, S. D., Chakraborty, A., Zhou, M. Y., Zeng, Q., Pitt, A. S., and Tweardy, D. J. (1998). Requirement of Stat3 but not Stat1 activation for epidermal growth factor receptor- mediated cell growth In vitro. J Clin Invest *102*, 1385-1392.

Grant, S. L., and Begley, C. G. (1999). The oncostatin M signalling pathway: reversing the neoplastic phenotype? Mol Med Today *5*, 406-412.

Graus-Porta, D., Beerli, R. R., Daly, J. M., and Hynes, N. E. (1997). ErbB-2, the preferred heterodimerization partner of all ErbB receptors, is a mediator of lateral signaling. EMBO J *16*, 1647-1655.

Grivennikov, S., Karin, E., Terzic, J., Mucida, D., Yu, G. Y., Vallabhapurapu, S., Scheller, J., Rose-John, S., Cheroutre, H., Eckmann, L., and Karin, M. (2009). IL-6 and Stat3 are required for survival of intestinal epithelial cells and development of colitis-associated cancer. Cancer Cell *15*, 103-113.

Gross, V., Andus, T., Caesar, I., Roth, M., and Scholmerich, J. (1992). Evidence for continuous stimulation of interleukin-6 production in Crohn's disease. Gastroenterology *102*, 514-519.

Gschwind, A., Fischer, O. M., and Ullrich, A. (2004). The discovery of receptor tyrosine kinases: targets for cancer therapy. Nat Rev Cancer *4*, 361-370.

Gschwind, A., Hart, S., Fischer, O. M., and Ullrich, A. (2003). TACE cleavage of proamphiregulin regulates GPCR-induced proliferation and motility of cancer cells. EMBO J *22*, 2411-2421.

Gschwind, A., Prenzel, N., and Ullrich, A. (2002). Lysophosphatidic acid-induced squamous cell carcinoma cell proliferation and motility involves epidermal growth factor receptor signal transactivation. Cancer Res *62*, 6329-6336.

Gschwind, A., Zwick, E., Prenzel, N., Leserer, M., and Ullrich, A. (2001). Cell communication networks: epidermal growth factor receptor transactivation as the paradigm for interreceptor signal transmission. Oncogene *20*, 1594-1600.

Higashiyama, S., Abraham, J. A., Miller, J., Fiddes, J. C., and Klagsbrun, M. (1991). A heparin-binding growth factor secreted by macrophage-like cells that is related to EGF. Science *251*, 936-939.

Holzer, R. G., Ryan, R. E., Tommack, M., Schlekeway, E., and Jorcyk, C. L. (2004). Oncostatin M stimulates the detachment of a reservoir of invasive mammary carcinoma cells: role of cyclooxygenase-2. Clin Exp Metastasis *21*, 167-176.

Hsieh, F. C., Cheng, G., and Lin, J. (2005). Evaluation of potential Stat3-regulated genes in human breast cancer. Biochem Biophys Res Commun *335*, 292-299.

Huang da, W., Sherman, B. T., and Lempicki, R. A. (2009). Systematic and integrative analysis of large gene lists using DAVID bioinformatics resources. Nat Protoc *4*, 44-57.

Hunder, N. N., Wallen, H., Cao, J., Hendricks, D. W., Reilly, J. Z., Rodmyre, R., Jungbluth, A., Gnjatic, S., Thompson, J. A., and Yee, C. (2008). Treatment of metastatic melanoma with autologous CD4+ T cells against NY-ESO-1. N Engl J Med *358*, 2698-2703.

Hutterer, M., Knyazev, P., Abate, A., Reschke, M., Maier, H., Stefanova, N., Knyazeva, T., Barbieri, V., Reindl, M., Muigg, A*., et al.* (2008). Axl and growth arrest-specific gene 6 are frequently overexpressed in human gliomas and predict poor prognosis in patients with glioblastoma multiforme. Clin Cancer Res *14*, 130-138.

Hynes, N. E., and Lane, H. A. (2005). ERBB receptors and cancer: the complexity of targeted inhibitors. Nat Rev Cancer *5*, 341-354.

Ishigami, S., Natsugoe, S., Tokuda, K., Nakajo, A., Che, X., Iwashige, H., Aridome, K., Hokita, S., and Aikou, T. (2000). Prognostic value of intratumoral natural killer cells in gastric carcinoma. Cancer *88*, 577-583.

Iwamoto, R., Yamazaki, S., Asakura, M., Takashima, S., Hasuwa, H., Miyado, K., Adachi, S., Kitakaze, M., Hashimoto, K., Raab, G.*, et al.* (2003). Heparin-binding EGF-like growth factor and ErbB signaling is essential for heart function. Proc Natl Acad Sci U S A *100*, 3221-3226.

Jaini, R., Kesaraju, P., Johnson, J. M., Altuntas, C. Z., Jane-Wit, D., and Tuohy, V. K. (2010). An autoimmune-mediated strategy for prophylactic breast cancer vaccination. Nat Med *16*, 799-803.

Jensen, L. J., Kuhn, M., Stark, M., Chaffron, S., Creevey, C., Muller, J., Doerks, T., Julien, P., Roth, A., Simonovic, M.*, et al.* (2009). STRING 8--a global view on proteins and their functional interactions in 630 organisms. Nucleic Acids Res *37*, D412-416.

Johansson, M., Denardo, D. G., and Coussens, L. M. (2008). Polarized immune responses differentially regulate cancer development. Immunol Rev *222*, 145-154.

Jones, G., and Ding, C. (2010). Tocilizumab: a review of its safety and efficacy in rheumatoid arthritis. Clin Med Insights Arthritis Musculoskelet Disord *3*, 81-89.

Jorcyk, C. L., Holzer, R. G., and Ryan, R. E. (2006). Oncostatin M induces cell detachment and enhances the metastatic capacity of T-47D human breast carcinoma cells. Cytokine *33*, 323-336.

Kanehisa, M. (1997). A database for post-genome analysis. Trends Genet *13*, 375-376.

Kessenbrock, K., Plaks, V., and Werb, Z. (2010). Matrix metalloproteinases: regulators of the tumor microenvironment. Cell *141*, 52-67.

Khazen, W., M'Bika J, P., Tomkiewicz, C., Benelli, C., Chany, C., Achour, A., and Forest, C. (2005). Expression of macrophage-selective markers in human and rodent adipocytes. FEBS Lett *579*, 5631-5634.

Khong, H. T., and Restifo, N. P. (2002). Natural selection of tumor variants in the generation of "tumor escape" phenotypes. Nat Immunol *3*, 999-1005.

Knupfer, H., and Preiss, R. (2010). Serum interleukin-6 levels in colorectal cancer patients-- a summary of published results. Int J Colorectal Dis *25*, 135-140.

Kong, L. Y., Abou-Ghazal, M. K., Wei, J., Chakraborty, A., Sun, W., Qiao, W., Fuller, G. N., Fokt, I., Grimm, E. A., Schmittling, R. J.*, et al.* (2008). A novel inhibitor of signal transducers and activators of transcription 3 activation is efficacious against established central nervous system melanoma and inhibits regulatory T cells. Clin Cancer Res *14*, 5759-5768.

Kortylewski, M., Kujawski, M., Wang, T., Wei, S., Zhang, S., Pilon-Thomas, S., Niu, G., Kay, H., Mule, J., Kerr, W. G.*, et al.* (2005). Inhibiting Stat3 signaling in the hematopoietic system elicits multicomponent antitumor immunity. Nat Med *11*, 1314-1321.

Kramer, C., Klasmeyer, K., Bojar, H., Schulz, W. A., Ackermann, R., and Grimm, M. O. (2007). Heparin-binding epidermal growth factor-like growth factor isoforms and epidermal growth factor receptor/ErbB1 expression in bladder cancer and their relation to clinical outcome. Cancer *109*, 2016-2024.

Kreider, J. W., Bartlett, G. L., and Butkiewicz, B. L. (1984). Relationship of tumor leucocytic infiltration to host defense mechanisms and prognosis. Cancer Metastasis Rev *3*, 53-74.

Laemmli, U. K. (1970). Cleavage of structural proteins during the assembly of the head of bacteriophage T4. Nature *227*, 680-685.

Lee, H., Herrmann, A., Deng, J. H., Kujawski, M., Niu, G., Li, Z., Forman, S., Jove, R., Pardoll, D. M., and Yu, H. (2009). Persistently activated Stat3 maintains constitutive NF-kappaB activity in tumors. Cancer Cell *15*, 283-293.

Leek, R. D., Hunt, N. C., Landers, R. J., Lewis, C. E., Royds, J. A., and Harris, A. L. (2000). Macrophage infiltration is associated with VEGF and EGFR expression in breast cancer. J Pathol *190*, 430-436.

Leong, P. L., Andrews, G. A., Johnson, D. E., Dyer, K. F., Xi, S., Mai, J. C., Robbins, P. D., Gadiparthi, S., Burke, N. A., Watkins, S. F., and Grandis, J. R. (2003). Targeted inhibition of Stat3 with a decoy oligonucleotide abrogates head and neck cancer cell growth. Proc Natl Acad Sci U S A *100*, 4138-4143.

Lewis, M. P., Lygoe, K. A., Nystrom, M. L., Anderson, W. P., Speight, P. M., Marshall, J. F., and Thomas, G. J. (2004). Tumour-derived TGF-beta1 modulates myofibroblast differentiation and promotes HGF/SF-dependent invasion of squamous carcinoma cells. Br J Cancer *90*, 822-832.

Li, G., Satyamoorthy, K., Meier, F., Berking, C., Bogenrieder, T., and Herlyn, M. (2003). Function and regulation of melanoma-stromal fibroblast interactions: when seeds meet soil. Oncogene *22*, 3162-3171.

Lin, E. Y., Nguyen, A. V., Russell, R. G., and Pollard, J. W. (2001). Colony-stimulating factor 1 promotes progression of mammary tumors to malignancy. J Exp Med *193*, 727-740.

Ling, X., and Arlinghaus, R. B. (2005). Knockdown of STAT3 expression by RNA interference inhibits the induction of breast tumors in immunocompetent mice. Cancer Res *65*, 2532-2536.

Liu, Y. J., Xu, Y., and Yu, Q. (2006). Full-length ADAMTS-1 and the ADAMTS-1 fragments display pro- and antimetastatic activity, respectively. Oncogene *25*, 2452-2467.

Lu, X., Wang, Q., Hu, G., Van Poznak, C., Fleisher, M., Reiss, M., Massague, J., and Kang, Y. (2009). ADAMTS1 and MMP1 proteolytically engage EGF-like ligands in an osteolytic signaling cascade for bone metastasis. Genes Dev *23*, 1882-1894.

Lucas, T., Waisman, A., Ranjan, R., Roes, J., Krieg, T., Muller, W., Roers, A., and Eming, S. A. (2010). Differential roles of macrophages in diverse phases of skin repair. J Immunol *184*, 3964-3977.

Malik, N., Kallestad, J. C., Gunderson, N. L., Austin, S. D., Neubauer, M. G., Ochs, V., Marquardt, H., Zarling, J. M., Shoyab, M., Wei, C. M., and et al. (1989). Molecular cloning, sequence analysis, and functional expression of a novel growth regulator, oncostatin M. Mol Cell Biol *9*, 2847-2853.

Mandal, P. K., Limbrick, D., Coleman, D. R., Dyer, G. A., Ren, Z., Birtwistle, J. S., Xiong, C., Chen, X., Briggs, J. M., and McMurray, J. S. (2009). Conformationally constrained peptidomimetic inhibitors of signal transducer and activator of transcription. 3: Evaluation and molecular modeling. J Med Chem *52*, 2429-2442.

Manning, C. B., Vallyathan, V., and Mossman, B. T. (2002). Diseases caused by asbestos: mechanisms of injury and disease development. Int Immunopharmacol *2*, 191-200.

Mantovani, A., Bottazzi, B., Sozzani, S., Peri, G., Allavena, P., Dong, Q. G., Vecchi, A., and Colotta, F. (1995). Cytokine regulation of monocyte recruitment. Arch Immunol Ther Exp (Warsz) *43*, 149-152.

Marikovsky, M., Breuing, K., Liu, P. Y., Eriksson, E., Higashiyama, S., Farber, P., Abraham, J., and Klagsbrun, M. (1993). Appearance of heparin-binding EGF-like growth factor in wound fluid as a response to injury. Proc Natl Acad Sci U S A *90*, 3889-3893.

Martin, P., and Leibovich, S. J. (2005). Inflammatory cells during wound repair: the good, the bad and the ugly. Trends Cell Biol *15*, 599-607.

Minn, A. J., Gupta, G. P., Siegel, P. M., Bos, P. D., Shu, W., Giri, D. D., Viale, A., Olshen, A. B., Gerald, W. L., and Massague, J. (2005). Genes that mediate breast cancer metastasis to lung. Nature *436*, 518-524.

Miyamoto, S., Hirata, M., Yamazaki, A., Kageyama, T., Hasuwa, H., Mizushima, H., Tanaka, Y., Yagi, H., Sonoda, K., Kai, M.*, et al.* (2004). Heparin-binding EGF-like growth factor is a promising target for ovarian cancer therapy. Cancer Res *64*, 5720-5727.

Mueller, M. M., and Fusenig, N. E. (2004). Friends or foes - bipolar effects of the tumour stroma in cancer. Nat Rev Cancer *4*, 839-849.

Nakagawa, T., Kollmeyer, T. M., Morlan, B. W., Anderson, S. K., Bergstralh, E. J., Davis, B. J., Asmann, Y. W., Klee, G. G., Ballman, K. V., and Jenkins, R. B. (2008). A tissue biomarker panel predicting systemic progression after PSA recurrence post-definitive prostate cancer therapy. PLoS One *3*, e2318.

Nefedova, Y., Nagaraj, S., Rosenbauer, A., Muro-Cacho, C., Sebti, S. M., and Gabrilovich, D. I. (2005). Regulation of dendritic cell differentiation and antitumor immune response in cancer by pharmacologic-selective inhibition of the janus-activated kinase 2/signal transducers and activators of transcription 3 pathway. Cancer Res *65*, 9525-9535.

Nishi, E., and Klagsbrun, M. (2004). Heparin-binding epidermal growth factor-like growth factor (HB-EGF) is a mediator of multiple physiological and pathological pathways. Growth Factors *22*, 253-260.

Nishino, T., Kaise, N., Sindo, Y., Nishino, N., Nishida, T., Yasuda, S., and Masui, Y. (1991). Promyelocytic leukemia cell line, HL-60, produces human hepatocyte growth factor. Biochem Biophys Res Commun *181*, 323-330.

Niu, G., Wright, K. L., Huang, M., Song, L., Haura, E., Turkson, J., Zhang, S., Wang, T., Sinibaldi, D., Coppola, D.*, et al.* (2002). Constitutive Stat3 activity up-regulates VEGF expression and tumor angiogenesis. Oncogene *21*, 2000-2008.

O'Sullivan, C., Lewis, C. E., Harris, A. L., and McGee, J. O. (1993). Secretion of epidermal growth factor by macrophages associated with breast carcinoma. Lancet *342*, 148-149.

Okabe, M., Kunieda, Y., Shoji, M., Nakane, S., Kurosawa, M., Tanaka, J., Hansen, S. R., and Asaka, M. (1995). Megakaryocytic differentiation of a leukemic cell line, MC3, by phorbol ester: induction of glycoprotein IIb/IIIa and effects on expression of IL-6, IL-6 receptor, mpl and GATA genes. Leuk Res *19*, 933-943.

Olsen, J. V., de Godoy, L. M., Li, G., Macek, B., Mortensen, P., Pesch, R., Makarov, A., Lange, O., Horning, S., and Mann, M. (2005). Parts per million mass accuracy on an Orbitrap mass spectrometer via lock mass injection into a C-trap. Mol Cell Proteomics *4*, 2010-2021.

Ong, S. E., Blagoev, B., Kratchmarova, I., Kristensen, D. B., Steen, H., Pandey, A., and Mann, M. (2002). Stable isotope labeling by amino acids in cell culture, SILAC, as a simple and accurate approach to expression proteomics. Mol Cell Proteomics *1*, 376-386.

Paez, J. G., Janne, P. A., Lee, J. C., Tracy, S., Greulich, H., Gabriel, S., Herman, P., Kaye, F. J., Lindeman, N., Boggon, T. J.*, et al.* (2004). EGFR mutations in lung cancer: correlation with clinical response to gefitinib therapy. Science *304*, 1497-1500.

Paget, S. (1889). THE DISTRIBUTION OF SECONDARY GROWTHS IN CANCER OF THE BREAST. The Lancet *133*, 571-573.

Peter, M. R., Fowkes, F. G. R., Jill, F. F. B., Hisao, O., Charles, P. W., and Tom, W. M. (2010a). Effect of daily aspirin on long-term risk of death due to cancer: analysis of individual patient data from randomised trials. The Lancet.

Peter, M. R., Michelle, W., Carl-Eric, E., Bo, N., Ale, A., Charles, P. W., and Tom, W. M. (2010b). Long-term effect of aspirin on colorectal cancer incidence and mortality: 20-year follow-up of five randomised trials. The Lancet *376*, 1741-1750.

Pollard, J. W. (2004). Tumour-educated macrophages promote tumour progression and metastasis. Nat Rev Cancer *4*, 71-78.

Pollard, J. W., and Hennighausen, L. (1994). Colony stimulating factor 1 is required for mammary gland development during pregnancy. Proc Natl Acad Sci U S A *91*, 9312-9316.

Queen, M. M., Ryan, R. E., Holzer, R. G., Keller-Peck, C. R., and Jorcyk, C. L. (2005). Breast cancer cells stimulate neutrophils to produce oncostatin M: potential implications for tumor progression. Cancer Res *65*, 8896-8904.

Ranger, J. J., Levy, D. E., Shahalizadeh, S., Hallett, M., and Muller, W. J. (2009). Identification of a Stat3-dependent transcription regulatory network involved in metastatic progression. Cancer Res *69*, 6823-6830.

Rappsilber, J., Ishihama, Y., and Mann, M. (2003). Stop and go extraction tips for matrix-assisted laser desorption/ionization, nanoelectrospray, and LC/MS sample pretreatment in proteomics. Anal Chem *75*, 663-670.

Rigo, A., Gottardi, M., Zamo, A., Mauri, P., Bonifacio, M., Krampera, M., Damiani, E., Pizzolo, G., and Vinante, F. (2010). Macrophages may promote cancer growth via a GM-CSF/HB-EGF paracrine loop that is enhanced by CXCL12. Mol Cancer *9*, 273.

Rose, T. M., and Bruce, A. G. (1991). Oncostatin M is a member of a cytokine family that includes leukemia-inhibitory factor, granulocyte colony-stimulating factor, and interleukin 6. Proc Natl Acad Sci U S A *88*, 8641-8645.

Rossi, J. F., Negrier, S., James, N. D., Kocak, I., Hawkins, R., Davis, H., Prabhakar, U., Qin, X., Mulders, P., and Berns, B. (2010). A phase I/II study of siltuximab (CNTO 328), an anti-interleukin-6 monoclonal antibody, in metastatic renal cell cancer. Br J Cancer *103*, 1154-1162.

Sano, S., Chan, K. S., Kira, M., Kataoka, K., Takagi, S., Tarutani, M., Itami, S., Kiguchi, K., Yokoi, M., Sugasawa, K.*, et al.* (2005). Signal transducer and activator of transcription 3 is a key regulator of keratinocyte survival and proliferation following UV irradiation. Cancer Res *65*, 5720-5729.

Schlessinger, J. (1988). Signal transduction by allosteric receptor oligomerization. Trends Biochem Sci *13*, 443-447.

Schroeder, J. A., and Lee, D. C. (1997). Transgenic Mice Reveal Roles for TGFα and EGF Receptor in Mammary Gland Development and Neoplasia. Journal of Mammary Gland Biology and Neoplasia *2*, 119-129.

Schust, J., Sperl, B., Hollis, A., Mayer, T. U., and Berg, T. (2006). Stattic: a small-molecule inhibitor of STAT3 activation and dimerization. Chem Biol *13*, 1235-1242.

Seitzer, N., Mayr, T., Streit, S., and Ullrich, A. (2010). A single nucleotide change in the mouse genome accelerates breast cancer progression. Cancer Res *70*, 802-812.

Shannon, P., Markiel, A., Ozier, O., Baliga, N. S., Wang, J. T., Ramage, D., Amin, N., Schwikowski, B., and Ideker, T. (2003). Cytoscape: a software environment for integrated models of biomolecular interaction networks. Genome Res *13*, 2498-2504.

Shevchenko, A., Wilm, M., Vorm, O., Jensen, O. N., Podtelejnikov, A. V., Neubauer, G., Mortensen, P., and Mann, M. (1996). A strategy for identifying gel-separated proteins in sequence databases by MS alone. Biochem Soc Trans *24*, 893-896.

Shirakata, Y., Kimura, R., Nanba, D., Iwamoto, R., Tokumaru, S., Morimoto, C., Yokota, K., Nakamura, M., Sayama, K., Mekada, E.*, et al.* (2005). Heparin-binding EGF-like growth factor accelerates keratinocyte migration and skin wound healing. J Cell Sci *118*, 2363-2370.

Shirasawa, S., Sugiyama, S., Baba, I., Inokuchi, J., Sekine, S., Ogino, K., Kawamura, Y., Dohi, T., Fujimoto, M., and Sasazuki, T. (2004). Dermatitis due to epiregulin deficiency and a critical role of epiregulin in immune-related responses of keratinocyte and macrophage. Proc Natl Acad Sci U S A *101*, 13921-13926.

Sica, A., Schioppa, T., Mantovani, A., and Allavena, P. (2006). Tumour-associated macrophages are a distinct M2 polarised population promoting tumour progression: potential targets of anti-cancer therapy. Eur J Cancer *42*, 717-727.

Slamon, D. J., Clark, G. M., Wong, S. G., Levin, W. J., Ullrich, A., and McGuire, W. L. (1987). Human breast cancer: correlation of relapse and survival with amplification of the HER-2/neu oncogene. Science *235*, 177-182.

Smyth, M. J., Godfrey, D. I., and Trapani, J. A. (2001). A fresh look at tumor immunosurveillance and immunotherapy. Nat Immunol *2*, 293-299.

Stransky, N., Vallot, C., Reyal, F., Bernard-Pierrot, I., de Medina, S. G., Segraves, R., de Rycke, Y., Elvin, P., Cassidy, A., Spraggon, C.*, et al.* (2006). Regional copy number-independent deregulation of transcription in cancer. Nat Genet *38*, 1386-1396.

Subimerb, C., Pinlaor, S., Lulitanond, V., Khuntikeo, N., Okada, S., McGrath, M. S., and Wongkham, S. (2010). Circulating CD14(+) CD16(+) monocyte levels predict tissue invasive character of cholangiocarcinoma. Clin Exp Immunol *161*, 471-479.

Sun, S., and Steinberg, B. M. (2002). PTEN is a negative regulator of STAT3 activation in human papillomavirus-infected cells. J Gen Virol *83*, 1651-1658.

Takahashi, H., Ogata, H., Nishigaki, R., Broide, D. H., and Karin, M. (2010). Tobacco smoke promotes lung tumorigenesis by triggering IKKbeta- and JNK1-dependent inflammation. Cancer Cell *17*, 89-97.

Takeda, K., Noguchi, K., Shi, W., Tanaka, T., Matsumoto, M., Yoshida, N., Kishimoto, T., and Akira, S. (1997). Targeted disruption of the mouse Stat3 gene leads to early embryonic lethality. Proc Natl Acad Sci U S A *94*, 3801-3804.

Tanaka, Y., Miyamoto, S., Suzuki, S. O., Oki, E., Yagi, H., Sonoda, K., Yamazaki, A., Mizushima, H., Maehara, Y., Mekada, E., and Nakano, H. (2005). Clinical significance of heparin-binding epidermal growth factor-like growth factor and a disintegrin and metalloprotease 17 expression in human ovarian cancer. Clin Cancer Res *11*, 4783-4792.

Tateishi, M., Ishida, T., Mitsudomi, T., Kaneko, S., and Sugimachi, K. (1990). Immunohistochemical evidence of autocrine growth factors in adenocarcinoma of the human lung. Cancer Res *50*, 7077-7080.

Tchirkov, A., Rolhion, C., Bertrand, S., Dore, J. F., Dubost, J. J., and Verrelle, P. (2001). IL-6 gene amplification and expression in human glioblastomas. Br J Cancer *85*, 518-522.

Thogersen, V. B., Sorensen, B. S., Poulsen, S. S., Orntoft, T. F., Wolf, H., and Nexo, E. (2001). A subclass of HER1 ligands are prognostic markers for survival in bladder cancer patients. Cancer Res *61*, 6227-6233.

Turkson, J., and Jove, R. (2000). STAT proteins: novel molecular targets for cancer drug discovery. Oncogene *19*, 6613-6626.

Turkson, J., Kim, J. S., Zhang, S., Yuan, J., Huang, M., Glenn, M., Haura, E., Sebti, S., Hamilton, A. D., and Jove, R. (2004). Novel peptidomimetic inhibitors of signal transducer and activator of transcription 3 dimerization and biological activity. Mol Cancer Ther *3*, 261-269.

Tyagi, P., and Mirakhur, B. (2009). MAGRIT: the largest-ever phase III lung cancer trial aims to establish a novel tumor-specific approach to therapy. Clin Lung Cancer *10*, 371-374.

Ueno, T., Toi, M., Saji, H., Muta, M., Bando, H., Kuroi, K., Koike, M., Inadera, H., and Matsushima, K. (2000). Significance of macrophage chemoattractant protein-1 in macrophage recruitment, angiogenesis, and survival in human breast cancer. Clin Cancer Res *6*, 3282-3289.

Ullrich, A., Coussens, L., Hayflick, J. S., Dull, T. J., Gray, A., Tam, A. W., Lee, J., Yarden, Y., Libermann, T. A., Schlessinger, J., and et al. (1984). Human epidermal growth factor receptor cDNA sequence and aberrant expression of the amplified gene in A431 epidermoid carcinoma cells. Nature *309*, 418-425.

Umekita, Y., Ohi, Y., Sagara, Y., and Yoshida, H. (2000). Co-expression of epidermal growth factor receptor and transforming growth factor-alpha predicts worse prognosis in breast-cancer patients. Int J Cancer *89*, 484-487.

Underhill-Day, N., and Heath, J. K. (2006). Oncostatin M (OSM) cytostasis of breast tumor cells: characterization of an OSM receptor beta-specific kernel. Cancer Res *66*, 10891-10901.

Venneri, M. A., De Palma, M., Ponzoni, M., Pucci, F., Scielzo, C., Zonari, E., Mazzieri, R., Doglioni, C., and Naldini, L. (2007). Identification of proangiogenic TIE2-expressing monocytes (TEMs) in human peripheral blood and cancer. Blood *109*, 5276-5285.

Wang, T., Niu, G., Kortylewski, M., Burdelya, L., Shain, K., Zhang, S., Bhattacharya, R., Gabrilovich, D., Heller, R., Coppola, D.*, et al.* (2004). Regulation of the innate and adaptive immune responses by Stat-3 signaling in tumor cells. Nat Med *10*, 48-54.

Wang, W., Goswami, S., Sahai, E., Wyckoff, J. B., Segall, J. E., and Condeelis, J. S. (2005). Tumor cells caught in the act of invading: their strategy for enhanced cell motility. Trends Cell Biol *15*, 138-145.

Wyckoff, J., Wang, W., Lin, E. Y., Wang, Y., Pixley, F., Stanley, E. R., Graf, T., Pollard, J. W., Segall, J., and Condeelis, J. (2004). A paracrine loop between tumor cells and macrophages is required for tumor cell migration in mammary tumors. Cancer Res *64*, 7022-7029.

Xin, H., Zhang, C., Herrmann, A., Du, Y., Figlin, R., and Yu, H. (2009). Sunitinib inhibition of Stat3 induces renal cell carcinoma tumor cell apoptosis and reduces immunosuppressive cells. Cancer Res *69*, 2506-2513.

Yamashita, S., Miyagi, C., Carmany-Rampey, A., Shimizu, T., Fujii, R., Schier, A. F., and Hirano, T. (2002). Stat3 Controls Cell Movements during Zebrafish Gastrulation. Dev Cell *2*, 363-375.

Yamazaki, S., Iwamoto, R., Saeki, K., Asakura, M., Takashima, S., Yamazaki, A., Kimura, R., Mizushima, H., Moribe, H., Higashiyama, S.*, et al.* (2003). Mice with defects in HB-EGF ectodomain shedding show severe developmental abnormalities. J Cell Biol *163*, 469-475.

Yang, F., Brown, C., Buettner, R., Hedvat, M., Starr, R., Scuto, A., Schroeder, A., Jensen, M., and Jove, R. (2010). Sorafenib induces growth arrest and apoptosis of human glioblastoma cells through the dephosphorylation of signal transducers and activators of transcription 3. Mol Cancer Ther *9*, 953-962.

Yeh, Y. T., Ou-Yang, F., Chen, I. F., Yang, S. F., Wang, Y. Y., Chuang, H. Y., Su, J. H., Hou, M. F., and Yuan, S. S. (2006). STAT3 ser727 phosphorylation and its association with negative estrogen receptor status in breast infiltrating ductal carcinoma. Int J Cancer *118*, 2943-2947.

Yu, C. L., Meyer, D. J., Campbell, G. S., Larner, A. C., Carter-Su, C., Schwartz, J., and Jove, R. (1995). Enhanced DNA-binding activity of a Stat3-related protein in cells transformed by the Src oncoprotein. Science *269*, 81-83.

Yu, H., and Jove, R. (2004). The STATs of cancer--new molecular targets come of age. Nat Rev Cancer *4*, 97-105.

Yu, H., Kortylewski, M., and Pardoll, D. (2007). Crosstalk between cancer and immune cells: role of STAT3 in the tumour microenvironment. Nat Rev Immunol *7*, 41-51.

Yu, H., Pardoll, D., and Jove, R. (2009). STATs in cancer inflammation and immunity: a leading role for STAT3. Nat Rev Cancer *9*, 798-809.

Zarling, J. M., Shoyab, M., Marquardt, H., Hanson, M. B., Lioubin, M. N., and Todaro, G. J. (1986). Oncostatin M: a growth regulator produced by differentiated histiocytic lymphoma cells. Proc Natl Acad Sci U S A *83*, 9739-9743.

Zhang, F., Li, C., Halfter, H., and Liu, J. (2003). Delineating an oncostatin M-activated STAT3 signaling pathway that coordinates the expression of genes involved in cell cycle regulation and extracellular matrix deposition of MCF-7 cells. Oncogene *22*, 894-905.

Zhong, Z., Wen, Z., and Darnell, J. E., Jr. (1994). Stat3: a STAT family member activated by tyrosine phosphorylation in response to epidermal growth factor and interleukin-6. Science *264*, 95-98.

IX. APPENDIX

1.   Abbreviations

°C	degree Celsius
µ	micro
µg	microgram
µl	microliter
µm	micrometer
AB	antibody
ABC	ammonium bicarbonate
Abl	Abelson murine leukemia viral oncogene homolog 1
ADAM	a disintegrin and metalloprotease
ADAMTS-1	a disintegrin and metalloproteinase with thrombospondin motifs 1
AG1478	tyrphostin AG1478; 4-(3'-Chloroanilino)-6,7-dimethoxyquinazoline
AKT	protein kinase B
APS	ammonium peroxodisulfate
AREG	amphiregulin
ATCC	American Type Culture Collection, USA
BCA	bicinchoninic acid
BSA	bovine serum albumin
BTC	betacellulin
CAF	cancer-associated fibroblast
CD	cluster of differentiation
CD11a	integrin alpha-L
CD11b	integrin alpha M
CD11c	integrin alpha-X
CD14	monocyte differentiation antigen CD14
CD16b	Fc fragment of IgG, low affinity IIIb, receptor
CD18	integrin beta-2
CD1C	CD1c molecule
CD33	myeloid cell surface antigen
CD45	leukocyte common antigen
CD54	intercellular adhesion molecule 1
CD64	IgG Fc receptor I
cDNA	complementary DNA
CNTF	ciliary neurotrophic factor
CT-1	cardiotrophin-1
Ctrl	control

CYR61	cysteine-rich angiogenic inducer 61
Da	Dalton
dATP	2´-deoxyadenosine 5´-triphosphate
DC	dendritic cell
DCIS	ductal carcinoma *in situ*
dCTP	2´-deoxycytidine 5´-triphosphate
dGTP	2´-deoxyguanosine 5´-triphosphate
DMSO	dimethylsulfoxide
DNA	deoxyribonucleic acid
DTT	dithiothreitol
dTTP	2´-deoxythymidine 5´-triphosphate
ECL	enhanced chemiluminescence
ECM	extracellular matrix
EDTA	ethylenediaminetetraacetic acid
EGF	epidermal growth factor
EGFR	epidermal growth factor receptor
EGTA	ethylene glycol tetraacetic acid
ELISA	enzyme-linked immunosorbent assay
EMR1	EGF-like module receptor 1
EPGN	epigen
ERBB	receptor tyrosine-protein kinase erbB
EREG	epiregulin
ERK	extracellular-signal-regulated kinase
F4/80	EGF-like module-containing mucin-like hormone receptor-like 1
Fc	immunoglobulin fragment, crystallisable
FCS	fetal calf serum
FDA	Food and Drug Administration
FITC	fluorescein isothiocyanate
g	gravitational force
gp130	membrane glycoprotein 130
Grb2	growth factor receptor-bound protein
HBEGF	heparin-binding EGF-like growth factor
HB-EGF	heparin-binding EGF-like growth factor
HDGF	hepatoma-derived growth factor
HEPES	N-(2-hydroxyethyl) piperazine-N'-(2-ethanesulfonic acid)
Her	human EGFR-related
HGF	hepatocyte growth factor
HGFR	hepatocyte growth factor receptor
HLA	human leukocyte antigen
HMEC	human mammary epithelial cells

HNTG	HEPES-, NaCl-, Triton X-100- and glycerol-containing buffer
hr	hour
HRP	horseradish peroxidase
hrs	hours
HSC	hematopoietic stem cell
Ig	immunoglobulin
IGFR	insulin-like growth factor receptor
IgG	immunoglobulin G
IL-10	interleukin-10
IL-11	interleukin-11
IL6	interleukin 6
IL-6	interleukin-6
IL6R	interleukin-6 receptor subunit alpha
IP	immunoprecipitation
IPI	International Protein Index
JAK	Janus kinase
kDa	kilodalton
LC	liquid chromatography
LDS	lithium dodecyl sulfate
LIF	leukemia inhibitory factor
LIFR	leukemia inhibitory factor receptor
M	molar
M2	alternatively activated macrophage
MAD-CM	MAD-NT-conditioned medium
MAD-NT	macrophage differentiation, non-terminal
MAPK	mitogen-activated protein kinase
MCP-1	monocyte chemoattractant protein 1
MDSC	myeloid-derived suppressor cells
MEK	MAPK/ERK kinase
min	minute
ml	milliliter
mM	millimolar
mRNA	messenger RNA
MS	mass spectrometry
mTOR	mammalian target of rapamycin
MW	molecular weight
MΦ	macrophage
NET	NaCl-, EDTA- and Tris-containing buffer
NFκB	nuclear factor NF-kappa-B
ng	nanogram

NK	natural killer cell
nM	nanomolar
NRG	neuregulin
NSAID	non-steroidal anti-inflammatory drug
NSCLC	non-small cell lung carcinoma
OSM	oncostatin-M
OSMRβ	oncostatin-M receptor beta
PAGE	polyacrylamide gel electrophoresis
pAKT	phospho-AKT
PBMC	peripheral blood monocytes
PBS	phosphate buffered saline
PCR	polymerase chain reaction
PDGFR	platelet-derived growth factor receptor
PE	phycoerythrin
pEGFR	phospho-EGFR
pg	picogram
PI3K	phosphatidylinositol 3 kinase
PLCγ1	phospholipase C-gamma-1
PMSF	phenylmethanesulfonylfluoride
pN>0	nodal positive tumour
pN0	nodal negative tumour
ppm	parts per million
pSTAT3	phospho-STAT3
pT1	invasive breast carcinoma, up to 2 cm in diameter
pT2	invasive breast carcinoma, 2 cm to 5 cm in diameter
pT3	invasive breast carcinoma, more than 5 cm in diameter
pTYK2	phospho-TYK2
pY	phospho-tyrosine
PyMT	polyoma middle T antigen
qPCR	quantitative polymerase chain reaction
Raf	rapidly accelerated fibrosarcoma
Ras	rat sarcoma small GTPase subfamily
RNA	ribonucleic acid
RP	reverse phase
RPMI	Roswell Park Memorial Institute cell culture media
RTK	receptor tyrosine kinase
RT-PCR	reverse transcriptase polymerase chain reaction
s	second
SCARA1	scavenger receptor A 1
SD	standard deviation

SDS	sodium dodecyl sulfate
SDS-PAGE	sodium dodecyl sulfate polyacrylamide gel electrophoresis
SEM	standard error of the mean
SF	serum-free
SH2	Src homology 2
SILAC	stable isotope labelling with amino acids in cell culture
siRNA	small interfering ribonucleic acid
SN	supernatant
Sos	son of sevenless
Src	proto-oncogene tyrosine-protein kinase Src
STAT	signal transducer and activator of transcription
TAE	Tris base-, acetic acid- and EDTA-containing buffer
TAM	tumour-associated macrophage
TCA	trichloroacetic acid
TE	Tris/EDTA
TEMED	N,N,N',N'-tetramethylethane-1,2-diamine
TGFA	transforming growth factor alpha
TGFα	transforming growth factor alpha
TGF-β	transforming growth factor beta
TKI	tyrosine kinase inhibitor
TMB	3,3′,5,5′-tetramethylbenzidine
TYK2	non-receptor tyrosine-protein kinase TYK2
UV	ultraviolet
VEGF	vascular endothelial growth factor
v-erbB	viral erbB protein
v-Src	v-Src sarcoma viral oncogene
WB	Western blot

2. Acknowledgments

Thorsten B., Claus, Carolin, Bianka, Jingui, Michaela, Angela G., Kerstin, Stefan H., Simone, Felix, Matthias S., Renate G., Susanne B., Susanne W., Silvia, Verena, Laura, Judith, Anne-Marie and Kathrin!

A big THANK YOU! goes to Johanna Trischberger and my family for their support and patience.

3.   *Curriculum vitae*

PERSONAL INFORMATION

- Name: Vlaicu
- First name: Philip Adrian
- Date of birth: 18.02.1977
- Place of birth: Reps, Romania
- Nationality: German and Romanian

EDUCATION

- November 1998 – April 2003 Scholarship at the Technical University Munich, Faculty of Biosciences
- July 2003 – April 2004 Diploma thesis at the Max Planck Institute of Biochemistry, Dept. of Molecular Biology, Martinsried Topic: Mechanisms of EGFR Transactivation
- June 2004 – January 2011 PhD thesis at the Max Planck Institute of Biochemistry, Dept. of Molecular Biology, Martinsried Topic: Interaction Pathways between Breast Cancer Cells and Macrophages

WORK EXPERIENCE

- November 1999 – July 2000 Teaching assistant at the Technical University Munich, Institute of Zoology, Garching
- January 2001 – April 2001 and August 2001 – Oktober 2001 Assistant at the Technical University Munich, Dept. of Landscape Management and Nature Protection, Weihenstephan
- August 2002 – September 2002 Assistant at the Technical University Munich, Dept. of Plant Genetics, Weihenstephan
- July 2003 – present Cancer research at the Max Planck Institute of Biochemistry, Dept. of Molecular Biology, Martinsried